

DISSERTATION

THE ROLE OF CELLULAR RNA DECAY PATHWAYS IN SINDBIS
VIRUS INFECTION

Submitted by
Nicole L. Garneau
Department of Microbiology, Immunology & Pathology

In partial fulfillment of the requirements
For the Degree of Doctor of Philosophy
Colorado State University
Fort Collins, Colorado
Spring 2009

UMI Number: 3374648

INFORMATION TO USERS

The quality of this reproduction is dependent upon the quality of the copy submitted. Broken or indistinct print, colored or poor quality illustrations and photographs, print bleed-through, substandard margins, and improper alignment can adversely affect reproduction.

In the unlikely event that the author did not send a complete manuscript and there are missing pages, these will be noted. Also, if unauthorized copyright material had to be removed, a note will indicate the deletion.

UMI[®]

UMI Microform 3374648
Copyright 2009 by ProQuest LLC
All rights reserved. This microform edition is protected against
unauthorized copying under Title 17, United States Code.

ProQuest LLC
789 East Eisenhower Parkway
P.O. Box 1346
Ann Arbor, MI 48106-1346

COLORADO STATE UNIVERSITY

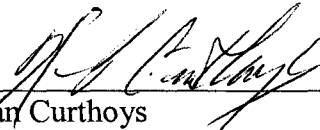
April 3, 2009

WE HEREBY RECOMMEND THAT THE DISSERTATION PREPARED UNDER OUR SUPERVISION BY NICOLE L. GARNEAU ENTITLED *THE ROLE OF CELLULAR RNA DECAY PATHWAYS IN SINDBIS VIRUS INFECTION* BE ACCEPTED AS FULFILLING IN PART REQUIREMENTS FOR THE DEGREE OF DOCTOR OF PHILOSOPHY.

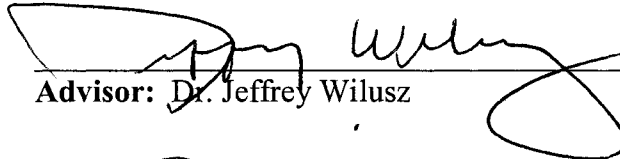
Committee on Graduate Work



Dr. Carol Blair



Dr. Norman Curthoys



Advisor: Dr. Jeffrey Wilusz



Co-Advisor: Dr. Carol Wilusz



Associate Department Head: Dr. Sandra Quackenbush

ABSTRACT OF DISSERTATION

THE ROLE OF CELLULAR RNA DECAY PATHWAYS IN SINDBIS VIRUS INFECTION

Sindbis virus is the prototypic species of the *Alphavirus* genus. Often transmitted by mosquitoes, members of this genus can cause febrile illness, arthritic pain and potentially fatal encephalitis. The alphaviral lifecycle generates single-stranded, positive-sense genomic and subgenomic RNAs which are capped on the 5' terminus, contain 5' and 3' untranslated regions (UTRs), and are polyadenylated at the 3' terminus. These characteristics make alphaviral RNAs similar in structure to cellular mRNAs, which carries both advantages and disadvantages for the virus. Such features allow alphaviruses, such as Sindbis, to benefit from the host cell translation process; however, they also could make the viral transcript vulnerable to the cellular mRNA decay enzymes. mRNA decay is a form of post-transcriptional regulation of gene expression that is found in both the mammalian and the mosquito hosts of Sindbis virus. The interaction between Sindbis viral RNAs and mRNA decay pathways was investigated in this dissertation.

First, we developed an *in vivo* viral RNA decay assay to accurately assess the rate of alphavirus RNA decay during infection in multiple cell types. Second, using this assay we identified a correlation between Sindbis viral RNA stability and viral replication efficiency, demonstrating mRNA decay potentially represents a novel host cell restriction factor. In light of this, we went on to establish the contribution of prominent cellular decay enzymes in the degradation of Sindbis viral RNAs. Based on knock down analysis we conclude that the RNAi pathway likely plays a dominant role in the decay of the viral

RNAs during infection in mammalian cells. These data represent a novel demonstration that the RNAi pathway is potentially an effective antiviral response in the mammalian host as it is in the mosquito host.

With the goal of examining the RNA turnover pathways more closely, we developed a highly sensitive method to assess poly(A) tail length, and demonstrated the importance of the viral 3'UTR as a repressor of deadenylation of viral RNAs *in vivo*. This point is particularly significant as it demonstrated that wild-type Sindbis viral RNAs are protected from the major decay pathway of the cell by the viral 3'UTR and thus undergo decay by a mechanism that is different from that found for the majority of cellular mRNAs. Finally, we found that Repeat Sequence Element 3 (RSE 3), the third and final in a series of three RSEs within the viral 3'UTR, hinders the processivity of the cellular deadenylases on viral RNAs *in vitro*, providing the first evidence for a function of this conserved alphaviral genome element.

Taken together, these results shed light on the much understudied area of viral RNA decay. Our data support the notion that the interaction between viral RNAs and the cellular RNA decay machinery is very important to the biology of the virus. Finally, this interaction may prove valuable in the pursuit to develop novel antiviral therapeutics.

Nicole L. Garneau
Department of Microbiology, Immunology & Pathology
Colorado State University
Fort Collins, Colorado 80523
Spring 2009

ACKNOWLEDGEMENTS

I want to foremost thank my advisors, Drs. Jeff and Carol Wilusz, who have continuously encouraged me to hypothesize and develop ideas. Specifically, Jeff has offered both scientific support and has generously offered unending enthusiasm for my work and belief in my potential. He was especially encouraging, despite his own deadlines and obligations, during the writing process of this dissertation. My thanks also go to my co-advisor Carol for her expertise for science and writing. Her comments and suggestions, as well as questions and critiques have contributed to the maturation of thought and technical aspects of this project. Without her help it would have been virtually impossible to for me to submit this dissertation in its corrected and polished shape by the stated deadline. Finally, I would like to extend my appreciation to my committee members, Dr. Carol Blair and Dr. Norm Curthoys. Dr. Blair is an experienced resource on Sindbis viral biology, and Dr. Curthoys offered a unique molecular perspective on aspects concerning mRNA decay. I was lucky to have a graduate committee composed of members that genuinely were interested in my success as a graduate student and who greatly contributed to the quality of my research and my dissertation.

I want to say thank you to past and present members of the Wilusz lab, all of whom have made my journey as a graduate student an entertaining experience. I would especially like to thank those members who have stood by me and offered kind words and support through the more challenging parts of my Ph.D. work. My “lab” recognition

is also extended to many members of the AIDL, both past and present, who lent their expertise on Sindbis virus and who helped me learn the ropes of virology.

I have also collected a handful of unofficial mentors to whom I am eternally grateful: Marcia Boggs for her warmth and kindness. Dr. Sandra Quackenbush (Q) for always making time to chat when I needed an objective ear. Dr. Gerry Callahan for encouraging me to embrace my love of science in any form it comes in. And finally, my thanks to Charlie Calisher for pointing out the right and the wrong in the world and for reminding me to never start a sentence with a conjunction, unless it's a good one.

My acknowledgments wouldn't be complete without offering my gratitude and my appreciation for my family and friends. To Lesley, Matt, Morgan and Jake Jones, for taking me in five years ago and for giving me support in every imaginable way. To Kiki Gilderhus, Della and Chris Fisher, I am very grateful that you were willing to open your home and family to me. To Katie Fogarty, Ann-Marie Waterhouse and Jenny Neves, I could not have kept a smile on my face under pressure without your friendship. To Gram and Gramps, Nana and Grampa, Mom and Wayne, Dad and Jay, and to the whole rest of the Garneaus and Therriens— I offer my gratitude for your love and support.

Lastly, my most sincere thanks goes to two people who have stood by me through thick and thin and who have exhibited unwavering support for me when I needed it the most. To my sister Alex, thank you for loving me unconditionally, for putting up with my infuriating dedication to work, and for reminding me that there is a world outside the lab. To my best friend Stew, who has selflessly supported me as I pursued my academic goals. His tireless love and encouragement is the backbone of my success.

TABLE OF CONTENTS

LITERATURE REVIEW.....	1
I. INTRODUCTION.....	1
II. MRNA DECAY.....	1
1. An Introduction to mRNA Decay.....	1
2. Deadenylation-Dependent mRNA Decay.....	2
3. Non-Conventional Pathways of mRNA Decay.....	7
a. Nonsense-Mediated Decay.....	7
b. Non-Stop Decay.....	10
c. No-Go Decay.....	11
4. 3'UTR Elements as Mediators of mRNA Decay.....	12
a. AU-Rich Elements and Their Binding Proteins.....	12
b. Pyrimidine-Rich Elements and Their Binding Proteins.....	12
c. Histone Stem-Loop Element and the Stem-Loop Binding Protein.....	13
5. Cytoplasmic Foci Associated with mRNA Stability.....	14
III. SINDBIS VIRUS.....	15
1. Enzootic Cycle.....	15
2. Virus Pathology.....	15
3. Molecular Biology and Replication Scheme.....	15
4. Non-Structural Proteins.....	18
5. Structural Proteins.....	20
6. Host cell Specificity.....	20
IV. THE CROSSROADS OF VIRUSES AND MRNA DECAY.....	21
1. mRNA Decay Machinery as a Possible Antiviral.....	21
a. Interferon-Stimulated RNA Decay.....	21
b. RNA Interference.....	23
c. Zinc-Finger Antiviral Protein (ZAP).....	26
2. Viral Induced Cellular RNA Decay.....	26
a. Viral Encoded Ribonucleases.....	27
b. Unknown Mechanisms of Viral Induced Host Shutoff.....	28
3. The Interaction of Viral RNAs with mRNA Decay-Associated Factors...	28
a. Viruses that Bind mRNA Stability Factors.....	29
b. Host Cell Factors that Bind and Protect Viral RNAs <i>in vitro</i>	30
RATIONALE.....	32

MATERIALS AND METHODS.....	33
I. CELL LINES.....	33
II. CELL EXTRACTS.....	38
III. VIRUS PREPARATION.....	38
1. Viral cDNA Clones.....	38
2. Viral Stocks.....	43
3. Plaque Assay.....	43
IV. PREPARATION OF RNA SUBSTRATES AND RNA PROBES.....	45
V. ONE-STEP VIRAL GROWTH CURVES.....	48
VI. <i>IN VIVO</i> VIRAL RNA DECAY ASSAY.....	49
VII. ANALYSIS OF <i>IN VIVO</i> VIRAL RNA DECAY.....	49
1. Quantitative Reverse Transcription PCR.....	49
2. RNase Protection Assay.....	51
3. Statistical Analysis of Viral RNA Half-Lives.....	52
VIII. ANALYSIS OF <i>IN VIVO</i> VIRAL POLY(A) TAIL LENGTH.....	54
1. RNase H/Northern Blotting.....	54
2. Linker Ligation-Mediated Poly(A) Tail Assay.....	55
IX. ANALYSIS OF <i>IN VITRO</i> DEADENYLATION.....	57
RESULTS.....	58
I. THE EFFICIENCY OF SINDBIS VIRUS REPLICATION IN HUMAN CELLS IS ASSOCIATED WITH RELATIVE RNA STABILITY.....	58
II. SINDBIS VIRUS RNA STABILITY IS A FUNCTION OF THE VIRAL 3'UTR.....	79
DISCUSSION.....	106
I. THE DEVELOPMENT OF AN <i>IN VIVO</i> VIRAL RNA DECAY ASSAY.....	106
II. SINDBIS VIRAL RNA STABILITY IS CORRELATED TO VIRAL GROWTH EFFICIENCY IN HOST CELLS.....	108

III. CELLULAR mRNA DECAY ENZYMES CONTRIBUTE TO THE TURNOVER OF SINDBIS VIRAL RNAS.....	111
IV. DEVELOPMENT OF THE LINKER LIGATION-MEDIATED POLY(A) TAIL ASSAY.....	115
V. SINDBIS VIRUS REPRESSES DEADENYLATION OF ITS RNA DUE TO A NOVEL FUNCTION OF THE VIRAL 3'UTR.....	117
VI. THE REPEAT SEQUENCE ELEMENT OF SINDBIS VIRUS CONTRIBUTES TO THE REPRESSION OF DEADENYLATION <i>IN VITRO</i>	121
CONCLUSIONS.....	124
LITERATURE CITED.....	126
APPENDIX A: ABBREVIATIONS.....	148
APPENDIX B: STUDENT'S T-DISTRIBUTION.....	152
APPENDIX C: LIST OF AUTHOR'S PUBLICATIONS.....	153

LIST OF FIGURES

FIGURE 1.	THE DEADENYLATION-DEPENDENT mRNA DECAY PATHWAY.....	4
FIGURE 2.	mRNA SURVEILLANCE PATHWAYS.....	8
FIGURE 3.	ORGANIZATION OF THE GENOME AND LIFECYCLE OF SINDBIS VIRUS..	17
FIGURE 4.	RNA INTERFERENCE-MEDIATED RNA DECAY (RNAi).....	24
FIGURE 5.	SINDBIS VIRUS GROWS EXPONENTIALLY IN 293T CELLS, BUT MAINTAINS ONLY A BASAL LEVEL OF INFECTION IN HELa CELLS.....	59
FIGURE 6.	METHODS FOR DISTINGUISHING BETWEEN THE GENOMIC AND SUBGENOMIC RNAs OF SINDBIS VIRUS.....	63
FIGURE 7.	SINDBIS VIRAL RNAs SHOW DRAMATICALLY DIFFERENT STABILITIES IN THE 293T VERSUS HELa HUMAN CELL LINES.....	66
FIGURE 8.	KNOCK DOWN OF mRNA TURNOVER ENZYMES WITHIN THE DEADENYLATION-DEPENDENT RNA DECAY PATHWAY.....	68
FIGURE 9.	EXO9 AND XRN1 CONTRIBUTE TO THE DECAY OF THE GENOMIC RNA OF SINDBIS VIRUS IN HELa CELLS.....	70
FIGURE 10.	EXO9 CONTRIBUTES TO THE DECAY OF THE SUBGENOMIC RNA OF SINDBIS VIRUS IN HELa CELLS.....	72
FIGURE 11.	KNOCK DOWN OF UPF1 AND DICER, TWO MAJOR PROTEINS IN NON- CONVENTIONAL PATHWAYS OF mRNA DECAY.....	75
FIGURE 12.	THE ENDONUCLEASE DICER CONTRIBUTES TO THE DECAY OF THE SINDBIS VIRAL RNA IN HELa CELLS.....	77
FIGURE 13.	THE NONSENSE-MEDIATED DECAY FACTOR UPF1 DOES NOT CONTRIBUTE TO THE DECAY OF THE SINDBIS VIRAL RNA IN HELa CELLS.....	78
FIGURE 14.	SINDBIS VIRAL RNAs ARE SUBJECT TO DECAY IN MOSQUITO CELLS...	80
FIGURE 15.	SINDBIS VIRAL RNAs DECAY IN A DEADENYLATION-INDEPENDENT FASHION.....	83

FIGURE 16.	SEQUENCE AND ORGANIZATION OF THE SINDBIS VIRUS 3'UTR.....	85
FIGURE 17.	THE 3'UTR OF SINDBIS VIRUS REPRESSES DEADENYLATION DURING INFECTION IN BHK-21 CELLS.....	87
FIGURE 18.	LINKER-LIGATION MEDIATED POLY(A) TAIL ASSAY (LLM-PAT).....	89
FIGURE 19.	THE 3'UTR OF SINDBIS VIRUS REPRESSES DEADENYLATION DURING INFECTION IN C6/36 CELLS.....	91
FIGURE 20.	THE 3'UTR OF SINDBIS VIRUS REPRESSES DEADENYLATION IN C6/36 CYTOPLASMIC EXTRACTS.....	94
FIGURE 21.	REPEAT SEQUENCE ELEMENT 3 (RSE 3) OF SINDBIS VIRUS REPRESSES DEADENYLATION IN C6/36 CYTOPLASMIC EXTRACTS.....	96
FIGURE 22.	PREDICTED SECONDARY STRUCTURE, PRIMARY SEQUENCE AND MUTANT CONSTRUCTS OF THE SINDBIS VIRUS RSE 3.....	98
FIGURE 23.	SEQUENCES IN LOOP 1 OF RSE 3 OF SINDBIS VIRUS CONTRIBUTE TO THE REPRESSION OF DEADENYLATION IN C6/36 CYTOPLASMIC EXTRACTS.....	100
FIGURE 24.	STEM-LOOP 1 OF RSE 3 ALONE REPRESSES DEADENYLATION IN C6/36 CYTOPLASMIC EXTRACTS.....	102
FIGURE 25.	REGION 1 OF RSE 3 CONTRIBUTES TO THE REPRESSION OF DEADENYLATION IN C6/36 CYTOPLASMIC EXTRACTS.....	103

LITERATURE REVIEW

I. INTRODUCTION

The species that comprise the genus *Alphavirus* have positive-sense RNA genomes and pose a significant risk to human and veterinary health. Since their discovery alphaviruses have become very well understood in terms of the method of transmission, the epidemiology of the diseases they cause, the pathology of infection and the molecular biology of the viral lifecycle. Despite this knowledge however, there are no specific antiviral treatments for alphavirus-induced diseases. An understudied area of research is the interplay between alphaviral RNAs and the host cell mRNA decay machinery. Cellular RNA turnover pathways rapidly and efficiently destroy unwanted cellular mRNAs. As alphaviral RNAs look and function like cellular mRNAs, it is unclear why these enzymes should not also represent an effective defense against viral transcripts. Delineating the interaction between viral RNAs and the cellular decay machinery is therefore necessary to fully understand viral lifecycles. A background of mRNA decay, an overview of the prototypic alphavirus Sindbis, and known interactions between mRNA decay factors and viruses are presented in this literature review.

II. MRNA DECAY

1. An introduction to mRNA decay. All levels of gene expression are highly regulated. The first regulated step is within the nucleus at the level of gene transcription. Following transcription, processing of the mRNA occurs and the mature transcripts are exported to the cytoplasm. Once in the cytoplasm, regulation due to the level of translation efficiency is very important, but protein production is ultimately dependent

upon all prior steps. mRNA decay however, as an additional facet of cytoplasmic regulation, can quickly and efficiently affect protein production by ridding the cell of the target transcript. This is best exemplified by studies that specifically examined the changes in gene expression that were a function of mRNA decay. Under certain conditions, including environmental stimuli and liver regeneration, up to 50% of changes in gene expression were due to alterations in mRNA turnover (Cheadle *et al.*, 2005b; Cheadle *et al.*, 2005a; Garcia-Martinez *et al.*, 2004; Kren & Steer, 1996). So while every step in the regulation of gene expression is critical, protein production can be efficiently altered by quickly removing the transcripts via mRNA decay.

Characteristics of an mRNA that can contribute to the regulation of mRNA decay include a 7-methyl guanosine cap on the 5' terminus, the open reading frame, 5' and 3' untranslated regions (UTRs) and a poly(A) tract at the 3' terminus. Some or all of these features are found in many viral RNAs. In addition to regulation of normal gene expression, mRNA decay plays an important role in surveillance and turnover of aberrant RNAs, as well as in processing of non-coding RNAs. As the range of transcripts requiring turnover is broad, the cell has evolved multiple pathways of decay to ensure accurate gene expression, to promote RNA processing, and to efficiently rid the cell of abnormal transcripts. Many of the characterized RNA decay pathways are described here and viral interactions are highlighted where applicable.

2. *Deadenylation-dependent mRNA decay.* A majority of eukaryotic mRNAs are turned over by the deadenylation-dependent mRNA decay pathway. As diagramed in Figure 1, this pathway is initiated by shortening of the 3' poly(A) tail. Deadenylation,

while being the first step in this pathway, is also the rate-limiting step and is reversible (Paynton & Bachvarova, 1994; Belloc *et al.*, 2008; Brewer & Ross, 1988; Shyu *et al.*, 1991; Wilson & Treisman, 1988). An important aspect of deadenylation is the built-in redundancy of function; there are four well-characterized deadenylases in mammalian cells as well as several less studied factors. The Carbon Catabolite Repression 4 protein (Ccr4p) and the Ccr4-Associated Factor (Caf1p) are part of the Ccr4-Not complex. Both of these proteins function as poly(A) specific exonucleases in the yeast *Saccharomyces cerevisiae* (Tucker *et al.*, 2001). While human homologues of Ccr4p and Caf1p were identified early on, the functional characterization of these proteins as deadenylases in mammalian cells did not come until later (Albert *et al.*, 2000; Gavin *et al.*, 2002; Zheng *et al.*, 2008; Schwede *et al.*, 2008; Yamashita *et al.*, 2005). Similarly, the Pab1p-dependent poly(A) nuclease 2 (Pan2), in complex with Pan3, forms a deadenylase complex which was also originally characterized in yeast. In this system, the presence of Pan3 is required for the catalytic activity of Pan2 (Brown *et al.*, 1996). In mammals, the Pan2-Pan3 complex is involved in the initial poly(A) tail shortening of the β -globin mRNA, but it is unclear if it is involved in the trimming of all poly(A) tails (Yamashita *et al.*, 2005). The final well-characterized mammalian deadenylase is the poly(A)-specific ribonuclease (PARN), originally termed the deadenylating nuclease (DAN) (Korner & Wahle, 1997). PARN is particularly unique because there are no known homologues in either yeast or in the fruit fly species *Drosophila melanogaster*. The enzyme is highly processive and its activity is strongly stimulated by the presence of a 5' cap structure (Dehlin *et al.*, 2000; Gao *et al.*, 2000; Liu *et al.*, 2009; Martinez *et al.*, 2000; Martinez *et al.*, 2001; Nilsson *et al.*, 2007; Wu *et al.*, 2009).

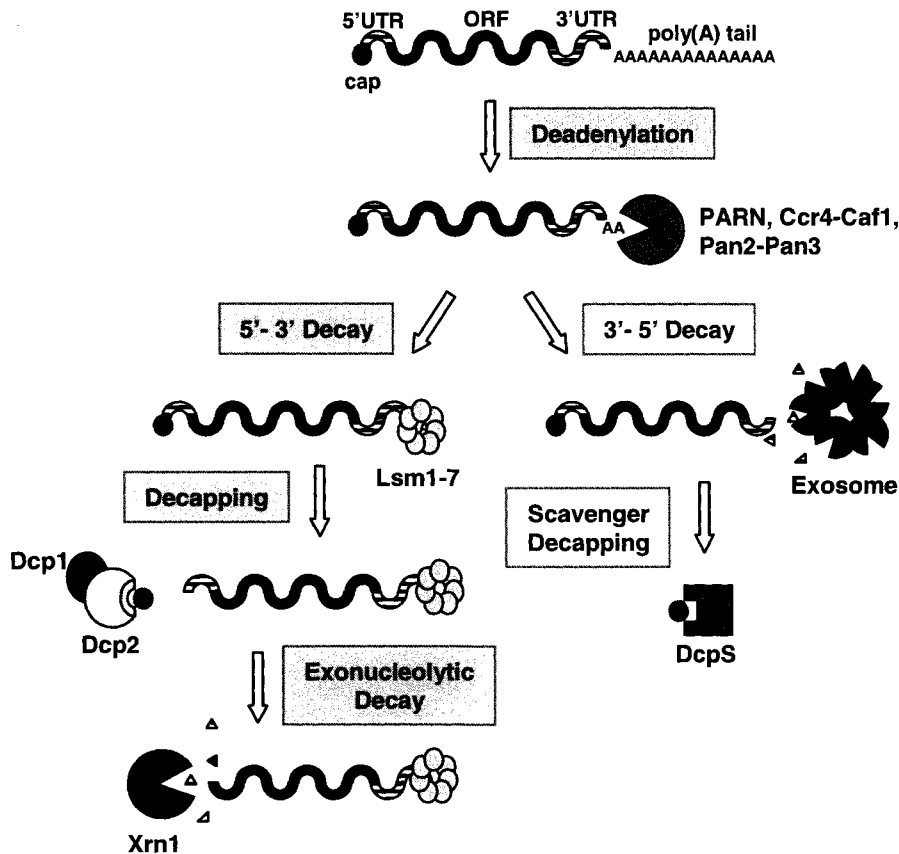


Figure 1 | The deadenylation-dependent mRNA decay pathway. A majority of mRNAs undergo decay through removal of the poly(A) tail by the activity of a deadenylase shown here as PARN, Ccr4-Caf1 or Pan2-Pan3. Following deadenylation, two branches of the pathway can occur. The first branch, shown on the left, begins with the binding of the Lsm1-7 complex to the 3' end of the transcript, which induces decapping of the mRNA by the Dcp2-Dcp1 complex. The body of the transcript is then susceptible to decay via the 5' to 3' exonuclease Xrn1. The second branch of the pathway, as shown on the right, commences with degradation of the body of the mRNA via the 3' to 5' exonucleolytic complex called the exosome. The remaining cap structure is then hydrolyzed by the scavenger decapping enzyme DcpS.

Following shortening of the poly(A) tail, a transcript destined for decay in mammalian cells will undergo one of two irreversible branches of the deadenylation-dependent decay pathway. The first branch in yeast cells initiates with the binding of the Sm-like 1-7 protein complex (Lsm1-7) to the 3' end of the transcript to promote decapping at the 5' end (Tharun *et al.*, 2000; Tharun & Parker, 2001; Tharun *et al.*, 2005). Although this association event has not yet been directly observed in mammalian cells, it has been found that the human Lsm1-7 complex does in fact co-localize with mRNA decay enzymes (Ingelfinger *et al.*, 2002). Additionally, with the reconstitution of the recombinant human Lsm1-7 complex, it is likely that the proposed function of the proteins in human cells will soon be confirmed (Zaric *et al.*, 2005).

Following the binding of Lsm1-7, the targeted transcript is then subject to decapping. Mammalian decapping is catalyzed by the Dcp2 protein as a component of the Dcp2-Dcp1 complex (Lykke-Andersen, 2002; Wang *et al.*, 2002; van Dijk *et al.*, 2002). The yeast Dcp2 enzyme, and its orthologues, are part of a class of proteins that contain the *mutT* motif (Dunckley & Parker, 1999; Piccirillo *et al.*, 2003). This motif has been shown to be critical to the hydrolysis of pyrophosphates (Safrany *et al.*, 1998); thus the decapping activity of Dcp2 is dependent upon *mutT*. In mammalian cells, it was found that the catalytic activity of Dcp2 is enhanced by the protein Hedls (Fenger-Gron *et al.*, 2005). Although not as well understood as the yeast systems, there are also other mammalian decapping accessory proteins, including Pat1 and Rck/p54, that redirect the fate of a transcript by blocking translation and stimulating decapping (Scheller *et al.*, 2007; Fenger-Gron *et al.*, 2005). Finally, the process of decapping leaves a 5' monophosphate on the targeted transcript, rendering it vulnerable to 5' to 3' decay via the

exoribonuclease Xrn1 in yeast cells and also in mammalian cells (Hatfield *et al.*, 1996; Stoecklin *et al.*, 2006).

If an mRNA is directed to the second branch of the deadenylation-dependent pathway, it is attacked at its vulnerable 3' end by the exosome. The mammalian exosome represents a large protein complex (Chen *et al.*, 2001; Allmang *et al.*, 1999; Brouwer *et al.*, 2000; Liu *et al.*, 2006). Six of the subunits (Exo4-9) contain Pleckstrin homology (PH) protein binding domains and function to form a ring structure. This structure is then bridged by three additional subunits (Exo1-3) (Liu *et al.*, 2006; Hernandez *et al.*, 2006). These nine components which form the core are highly conserved among all eukaryotes, and thus our understanding of the mammalian exosome is based primarily on in-depth studies conducted in yeast. From this work, it is now widely believed that this core is in fact catalytically inactive, although all subunits are required for viability in yeast (Allmang *et al.*, 1999). Interestingly, it was found that the 3' to 5' exonucleolytic activity of the exosome is due to a single subunit termed Dis3 or Rrp44 that is not part of the core (Dziembowski *et al.*, 2007). Recent reports have also described a novel endonucleolytic activity of the Dis3/Rrp44 component of the exosome in yeast, in addition to its well-described exonuclease activity (Schaeffer *et al.*, 2009; Lebreton *et al.*, 2008). Finally, what remains following 3' to 5' exonucleolytic decay is the recycling of the 5' cap structure by the scavenger decapping enzyme DcpS (Liu *et al.*, 2002).

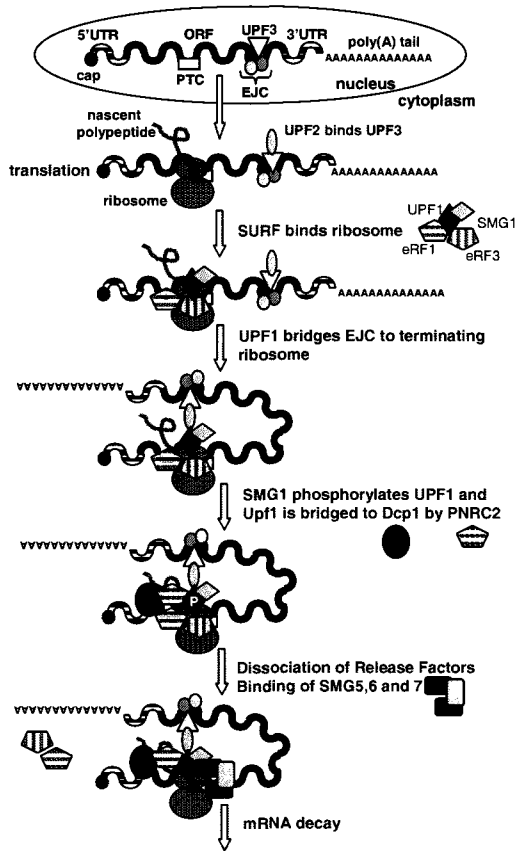
Many positive-strand RNA viruses contain characteristics that are important in the regulation of the deadenylation-dependent decay pathway, such as a 5' cap structure and a 3' poly(A) tail. As these features play a distinct role in the deadenylation-dependent

pathway of mRNA decay, it is unclear why this mechanism of RNA turnover would not also act on viral RNAs.

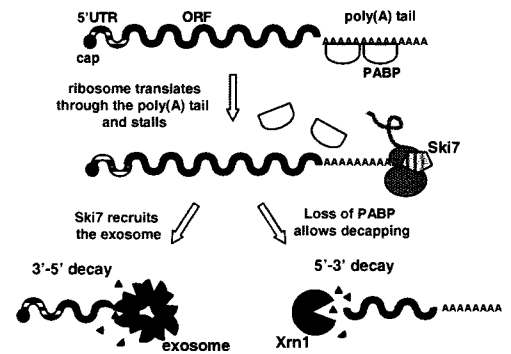
3. Non-conventional pathways of mRNA decay. While the deadenylation-dependent RNA decay pathway described above is responsible for the bulk of mRNA degradation, there are specialized RNA turnover pathways that ensure faulty transcripts are decayed, and therefore remain untranslated. The surveillance pathways listed below detect and degrade such transcripts, thus protecting the cell from potentially toxic protein products.

a. Nonsense-mediated mRNA decay. Nonsense-mediated decay (NMD) is the best studied of the quality control and surveillance pathways and is found in all eukaryotes. Mammalian NMD begins with the recognition of an aberrant messenger ribonucleoprotein (mRNP) structure due to an extended 3' UTR or a premature termination codon (PTC). PTCs can arise from mutations, frame-shifts, inefficient processing, and leaky translation initiation. During splicing, a normal mRNA acquires a protein mark called an exon junction complex (EJC). EJCs are deposited upstream of each exon junction within the open reading frame of the transcripts (Le Hir *et al.*, 2000). In PTC containing mRNAs the EJC is inappropriately located downstream of the faulty stop codon. EJCs are normally displaced by translating ribosomes, but in PTC-containing transcripts the ribosome does not translate past the stop codon, and so the EJC remains inappropriately associated with the mRNA. The cell recognizes this aberrant mRNP structure, and targets the transcript for decay. Alternatively, in PTC-containing immunoglobulin μ transcripts, NMD is initiated by the recognition of an aberrant mRNP

A Nonsense-Mediated Decay



B Non-Stop Decay



C No-Go Decay

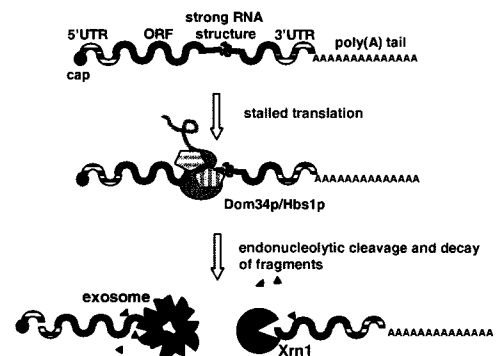


Figure 2 | mRNA-surveillance pathways. A | Nonsense-mediated decay (NMD). Following splicing in the nucleus, the exon junction complex (EJC), which contains Upf3 (a core protein of the NMD pathway), is associated with the transcript, and the resulting messenger ribonucleoprotein is exported to the cytoplasm. In the cytoplasm, a second NMD core protein, Upf2 binds to Upf3. Translation begins, but the ribosomes become stalled at the premature termination codon (PTC). This results in binding of the SURF complex (which contains Smg1, Upf1, eRF1 and eRF3) to the ribosome. Upf1 binds to Upf2, thereby linking the EJC to the PTC. The nuclear receptor coregulatory protein PNRC2 binds Upf1 and Dcp1, and bridges the PTC to the decay machinery. Phosphorylation of Upf1 by Smg1 leads to dissociation of eRF1 and eRF3. The Smg7 adaptor protein binds, and with it Smg5 and Smg6 (which contains endonucleolytic activity), triggering the dephosphorylation of Upf1, and subsequent decay of the transcript. B | Non-stop decay. Translation of an mRNA that lacks a stop codon results in ribosomes translating into the poly(A) tail, displacing poly(A) binding protein (PABP) and stalling the ribosomes. Two models exist to explain the mechanism of non-stop decay. The first proposes that the adaptor protein Ski7 binds to the A site on the stalled ribosome to release the transcript, and then recruits the exosome to decay the poly(A) tail and the mRNA. In the second described pathway, an absence Ski7 and the displacement of PABP leads to decapping and 5' to 3' turnover via Xrn1. C | No-go decay. Ribosomes stalling can occur in the open reading frame (ORF), due to for example a strong secondary structure. Dom34p and Hbs1p bind the transcript near the stalled ribosome and initiate an endonucleolytic cleavage event near the stall site. This releases the ribosomes and generates two mRNA fragments, each with a free end exposed for exonucleolytic decay by the exosome and Xrn1, respectively. Figure adapted from Garneau *et al.*, 2007.

structure due to the increased distance between the stop codon and the poly(A) tail (Buhler *et al.*, 2006).

As seen in panel A of Figure 2, ribosome stalling at the PTC in EJC-dependent NMD allows for Smg1 kinase, and Upf1 to bind to the peptide release factors eRF1 and 3, forming a complex called SURF (Kashima *et al.*, 2006). Upf2 then is recruited to the EJC by Upf3 (Lykke-Andersen *et al.*, 2000). Upf2 and Upf3 then bridge Upf1 to the EJC, which stimulates both the ATPase and 5' to 3' helicase activity of Upf1 (Chamieh *et al.*, 2008). This bridging between the SURF complex, the stalled ribosome, and the EJC leads to phosphorylation of Upf1 by Smg1 and dissociation of the release factors (Kashima *et al.*, 2006). It was recently reported that PNRC2, a proline-rich nuclear receptor coregulatory protein, also interacts with the phosphorylated Upf1, and by doing so bridges the targeted transcript to Dcp1 (Cho *et al.*, 2009). The authors suggest that connecting the decapping machinery to the PTC-containing RNA initiates the decay of the aberrant transcript. Smg5, 6 and 7 then associate with the complex and trigger dephosphorylation of Upf1 (Fukuhara *et al.*, 2005; Unterholzner & Izaurralde, 2004; Glavan *et al.*, 2006). Finally, the activities of both the endonuclease Smg6 and a deadenylase contribute to decay of NMD transcripts in mammalian cells (Glavan *et al.*, 2006; Chen & Shyu, 2003; Eberle *et al.*, 2009).

In addition to the surveillance role of NMD, genome-wide studies in many species have revealed a role for the pathway in the turnover of select natural targets (Mendell *et al.*, 2004; He *et al.*, 2003). These targets include pseudogenes, a transcription activator, ancient transposons and endogenous retroviruses (Mendell *et al.*, 2004; Taylor *et al.*, 2005; Mitrovich & Anderson, 2005; Wittmann *et al.*, 2006). In addition a recent

report demonstrates that wild-type RNAs containing long 3' UTRs are similarly targeted by this pathway (Kebaara & Atkin, 2009).

Importantly, NMD has been implicated in the decay of the RNAs from the retrovirus Rous sarcoma virus during infection in chicken embryo fibroblasts (LeBlanc & Beemon, 2004). The lifecycle of retroviruses requires a nuclear experience. The genomic RNA copies, which are not spliced prior to export, are therefore recognized as aberrant, and targeted as such. Finally, it was demonstrated that the 3'UTR was critical to viral stability (Weil & Beemon, 2006; Weil *et al.*, 2009).

b. Non-stop Decay. Non-stop decay targets mRNAs that lack an in-frame stop codon. This can be due mutations and frame shifting, but is often due to an incomplete or “broken” transcript that is missing its 3'UTR. The result of this defect is that the translation machinery proceeds through the 3' UTR and into the poly(A) tail, where the ribosomes become stalled. This surveillance pathway, described in both yeast and mammalian cells, was found to function without Upf1, deadenylation, decapping or the 5' to 3' exonuclease activity of Xrn1, making it extremely unique in mechanism (Frischmeyer *et al.*, 2002).

Since its discovery, two separate models of non-stop decay have been proposed, both of which are highlighted in panel B of Figure 2. The first provides evidence that the exosome is responsible for both deadenylating the target mRNA and also degrading it in a 3' to 5' manner (van Hoof *et al.*, 2002; Frischmeyer *et al.*, 2002). This is accomplished by the binding of Ski7p to the empty A site of the stalled ribosome, which consequently releases the ribosome from the faulty transcript. The exosome is then recruited by the Ski complex and decay ensues. The second pathway came to light after

results showed that non-stop decay was still highly functional in the absence of Ski7p (Inada & Aiba, 2005). The authors demonstrated that removal of the poly(A) binding protein from the poly(A) tail rendered the transcripts susceptible to decapping and 5' to 3' exonucleolytic decay. It is likely that these proposed pathways are both functional in non-stop decay and that they may in fact work in concert with one another.

c. No-Go Decay. This final characterized surveillance pathway has only been described in yeast to date. It recognizes stalled ribosomes within the open reading frame of an mRNA and consequently targets the transcript for decay. It was found that this pathway of turnover was independent of both decapping and exosome function (Doma & Parker, 2006). As diagrammed in panel C of Figure 2, the mechanism by which degradation occurs is via endonucleolytic cleavage of the target mRNA near the site of the stalled ribosome. Furthermore, under the rationale that translation termination-like factors might function in no-go decay, the roles of Dom34p and Hbs1p (which are similar to such factors) were examined. They found that Dom34p appeared to be the major contributor to the pathway, with Hbs1p playing a minor role (Doma & Parker, 2006). In support of these data, a more recent study showed that Domain 1 of Dom34p possesses endonucleolytic activity *in vitro* (Lee *et al.*, 2007). Finally, no-go decay has also been implicated in the decay of a viral RNA. When a ribosome-inactivating antiviral factor called PAP (Pokeweed Antiviral Protein) was used against the alphavirus-like bromemosaic virus (family *Bromoviridae*) during an infection in yeast, PAP was observed to cause ribosome stalling on the viral RNA by an unknown mechanism which resulted in no-go decay (Gandhi *et al.*, 2008).

4. *3' UTR elements as mediators of mRNA decay.* The stability of an mRNA is often influenced by *cis*-elements located in the 3' UTR of a transcript. Through either secondary structure or the primary sequence, these elements are able to mediate stability of the transcript. The following examples of well-characterized cellular 3' UTR elements were chosen based on reports that viruses contain similar elements which may regulate stability of the viral RNAs.

a. AU-rich elements and their binding proteins. AU-rich elements (AREs) vary in the sequence and composition of As and Us. Class I and II AREs contain tandem copies of the pentamer AUUUA. Class III AREs, while very AU-rich, do not contain this canonical pentamer (Chen & Shyu, 1995). AREs are found in the 3' UTR of many transcripts, including cytokines, proto-oncogenes and transcription factors (Bakheet *et al.*, 2006; Khabar, 2005). The stability of the ARE-containing mRNA is dependent on ARE-binding proteins and the decay enzymes they modulate. The ARE-binding protein HuR (Human antigen R) generally stabilizes the ARE-containing transcripts it binds (Chen *et al.*, 2002). Conversely, Tristetraprolin (TTP) promotes rapid degradation by recruiting the decay enzymes directly to the transcript (Hau *et al.*, 2007). Interestingly, the alphavirus Sindbis bears a 3' UTR with high AU-rich content which may or may not function as AREs (Saleh *et al.*, 2003; Ou *et al.*, 1981).

b. Pyrimidine-rich elements and their binding proteins. Like AREs, pyrimidine-rich elements (PREs) are located in the 3' UTR, but rather than AUs, they contain C and/or U-rich motifs. One group of proteins that bind PREs, known as poly(C)-binding proteins (PCBPs) or α CPs, bind to the elements based on the primary and secondary structures (Thisted *et al.*, 2001). Unlike AREs which normally regulate

stability in response to cellular conditions, the presence of a PRE within the 3' UTR uniformly stabilizes the transcript. Human mRNAs that contain PREs and which are stabilized by the α CP complex that bind them include those encoding collagen, α -globin, β -globin, and tyrosine hydroxylase (Paulding & Czyzyk-Krzeska, 1999; Stefanovic *et al.*, 1997; Kiledjian *et al.*, 1995; Wang *et al.*, 1995; Yu & Russell, 2001). An additional pyrimidine-rich binding protein is PTB (Poly-pyrimidine Tract Binding protein). Studies on insulin mRNA stability have shown that this protein binds and stabilizes this mRNA (Fred & Welsh, 2005; Fred & Welsh, 2009; Fred *et al.*, 2006). Finally, it was found that PCBPs not only bind cellular transcripts, but also interact with the highly structured cloverleaf in the 5' UTR of poliovirus (family *Picornaviridae*) (Gamarnik & Andino, 1997). This interaction was observed to stabilize the viral RNA *in vitro* (Murray *et al.*, 2001).

c. Histone stem-loop element and the stem-loop binding protein. The 3' ends of histone mRNAs are unique in that they do not have poly(A) tails. Instead, they have a highly conserved 3' stem-loop structure consisting of a 6 base-pair stem and a 4 base loop (Busslinger *et al.*, 1979). The histone stem-loop element regulates many functions including the mediation of turnover of the mRNA (Graves *et al.*, 1987; Graves & Marzluff, 1984; Pandey & Marzluff, 1987; Sittman *et al.*, 1983). The process of degradation of histone RNAs is unique in that the initial step is polyuridylylation (Mullen & Marzluff, 2008). Following polyuridylylation, a complex including the Sm-like protein Lsm1, the nonsense-mediated decay protein Upf1 and the stem-loop binding protein (SLBP) degrades the histone mRNA (Kaygun & Marzluff, 2005; Mullen & Marzluff, 2008).

Although the SLBP has been shown to be highly specific to the histone mRNAs within mammalian cells (Townley-Tilson *et al.*, 2006), histone mRNAs are the most notable eukaryotic transcripts that do not have poly(A) tails. Many viral RNAs however, also do not have poly(A) tails, including those in the genus *Flavivirus* (Wengler *et al.*, 1978). Interestingly, these viruses also contain highly structured 3' ends. Despite this, studies to examine if an interaction of the histone SLBP with flaviviral RNAs exists has not been performed to date.

5. *Cytoplasmic foci associated with mRNA stability.* Two distinct types of cytoplasmic foci, termed stress granules and processing bodies (P-bodies), form during periods of translational arrest induced by cellular stress (Kedersha *et al.*, 2005). While stress granules are defined by the presence of arrested translation initiation complexes, P-bodies contain mRNA decay factors (Kedersha & Anderson, 2002; Kimball *et al.*, 2003; Sheth & Parker, 2003). It is important to note however, that the proteins used to define stress granules and P-bodies are not exclusive to these foci. To that end, it is speculated that P-bodies may be sites of mRNA decay in mammalian cells, but it is unclear the degree of degradation that occurs there when compared to the cytoplasm as a whole (Eulalio *et al.*, 2007; Cougot *et al.*, 2004). Finally, the Sindbis virus encoded protein nsP3, as well as the RNAs from the flaviviruses West Nile and Dengue have been shown to interact with P-body associated proteins (Li *et al.*, 2002b; Gorchakov *et al.*, 2008b), potentially linking these putative sites of mRNA decay to aspects of positive-strand RNA viral lifecycles.

III. SINDBIS VIRUS

1. *Enzootic cycle.* Sindbis virus is the prototypic species of the genus *Alphavirus* within the viral family *Togaviridae*. It is transmitted in an enzootic cycle via mosquitoes which acquire the virus during blood feeding from an infected vertebrate host. The virus replicates in the posterior midgut epithelial cells of the mosquito vector (Jackson *et al.*, 1993). From there it must migrate to the salivary glands of the vector host to be passed on to susceptible vertebrate hosts during a subsequent blood meal. Once infected, mosquitoes are carriers for life. In the enzootic cycle, birds represent the major vertebrate host, with mammals being an alternative host (Griffin, 2001).

2. *Virus pathology.* Infection of Sindbis virus in an invertebrate host, such as the mosquito vector, does not cause overt cellular pathology. Conversely, infections in human hosts can be characterized by coincident onset of fever with rash and arthritic pain. The skin irritation can be widely distributed over the body, but usually dissipates within a few weeks. Joint pain can be mild to severe, and in contrast to the rash, it can last for months to years (Griffin, 2001).

3. *Molecular biology and replication scheme.* Sindbis virus has a single-stranded, positive-sense RNA genome of 11.7 kb. As diagramed in panel A of Figure 3, the genomic and the subgenomic viral RNAs have a 7-methyl guanosine cap on the 5' terminus, contain 5' and 3' untranslated regions (UTRs), and are polyadenylated at the 3' terminus. The 5' two-thirds of the genomic RNA codes for the non-structural proteins

(nsPs), and the 3' third of the genomic RNA codes for the structural proteins (sPs) (Strauss & Strauss, 1994).

The 3' UTRs of the genomic and subgenomic RNAs are identical, and play a well defined role in Sindbis virus replication (Levis *et al.*, 1986; Hardy & Rice, 2005; Thal *et al.*, 2007). Just as the 3' UTRs of cellular mRNAs contain defined sequences, the viral 3' UTR contains its own specific elements. The elements within the 3' UTR of Sindbis virus include three Repeat Sequence Elements (RSE 1, 2 and 3), a U-Rich Element (URE) and a Conserved Sequence Element (CSE). RSEs of varying sizes and compositions are found in all alphaviral 3' UTRs, however their function has not been identified to date. The Sindbis viral RSEs are 40 nucleotides in length and are predicted to be highly structured according to computations based on thermodynamic stability (Pfeffer *et al.*, 1998; Ou *et al.*, 1981). The URE, which is located immediately upstream of the CSE is also 40 nucleotides in length and as its name suggests, it is composed of a high concentration of uridines (Ou *et al.*, 1981). Finally, the CSE, which is also U-rich, is composed of the 19 nucleotides which immediately precede the poly(A) tail, and it has been shown to be required for viral replication (Kuhn *et al.*, 1990; Levis *et al.*, 1986).

Sindbis virus is categorized as a class IV virus based on the Baltimore classification scheme (Baltimore, 1971). As diagramed in Figure 3, panel B, members of this class have positive-sense RNA genomes which are immediately translated by host cell translational machinery upon entry into the host cell cytoplasm. Translation of the genomic RNA yields the non-structural proteins, including nsP4 which is the RNA-dependent RNA polymerase. This viral enzyme is responsible for replication of the minus strand RNA from the genomic template. The minus strand itself then serves as a template

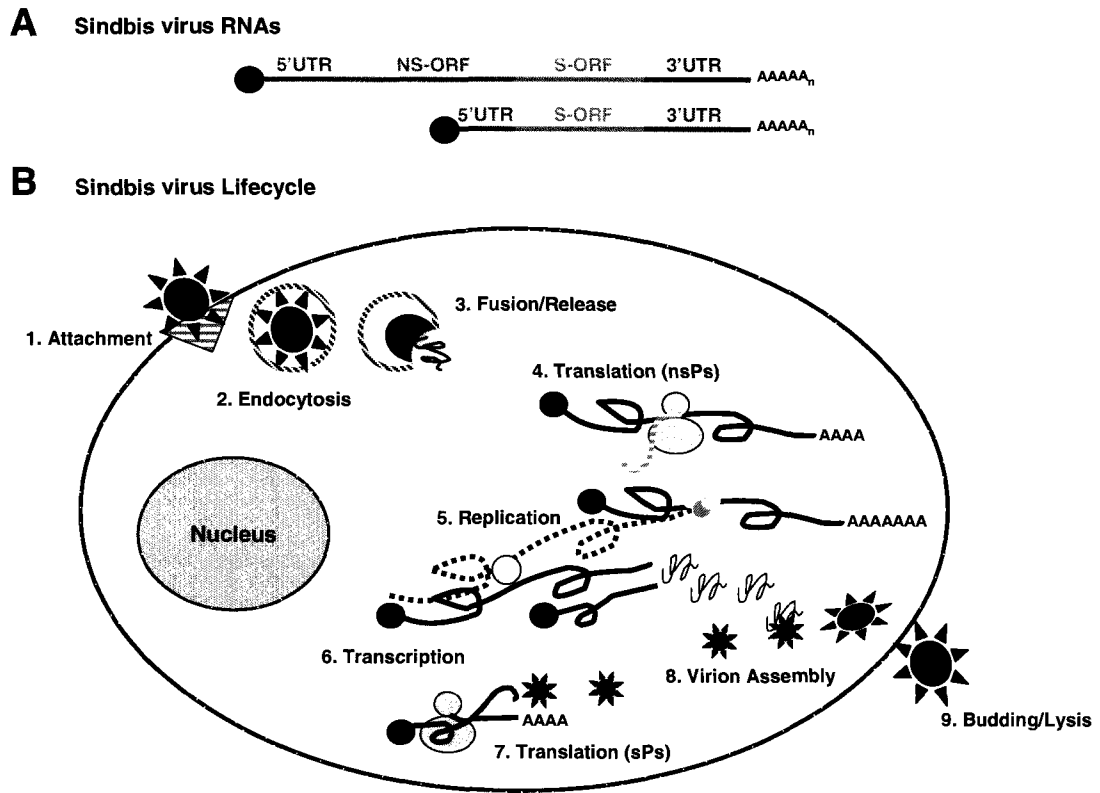


Figure 3 | Organization of the genome and lifecycle of Sindbis virus. **A** | The Sindbis virus genome contains a 5' cap structure, a 5' untranslated region (UTR), two large open reading frames (ORF) which code for the non-structural proteins (nsPs) and the structural proteins (sPs), and a 3' UTR which is followed immediately by a poly(A) tail. **B** | The lifecycle of Sindbis virus begins with infection of a host cell by a mature virion through binding to the host cell membrane receptor (1). The virus then enters the cell via endocytosis (2). A pH change in the vesicle allows for fusion of the nucleocapsid with the vesicle membrane and subsequent release of the genomic RNA into the cytoplasm (3). The host cell translational machinery translates the ns-ORF to synthesize nsPs, including the RNA-dependent RNA polymerase (4) which then replicates a minus strand copy of the genomic RNA (5). The minus strand serves as a template for transcription of multiple copies of both genomic and subgenomic RNAs (6). The subgenomic RNA is then translated by the host cell translation machinery to synthesize the sPs which includes nucleocapsid, and the glycoproteins E1 and E2 (7). The structural proteins combine with the genomic RNA to form virus particles (8). The virus particles become enveloped during their exit from the host cell via budding (mosquito cells) or lysis (mammalian cells), forming a mature virion (9).

for transcription of the subgenomic RNA species as well as for many more copies of the genomic RNA. Translation of the subgenomic RNA yields the structural proteins. A mature virion is composed of a genomic copy of the viral RNA and the structural proteins.

4. Non-structural proteins. The four non-structural proteins (nsPs) are translated as polyproteins, either P123 or P1234. P1234 is the result of a leaky opal stop codon located at the end of the nsP3 open reading frame which allows for a small amount of nsP4 to be made (Hardy & Strauss, 1988; Li & Rice, 1989; Lopez *et al.*, 1985). Both cellular proteases and the viral encoded protease activity of nsP2 contribute to the cleavage events that produce the individual non-structural proteins, nsP1,2,3 and 4 (de Groot *et al.*, 1990; Hardy *et al.*, 1990; Hardy & Strauss, 1989; Shirako & Strauss, 1990; Hahn *et al.*, 1989b). Protease-deficient mutants are able to replicate in mammalian cells, albeit more slowly than wild-type virus, but are not viable in mosquito cells (Gorchakov *et al.*, 2008a).

Based on studies of temperature-sensitive mutants, nsP1 is required for the initiation of minus-strand synthesis (Hahn *et al.*, 1989b; Sawicki *et al.*, 1981; Wang *et al.*, 1991b). Additionally, nsP1 has methyltransferase and guanylyltransferase activity, and therefore plays an important role in the capping of viral RNAs (Ahola & Kaariainen, 1995; Mi *et al.*, 1989).

The RNA triphosphatase activity of nsP2 also aids in the process of capping Sindbis viral RNAs (Vasiljeva *et al.*, 2000). In addition, nsP2 plays a role in the following three viral functions. First, it possesses NTP-binding activity which allows the protein to function as a helicase. Second, it has protease activity to process the non-

structural polyprotein. Finally, it functions in the internal initiation of subgenomic RNA synthesis (Hahn *et al.*, 1989b; Sawicki & Sawicki, 1985; Gorbalenya *et al.*, 1988; Ding & Schlesinger, 1989).

In contrast to the well-defined roles of the other three nsPs, the role of nsP3 during Sindbis infection is poorly understood. Analysis of temperature-sensitive mutants demonstrates that the protein is required for RNA synthesis, both as part of an nsP23 polyprotein and in the cleaved individual form (De *et al.*, 2003; Hahn *et al.*, 1989b; LaStarza *et al.*, 1994b; LaStarza *et al.*, 1994a; Wang *et al.*, 1994). It has also been shown that cleavage of the non-structural polyprotein is more efficient when nsP3 is present (de Groot *et al.*, 1990). Finally, it was recently reported that nsP3 is an integral part of the Sindbis viral replication complex (Frolova *et al.*, 2006). Although these studies demonstrate the importance of nsP3, it is unclear the exact mechanistic role the protein plays in each of these processes.

The final nsP, nsP4, is the RNA-dependent RNA polymerase of Sindbis virus (Kamer & Argos, 1984). It has been recently purified and characterized *in vitro* (Rubach *et al.*, 2009). Several temperature-sensitive mutants of nsP4 have been shown to be RNA negative, in that they are unable to replicate at the non-permissive temperature (Hahn *et al.*, 1989a). One specific RNA-negative mutant of nsP4, ts6, is conditional lethal; it is active at the permissive temperature, but upon shifting to the non-permissive temperature the protein ceases to function. The loss of activity is due to a point mutation from guanine to adenine resulting in an amino acid change of a glycine to a glutamic acid (Burge & Pfefferkorn, 1966; Hahn *et al.*, 1989a). As will become evident, the ts6 mutated strain of Sindbis virus played a vital role in the study presented in this dissertation.

5. *Structural proteins.* The structural proteins are translated from the subgenomic RNA of Sindbis virus. Similar to the non-structural proteins, the structural proteins are first translated as a polyprotein and then cleaved to form the individual peptides. The capsid functions as an autocatalytic protease during translation, folding to form a serine-protease active site (Hahn *et al.*, 1985; Aliperti & Schlesinger, 1978). In this manner, the capsid protein is cleaved from the growing polyprotein. After synthesis is complete, final cleavage events occur and the produced glycoproteins, E1 and E2, are ready to be incorporated into the mature virion. The capsid protein binds the genomic RNA to initiate nucleocapsid formation, the virion then acquires the glycoproteins, and becomes enveloped upon exit from the cell via the plasma membrane (Geigenmuller-Gnirke *et al.*, 1993; Weiss *et al.*, 1989).

6. *Host cell specificity.* Alphaviruses (including Sindbis) have very different effects on cells from a vertebrate host (birds and mammals) versus cells from an invertebrate host (mosquitoes). Although the kinetics of virus replication are similar, virion release via exocytosis during infection in cells from an invertebrate host does not disrupt the integrity of the cell, whereas the virus causes lysis in cells from a vertebrate host during virion release (Karpf & Brown, 1998). In this way, alphaviruses induce chronic infections in invertebrates, but exhibit short, lytic infections in vertebrate hosts.

Various species of mosquitoes, including *Aedes albopictus*, *Aedes aegypti* and *Culex pipiens* have been shown to transmit Sindbis virus (Dohm *et al.*, 1995). In addition, many cell lines have been shown to support Sindbis viral growth. Two widely used cell

lines in Sindbis studies are the C6/36 *Aedes albopictus* mosquito cell line and BHK-21 Baby Hamster Kidney mammalian cell line (Renz & Brown, 1976). Human cell lines have also been used in Sindbis viral studies. The human 293T cell line is an embryonic kidney cell line transformed by the T-antigen of the virus SV40 which supports robust growth of the virus (Wahlfors *et al.*, 2000). Interestingly, the few published studies conducted with the human cervical adenocarcinomas cell line (HeLa) show varying degrees of Sindbis viral growth (Wahlfors *et al.*, 2000; Snyder & Sreevalsan, 1974; Buckley, 1964; Li *et al.*, 1997; Ohno *et al.*, 1997; Unno *et al.*, 2005; Rosemond & Sreevalsan, 1973; Taylor *et al.*, 1955; Frothingham, 1955). Based on these studies, the viral growth kinetics of the virus in HeLa cells are unclear.

IV. THE CROSSROADS OF VIRUSES AND MRNA DECAY

The collective studies concerning viruses and mRNA decay-associated factors are wide ranging in relation to the viruses they address, however the field as a whole remains greatly understudied. The information presented in this section will summarize what is known to date. In addition, it will put forth a number of indications that the interface of viral RNAs with the host cell decay factors is integral to completely understanding the biology of the viruses we study.

1. mRNA decay machinery as a possible antiviral.

a. Interferon-stimulated RNA decay. The 2-5A oligo-adenylate synthetase/RNase L decay pathway was the first described interferon-stimulated RNA decay mechanism. RNase L is an endonuclease that promotes the cleavage of both viral

and cellular RNAs. The activation of the enzyme is the result of a complex series of events beginning with the recognition of viral RNAs. Depending on the virus, double-stranded RNAs can be recognized by the pattern recognition receptor TLR-3 (Toll-Like Receptor), or by either the RIG-I helicase (Retinoic Acid Inducible Gene I) or the MDA5 helicase (Melanoma-Differentiation-Associated Gene 5) (Kato *et al.*, 2006; Yoneyama *et al.*, 2004; Kang *et al.*, 2002; Rothenfusser *et al.*, 2005; Alexopoulou *et al.*, 2001; Matsumoto *et al.*, 2002). Recognition of single-stranded viral RNAs is through the related pattern recognition receptors TLR 7 and 8 (Lund *et al.*, 2004). Through a signaling cascade, viral recognition by any of the above listed methods leads to induction of type-1 interferon (IFN). IFN is a potent transcription factor and induces the expression of the 2-5A oligo-adenylate synthetase (OAS), as well as many other IFN-stimulated genes (ISGs) (Rutherford *et al.*, 1988). OAS, also a pathogen recognition receptor, is activated directly by the dsRNA and synthesizes small 2-5A oligonucleotides from ATP (Hovanessian *et al.*, 1977; Kerr *et al.*, 1979; Kerr *et al.*, 1977; Roberts *et al.*, 1976). Cytoplasmic RNase L which is constitutively dormant, is subsequently activated by these small 2-5A oligonucleotides and is then able to cleave any single-stranded portions of RNA (Floyd-Smith *et al.*, 1981; Wreschner *et al.*, 1981; Zhou *et al.*, 1993). The remaining segments of the RNA are then rapidly degraded (Kubota *et al.*, 2004; Silverman *et al.*, 1981). In this manner both viral RNAs and cellular RNAs are cleaved, leading to inhibition of both viral and cellular protein synthesis, and eventually apoptosis of the infected cell (Zhou *et al.*, 1998; Castelli *et al.*, 1998).

The second, more recently described IFN-stimulated RNA decay mechanism is the ISG20 (IFN-Stimulated Gene 20) pathway. ISG20 is a 3' to 5'

exonuclease with specificity for ssRNA, and to a lesser extent for DNA (Gongora *et al.*, 1997; Nguyen *et al.*, 2001). Although the pathway is not fully characterized, the 3' to 5' exonuclease activity of ISG20 does confer cellular resistance to some RNA viruses, including alphaviruses (Espert *et al.*, 2003; Espert *et al.*, 2005; Zhang *et al.*, 2007; Jiang *et al.*, 2008).

b. RNA Interference. Small interfering RNAs (siRNAs) are short non-coding RNAs which were originally presumed to be cellular by-products, but have since been found to be potent regulators of gene expression. siRNAs work in a sequence-specific manner to post-transcriptionally silence gene expression (Fire *et al.*, 1998). Additionally, siRNAs have also been exploited extensively as a research tool for silencing gene expression (Lehner *et al.*, 2004). The RNAi pathway and its potential role as an antiviral are discussed here.

As diagramed in Figure 4, the mammalian siRNA-mediated decay pathway begins with the cleavage of double-stranded RNAs (dsRNAs) into short 21-22 nucleotide siRNAs by the RNase III-like endonuclease Dicer (Bernstein *et al.*, 2001; Zamore *et al.*, 2000; Elbashir *et al.*, 2001). The double-stranded siRNAs are then loaded into an RNA-induced silencing complex (RISC) (Matranga *et al.*, 2005). The components of the mammalian RISC include Argonaute 2 (Ago2), Dicer, and the accessory proteins TRBP, PACT and RHA (Chendrimada *et al.*, 2005; Haase *et al.*, 2005; Lee *et al.*, 2006; Robb & Rana, 2007; MacRae *et al.*, 2008). The cleavage enzyme Ago2 then clips and releases the passenger strand, which is subsequently degraded, leaving the remaining strand as a guide within the RISC (Matranga *et al.*, 2005). The complex locates its target mRNA based on the sequence of the guide strand, and if the sequence is a perfect match,

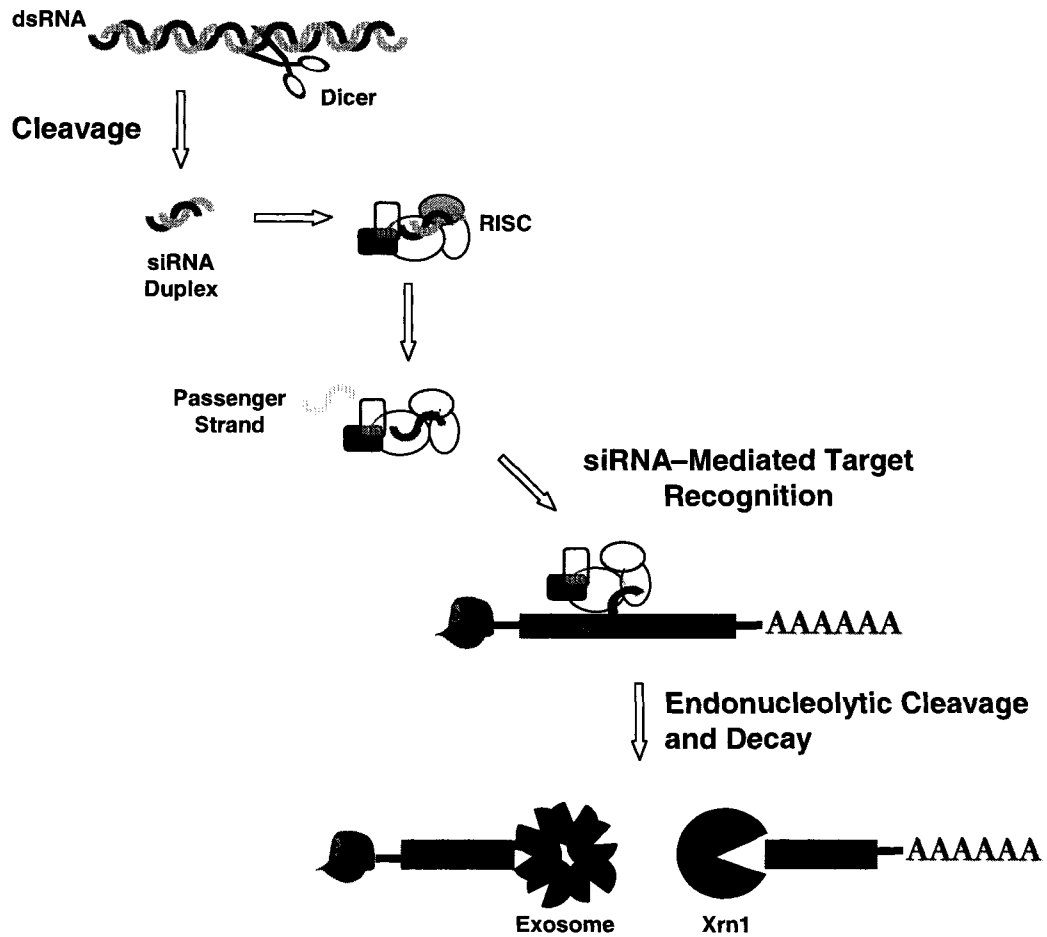


Figure 4 | RNA interference-mediated RNA decay (RNAi). Double stranded RNAs (dsRNA) are recognized by the endonuclease Dicer which cleaves the dsRNA into small interfering RNA (siRNA) duplexes. These siRNA duplexes are incorporated into the RNA Induced Silencing Complex (RISC), which is activated by the release and subsequent cleavage of the passenger strand of the duplex leaving the remaining strand as a guide. Based on the sequence of the guide siRNA, the activated RISC can target and degrade an mRNA with the complimentary sequence.

mRNA cleavage of the target transcript is catalyzed by the PIWI domain of Ago2 (Liu *et al.*, 2004).

Decay of the body of the RNA in mammalian cells is likely carried out by Xrn1 and the exosome, as was shown to occur in *Drosophila melanogaster* (Orban & Izaurralde, 2005). Additionally, a partial match with the target mRNA leads to inhibition of translation (Doench *et al.*, 2003). The end result of RNAi is silencing of the target mRNA which inhibits the expression of that gene.

The lifecycles of all RNA viruses contain potential dsRNA intermediates. Additionally, the secondary structure of viral RNAs could also be recognized as double-stranded. For this reason, siRNAs have been studied extensively in the context of host cell antiviral responses. Evidence to support the role of RNAi as an antiviral is best found in studies that document the viral suppression of the process and also in studies that use siRNAs to confer protection against infection. The Flock house virus and the related nodamura virus both encode the B2 protein. The B2 protein has been shown to prevent RNAi from acting on the viral RNAs during infection (Johnson *et al.*, 2004; Li *et al.*, 2002a). The mechanism of action of the viral B2 protein is through both non-specific binding of dsRNAs and by an interaction with Dicer through the PAZ domain (Singh *et al.*, 2009; Chao *et al.*, 2005). Three other viral associated inhibitors of RNAi include the VA1 RNA of adenovirus which binds and inhibits the function of Dicer *in vitro*, the E3L protein of vaccinia virus which sequesters dsRNAs, and the NS1 protein of influenza A virus which is presumed to function by binding the siRNAs directly (Li *et al.*, 2004; Lu & Cullen, 2004). Interestingly, although RNAi is well-accepted to be a potent antiviral pathway in insects, it is less understood how effective it is in mammalian hosts. Only a

limited amount of mammalian studies demonstrate the success of RNAi as a potential antiviral (Gitlin *et al.*, 2002; Kahana *et al.*, 2004; Ge *et al.*, 2003; Hui *et al.*, 2004; Wang *et al.*, 2004; Liu *et al.*, 2008).

c. Zinc-finger antiviral protein (ZAP). ZAP, like the cellular mRNA stability factor TTP, is a CCCH-type zinc finger protein. ZAP has been tested on a wide range of viruses, and has been found to inhibit infection of many alphaviruses, including Sindbis virus (Bick *et al.*, 2003; Muller *et al.*, 2007; Guo *et al.*, 2004). Further work to determine the mechanism of action of ZAP found that the protein binds directly to viral RNA via its zinc-finger motifs (Guo *et al.*, 2004). Studies then showed that ZAP recruits the exosome to degrade the viral RNA (Guo *et al.*, 2007). Finally, ZAP has been recently shown to also interact with a cellular RNA helicase, and based on co-immunoprecipitation studies the authors speculate that these proteins along with the exosome form a tertiary complex necessary for degradation of viral RNAs (Chen *et al.*, 2008).

2. Viral induced cellular RNA decay. As obligate parasites, viruses must hijack cellular processes to promote viral replication. Down-regulating cellular gene expression during infection is advantageous to the virus for two reasons. First, it ensures that viral proteins are made with minimal competition for translational machinery and substrates, and second it prevents antiviral proteins from being produced, thus helping the virus to evade the immune response. Therefore, it is not surprising that many viruses have evolved a means for modulating gene expression. This can occur by a variety of

mechanisms including the blocking of cellular transcription, inhibiting mRNA processing and export, altering cellular translation machinery, and finally, by regulating the rate of mRNA decay, which is discussed here.

a. Viral encoded ribonucleases. Members of the α - and γ -herpesviruses have a highly evolved means of turning off host gene expression through regulation of mRNA decay. The prototypic α -herpesvirus, Herpes Simplex I, does so through the action of the virion host shut-off protein (Vhs). Vhs is an endonuclease that is encoded by the virus and packaged into mature virions (Kwong *et al.*, 1988; Smibert *et al.*, 1992; Read & Patterson, 2007). Upon entry into a host cell, Vhs is able to immediately mediate RNA decay. It has been speculated that Vhs requires a mammalian factor to fully decay cellular mRNAs. This is supported by studies in mammalian extracts that show higher activity of the nuclease compared to studies in yeast, and that activity in yeast can be restored by the addition of rabbit reticulocyte lysate (Doepker *et al.*, 2004). Additionally, partially purified Vhs does not exhibit the same activity as compared to that within rabbit reticulocyte lysate and also compared to the *in vivo* activity of the protein (Zelus *et al.*, 1996). Finally, sequence studies have shown that all α -herpesviruses contain a Vhs homologue that is able to regulate host cell gene expression by means of mRNA decay (Berthomme *et al.*, 1993).

Interestingly, the γ -herpesviruses, including Kaposi's sarcoma-associated herpesvirus (KSHV) and Epstein-Barr virus (EBV), also shut down host gene expression by inducing cellular RNA decay, but do not contain a Vhs homologue. The search for a candidate host shutoff protein in KSHV yielded SOX (shut-off and exonuclease protein), and the protein was shown to in fact be responsible for the decay of cellular mRNAs

(Glaunsinger *et al.*, 2005). Following this discovery, the EBV SOX homologue, BGLF5, was identified, and was determined to contain DNase activity in addition to host shut-off activity, which were found to be separate functions (Rowe *et al.*, 2007; Zuo *et al.*, 2008).

Finally, vaccinia virus, a member of the poxvirus family, has long been known to induce cellular mRNA degradation (Rice & Roberts, 1983). The viral proteins D9 and D10 were found to be responsible for the down regulation of gene expression. These proteins contain the *mutT* motif, a characteristic of proteins like the decapping protein Dcp2 which cleaves nucleoside diphosphates (Bessman *et al.*, 1996; Koonin, 1993). More recently, the D10 and the D9 proteins were demonstrated to in fact exhibit mRNA decapping activity due to the *mutT* motif which was shown to accelerate mRNA degradation (Parrish *et al.*, 2007; Parrish & Moss, 2007).

b. Unknown mechanisms of viral induced host shutoff. The non-structural protein 1 (Nsp1) of two coronaviruses, severe acute respiratory syndrome (SARS) and group 2 bat coronavirus, is critical to the viral induced suppression of host gene expression by mRNA degradation (Kamitani *et al.*, 2006; Tohya *et al.*, 2009). Additionally, the SARS Nsp1 protein has been shown to affect levels of type I interferon indicating it may play a role in virulence of the virus (Narayanan *et al.*, 2008). Suppression of host gene expression via mRNA decay has also been reported during infection with influenza virus, although the mechanistic details are unclear (Beloso *et al.*, 1992).

3. The interaction of viral RNAs with mRNA decay-associated factors. mRNA decay enzymes have the potential to create a hostile host cell environment for viral

replication, yet viral infections are successful. As reported above, several viruses induce degradation of host cell mRNAs; the question is how these viruses are able to selectively prevent decay of their own RNAs under these circumstances. Additionally, there are viruses that have been shown to actually prevent universal mRNA turnover, presumably to circumvent viral RNA decay. Under both these conditions, we assume that the virus must aim to protect its RNA from degradation. Studies beginning to examine this phenomenon hint at the possibility of the recruitment of host cell *trans*-factors to bind *cis*-elements on viral RNAs, thus protecting the transcripts.

a. Viruses that bind mRNA stability factors. The first way in which viruses could potentially inhibit degradation of viral RNAs is by binding known RNA stability factors. This binding, similar to what is observed for cellular mRNAs, is facilitated by specific RNA sequences such as those reported to be in flavivirus and alphavirus RNAs. The viral RNA of the flavivirus hepatitis C does not contain a poly(A) tail which lends an additional degree of vulnerability to the viral 3' end. So it is not surprising that the U-rich regions of the 3' UTR of the viral RNA have been shown to bind HuR (Spangberg *et al.*, 2000; Spangberg *et al.*, 1999). HuR is a well known stabilizer of mRNAs and through binding to the hepatitis C viral RNA it is postulated that HuR may mediate viral RNA stability (Spangberg *et al.*, 2000).

Two other flaviviruses that bind mRNA decay-associated factors are West Nile and Dengue virus. It was first observed that the cellular proteins TIA-1 and TIAR interacted with the stem-loop of the WNV minus strand to facilitate viral replication (Li *et al.*, 2002b). These proteins are known to regulate translational arrest during cellular stress by promoting the assembly of stress granules, foci of stalled translational

complexes which can regulate mRNA stability and translation (Gilks *et al.*, 2004; Kedersha *et al.*, 1999; Kedersha & Anderson, 2002). Therefore, the studies on the interaction of TIA-1 and TIAR with the WNV minus strand were followed by work to delineate the effect the binding was having on the cellular processes in which the proteins were involved. It was observed that the interaction of TIA-1 and TIAR with WNV, and also with Dengue virus, interfered with stress granule formation (Emara & Brinton, 2007). It is suggested that the deregulation of the stress granule formation may inhibit RNA decay and potentially prevents viral RNAs from being targeted as well, but this has yet to be directly shown.

In addition to flaviviruses, the alphavirus Sindbis has also been found to interact with stress granule associated factors. During infection, the Sindbis virus nsP3 protein co-localizes with the stress granule-associated proteins G3BP1 and 2. This co-localization alters the dispersed distribution of G3BP1 and 2 to more punctuate foci (Gorchakov *et al.*, 2008b). Although the implications of this are unclear, the authors speculate that nsP3 is involved in abrogating stress granule formation, thus modifying cellular translation and redirecting cellular resources to viral-specific production.

b. Host cell factors that bind and protect viral RNAs in vitro. The viral RNA of poliovirus lacks a 5' cap, imparting a greater need for protection from the host cell RNA turnover machinery. However, the 5' end of the viral RNA is not wholly unprotected. It contains a highly structured cloverleaf which has been observed to recruit the poly(rC) binding proteins 1 and 2 (Gamarnik & Andino, 1997). An *in vitro* study on this interaction suggests that the poly(rC) proteins block the 5'-3' exonuclease Xrn1 from

acting on the viral RNA (Murray *et al.*, 2001). The authors propose that inhibiting the action of Xrn1 effectively stabilizes the viral RNA and thus prevents decay.

As mentioned earlier, the flavivirus Hepatitis C does not contain a poly(A) tail. The U-rich 3' UTR of the virus is a hot bed for RNA binding proteins. In addition to the binding of HuR to this region, the La protein has also been shown to interact with the viral RNA through the 3' UTR. Furthermore, the binding of La to the viral RNA has been demonstrated to stabilize the hepatitis C transcripts *in vitro*, but *in vivo* studies have not been performed to date (Spangberg *et al.*, 2001).

Finally, our laboratory has found that the non-templated poly(A) tract found at the 5' end of the viral RNA of vaccinia virus attracts the cytoplasmic heptameric complex of Lsm1-7 proteins to protect the RNA from decay (Bergman *et al.*, 2007). The Lsm1-7 complex normally functions in the binding of the 3' end of a deadenylated transcript, thereby inhibiting further shortening of the 3' end while promoting decapping and decay from the 5' end. In the case of vaccinia virus, the Lsm1-7 complex binds to the 5' poly(A) tract and it is hypothesized that a simultaneous interaction with the 3' end circularizes the transcript and hinders both branches of the deadenylation-dependent decay pathway, thus ensuring a productive infection.

RATIONALE

The genomes of positive-strand RNA viruses, such as Sindbis virus, look and function like cellular mRNAs in that they contain characteristics reminiscent of cellular mRNAs and that they are translated by the host cell translation machinery. The lifecycle of Sindbis virus is carried out exclusively in the cytoplasm, and it is there that cellular mRNAs are subjected to the highly regulated process of mRNA turnover. Although mRNA decay and positive-strand RNA virus biology are individually well-studied areas of research, the subject of viral RNA decay as a factor of viral growth is virtually uncharted. In order to have a thorough understanding of a virus, all viral-host interactions must be delineated. Therefore, the potential interface of the host cell RNA decay machinery with Sindbis viral RNAs was examined in this dissertation, with the hopes that a better understanding of the host interactions of positive-strand RNA viruses could become a foundation for the development of effective antiviral treatments.

MATERIALS AND METHODS

I. CELL LINES

1. BHK-21 (Baby hamster kidney, ATCC CCL-10) cells were obtained from Drs. Ken Olson and Carol Blair (Colorado State University) and grown at 37°C in complete medium [comprised of HyQ MEM/EBSS medium (HyClone) supplemented with 10% heat-inactivated fetal bovine serum (FBS; Atlanta Biologics), and 1% of each of the following: 100X non-essential amino acids (Cellgro), 100X (200 µM) L-glutamine (HyClone), and penicillin (10,000 µg/mL) /streptomycin (10,000 units/mL) (HyClone)]. A T-175 stock flask was maintained by splitting every 2 days. Briefly cells were washed with 1X phosphate buffered saline (PBS; HyClone), and treated with 1 mL 0.05% Trypsin-EDTA (Cellgro) diluted in 5 mL PBS for 1 minute, after which time the solution was removed and the cells sat for an additional minute at room temperature. Detached cells were then resuspended in 10 mL complete medium. To replenish the stock flask, 1 mL of the resuspension was diluted into 34 mL complete medium.

2. Vero (African green monkey, ATCC CCL-81) cells were also obtained from Drs. Ken Olson and Carol Blair (Colorado State University), and grown at 37°C in complete medium. A T-175 stock flask was maintained by splitting every 3-4 days. Briefly cells were washed with 1X PBS, and treated with 4 mL 0.05% Trypsin-EDTA (Cellgro) for 5 minutes, after which time the solution was removed and the cells sat for an additional 5 minutes at room temperature. Detached cells were then resuspended in 10

mL complete medium. To replenish the stock flask, 1 mL of the resuspension was diluted into 34 mL complete medium.

3. HeLa S3 (ATCC CCL-2.2) cells were grown at 37°C in complete medium. A T-175 stock flask was maintained by splitting every 3-4 days. Briefly cells were washed with 1X PBS, and treated with 2.5 mL 0.05% Trypsin-EDTA (Cellgro) diluted in 2.5 mL PBS for 5 minutes, after which time the solution was removed and the cells sat for an additional 5 minutes at room temperature. Detached cells were then resuspended in 10 mL complete medium. To replenish the stock flask, 1 mL of the resuspension was diluted into 34 mL complete medium.

4. C6/36 (Adherent *Aedes albopictus*, ATCC CRL-1660; (Igarashi, 1978)) cells were grown at 28°C in complete medium. A T-175 stock flask was maintained by splitting every 2-3 days. Briefly, the medium is removed and cells were scraped into 10 mL of fresh complete medium. To replenish the stock flask, 1 mL of the resuspension was diluted into 34 mL complete medium.

5. 293T (ATCC CRL-11268) cells were grown at 37°C in complete medium. A T-175 stock flask was maintained by splitting every 2-3 days. Briefly cells were washed with 1X PBS, and treated with 2.5 mL 0.05% Trypsin-EDTA (Cellgro) diluted in 2.5 mL PBS for 5 minutes, after which time the solution was removed and the cells sat for an additional 1-2 minutes at room temperature. Detached cells were then resuspended in 10

mL complete medium. To replenish the stock flask, 1 mL of the resuspension was diluted into 34 mL complete medium.

6. HeLa S3 Knock Down Cells

Stable Cell Lines. The Upf1 and Dicer knock down cell lines were acquired from Emily Chaskey. The stable cell lines were made using lentivirus constructs expressing shRNAs against the protein of interest (Sigma-Aldrich). Single colonies were selected using two independent shRNAs per protein. For Dicer, the shRNAs used were TRCN0000051262 and TCRN0000051261. For Upf1, the shRNAs used were TRCN0000022254 and TCRN0000022257. The cells were maintained in complete medium supplemented with 1 µg/mL Puromycin, and split as indicated for the wild-type HeLa S3 cell line. Knock down efficiency was determined by qRT-PCR using the primer sets listed below.

DicerB L- 5'TTG GCT TCC TCC TGG TTA TG, R- 5'CAC ATC AGG CTC
TCC TCC TC (Product size = 138 nucleotides, with a PCR efficiency of 98.8%).

Upf1 L- 5'CCC TCC AGA ATG GTG TCA CT, R- 5'CCT GTT CAG GTA
GGA GGT GC (Product size = 143 nucleotides, with a PCR efficiency of 114%).

Transient Knock Down Cells. Transient knock down cells were made by introducing siRNAs into the wild-type HeLa S3 cell line. To knock down Dcp2, the siGENOME SMARTpool from Thermo Scientific Dharmacon was utilized (sequences listed below). To knock down PARN, Xrn1 and Exo9, siRNA constructs were purchased from Invitrogen (sequences listed below). All siRNAs were transfected in the following

manner. On day 0, a confluent T-75 flask of HeLa cells was trypsinized and resuspended in 10 mL of complete media without antibiotics. For every well in a 12 well plate, 0.15 mL of cells were added to 0.85 mL complete media without antibiotics (scaled up to make a master mix for the total number of wells needed) and 1 mL of the cell mixture was aliquoted into each well. This equates to seeding approximately 1×10^4 cells per well of a 12-well plate. On day 1, the cells were approximately 50% confluent and were transfected as follows. Using a 1.5 mL tube, 3 μ L of 20 μ M stock of siRNA plus 125 μ L of OPTI-MEM (1X Reduced Serum Medium from Gibco) were mixed gently. In a separate 1.5 mL tube 2.5 μ L Lipofectamine RNAiMAX (Invitrogen) and 125 μ L of OPTI-MEM were mixed gently. The contents of the second tube were added to the first tube containing the siRNA mix. The mixture was gently mixed and was incubated for 20 minutes at room temperature. All reactions were scaled up when multiple wells were needed per siRNA treatment. Following the incubation at room temperature, the mixture (255.5 μ L) was added to the designated well. The plates were rocked gently and returned to the 37°C to incubate until either collected to test knock down or used in a viral RNA half-life or viral growth curve experiment. Knock-downs were identified by qRT-PCR using the primer sets listed following the siRNA sequences.

siRNA sequences

Dcp2 SMARTpool: siRNA 1: GAA AUU GCC UUG UCA UAG A
siRNA 2: GAU AAG AGA CUU UGC UAA A
siRNA 3: GAA GAG AAA UUC GGA ACA U
siRNA 4: GGA AAC UUC AGG AUA AUU U

PARN Stealth RNAi: siRNA 2: AAA GAA CCU AGG UAA UUG GCC AUG G

siRNA 3: AUC AAU UUA GUA UCC AAG AGU CUG G

Xrn1 Stealth RNAi: siRNA 2: AAA CAG GGA UUU CAU UAG CAA UCU G
siRNA 3: AAA GUA UUG CAU CUU UCC AGA UCC C

Exo9 Stealth RNAi: siRNA 2: AAU GAC AUA AGG CCA CGA UUG CAG C
siRNA 3: GCA AAU ACG UGU AGA CCU ACA UUU A

Quantitative Real-Time PCR Primers

PARN: L-5'CAG CCC GAG CAA GTA AAG AT
R-5'CTC TTC CTG TTT TCT CCC CA
Product size = 99 nucleotides
PCR efficiency of 121.6%)

Dcp2 L: L-5'GAT GCA CTG TTC CTG CTG TG
R-5'TGA AAA CAC ACT CGG ATT GC
Product size = 143 nucleotides
PCR efficiency of 120%

Exo9A: L-5'CGT GGC CTT ATG TCA TTT CC
R-5'ATG GGC ATG TGG TGG ATA CT
Product size = 114 nucleotides
PCR efficiency of 94.5%

XRNA: L-5'TCA GAA GTT GAC AGC CAT CG
R- 5'GTG ATT GAG GGG AAT GGT TG
Product size = 110 nucleotides
PCR efficiency of 112.5%

II. CELL EXTRACTS

C6/36 cytoplasmic S100 extracts (acquired from Kevin Sokoloski) and HeLa cytoplasmic S100 extracts (acquired from Dr. Hend Ibrahim) were prepared as described previously (Sokoloski *et al.*, 2007; Ford & Wilusz, 1999a; Opyrchal *et al.*, 2005). Briefly, cells were collected by centrifugation and washed in ice-cold PBS. The washed cells were suspended in 3 packed cell volumes of Buffer A (10 mM HEPES pH 7.9, 1.5 mM MgCl₂, 10 mM KCl, 1 mM DTT) and allowed to swell on ice for 10 minutes. Following a brief centrifugation, the swollen cells were resuspended in one volume of Buffer A and lysed by Dounce homogenization. The lysate was centrifuged at 2000 x g to remove nuclei and the supernatant was transferred to a fresh tube. The salt concentration was adjusted by addition of 0.11 volumes of Buffer B (300 mM HEPES pH 7.9, 30 mM MgCl₂, 1.4 mM KCl, 1 mM DTT) and the lysate was centrifuged at 100,000 x g for 1 hour. Glycerol was added to the supernatant to a final concentration of 20% and the aliquots were stored at the temperature of -80°C. The S100 extracts were stable at this temperature for several months.

III. VIRUS PREPARATION

1. VIRAL CDNA CLONES

a. pToto1101/wt and pToto1101/ts6. The AR339 Sindbis viral cDNA clone (pToto1101/ luc/wt) and the AR339 Sindbis viral cDNA clone with a temperature-sensitive point mutation at nucleotide 7879 in the original clone (pToto1101/ luc/ts6) were kindly provided by Dr. Margaret Macdonald (Rockefeller University, NY) (Bick *et al.*, 2003; Taylor *et al.*, 1955). The 1.6 kb luciferase fragment was excised out of both the

DNA Technologies) were ligated, the RNA was reverse transcribed using the “RT and PCR Primer for Linker-3”. The subsequent DNA was amplified with PCR using the “RT and PCR Primer for Linker-3” and either the “Primer for pToto/1101/ts6” specific to the wild-type virus or the “Primer for pToto/1101/ts6/Δ3’ UTR” specific to the mutant virus. Following PCR amplification, the PCR products were run on a 0.8% agarose gel, visualized with ethidium bromide, excised from the gel and then extracted. Finally, they were ligated into the pGEM T-easy vector (Promega), transformed into DH5α *Escherichia coli* cells, and plated for colony growth on LB-Ampicillin agar plates. Individual colonies were then selected and grown for mini-preparations of the plasmid DNA. The preps were screened for positive clones by digestion with NcoI (pToto/1101/ts6 yielded a 370 nucleotide band plus the length of the primer, the addition of the plasmid sequence, and the length of the poly(A) tail; pToto/1101/ts6/Δ3’ UTR yielded a 294 nucleotide band plus the length of the primer, the addition of the plasmid sequence, and the length of the poly(A) tail). The plasmid DNA of positive clones was PEG-precipitated to ensure purity and then sequenced through the Proteomics and Metabolomics Facility of Colorado State University.

RT and PCR Primer for Linker-3: CTG GAA TTC GCG GGT

Primer for pToto/1101/ts6: GGA CTT ATG ATT TTT GCT TGC AG

Primer for pToto/1101/ts6/Δ3’ UTR: GAA AGG AGC GGT GAC AGT CA

c. pToto/1101/ts6/3XRSE and pToto/1101/ts6/URE. These clones represent viral sequence either deleted of 40 nucleotides representing the URE within the viral 3’ UTR

or deleted of 240 nucleotides representing the 5' end of the viral 3' UTR containing the RSEs. They were made using a subclone from the pToto1101/ts6 vector and PCR-based site-directed mutagenesis (based on the ExSite Kit from Stratagene, although kit was not used). To subclone, the 3' end of the virus was selected by PCR amplification using primers to amplify the products that end with restriction sites specific to the pGEM-4 plasmid (Promega) multiple cloning site (5' Bam-SinV: CAT GGA TCC CGT ACG TCG AAT TGT CAG CA; 3' HinD-SinV: CAT AAG CTT CTT CAA GAA TTA ATT CCC CTC G). The PCR product and pGEM-4 plasmid were both digested with BamHI and HindIII and gel purified, and the vector was dephosphorylated with CIAP (Fisher, as per manufacturer's instructions). The insert was ligated into the digested vector, transformed into DH5 α *Escherichia coli* cells, and PCR screened for positive clones. Once a positive clone was identified, it was used as the starting point for the site-directed mutagenesis. Primers were designed to amplify in both directions away from the portion of the sequence wished to be deleted and the product was then kinased using T4 PNK (Fermentas) as per manufacturer's instruction. The kinase was then heat inactivated by incubating the reaction mixture at 65°C for 20 minutes. The 3xRSE denotes that that portion of the 3' UTR was kept and that the URE was deleted. Similarly, the URE notation represents the portion that was kept, with the 3xRSE portion deleted. The primers for the PCR are listed below.

3xRSE Downstream: 5' ATT TTG TTT TTA ACA TTT CAA AAA AAA AAA AAA
AAA AAA AAA AAA AAA AAA AAA AAG GGA ATT C
3xRSE Upstream: 5' TTA TGC AGA CGC TGC GTG GCA TTA TGC

URE Downstream: 5' CTT TTA TTA TTT CTT TTA TTA ATC AAC AAA ATT
TTG TTT TTA ACA TTT CAA AAA AAA AAA AAA AAA
AAA AAA AAA AAA AAA AAA AAG GGA ATT C

URE Upstream: 5' TCA TCT TCG TGT GCT AGT CAG CAT CAT GCT GC

The phosphorylated primers were then used in the following PCR reaction (5 ng SinV/pGEM, 1X PFU Buffer (Stratagene), 1 mM dNTPs, 15 pmol each kinased primer, 2.5U *pfu* DNA Polymerase (Stratagene), total volume 50 μ L with H₂O), under the conditions: 1 Cycle at 94°C for 4 minutes, 65°C for 2 minutes, 72°C for 6 minutes; 12 cycles at 94°C for 1 minute, 70°C for 2 minutes, 72°C for 6 minutes; 1 cycle at 72°C for 10 minutes; 4°C to complete and store. Following the PCR, the 50 μ L reaction was treated with 20U DpnI (20 U/ μ L) for 30 minutes at 37°C to digest away the methylated template, while leaving the un-methylated PCR product intact. Reaction products were recovered by phenol/chloroform extraction and ethanol precipitation, and resuspended in 100 μ L H₂O. 5 μ L of the solution was then used in a reaction to ligate the ends of the PCR product. The ligation was transformed into DH5 α *Escherichia coli* cells, PCR screened for positive clones, and positive clones were sequenced. The positive clones and the pToto1101/ts6 vector were digested with BsiWI and XhoI. The inserts were ligated into the digested vector, transformed using DH5 α *Escherichia coli* cells, PCR screened for positive clones, and positive clones were sequenced. The viral cDNAs were linearized with XhoI and used as templates for *in vitro* transcription with Sp6 RNA polymerase.

2. VIRAL STOCKS

All Sindbis viral stocks were produced by electroporation of transcription products into BHK-21 cells using a BTX EMC 630 apparatus (2 pulses at 400 LV, 800 Ω , and 25 μ F), 400 μ L cells at 1×10^7 cells/mL (BTX Model 620 2 mm Gap Cuvette). Virus present in the medium 24-48 hr later was harvested (stored as 1 mL aliquots at -80°C) and amplified by inoculating 1 mL virus plus 2 mL complete medium unto an 80% confluent T-75 flask of BHK-21 cells. Amplified virus (BHK-21 passage 1) was collected 24-48 hours post-infection (stored at -80°C) and plaque assays were performed on Vero cells to determine viral titers.

3. PLAQUE ASSAY

1. Preparation of cells. Using a confluent T-175 of Vero cells, the cells were split and resuspended into 12 mL complete medium. A mastermix containing 0.5 mL of cells and 24 mL of fresh media used was made and scaled up for each 12 well plate that was required. Each sample required 6 wells, and an extra plate was required for positive and negative control samples. The cells were mixed and 2 mL of the mix was seeded into each well. The assay was performed when the cells were confluent.

2. Preparation of virus dilutions and agar overlay. Using 48 well plates (6 samples per plate), 225 μ L complete medium were added to each well (8 wells per sample), 25 μ L of the virus sample was added to the first well in the series of 8, and mixed well by pipetting the sample up and down. 25 μ L of the diluted sample (dilution 10^{-1}) was then added to the next well (dilution 10^{-2}), and this was repeated until the dilution series was complete (all 8 wells).

For every 3 plates, 1 g agar was combined with 74 mL H₂O (Millipore) in a suitable sized bottle and autoclaved for 15 minutes using the liquid cycle. Once completed, the bottle was immediately placed into a pre-heated (44°C) water-bath to slow cool. Once cooled to approximately 50-60°C, the following pre-mixed solution was added and the final mix was well combined. To prevent precipitates from forming the components were added in the following order: 10 mL 10X Medium 199 (Sigma), 10 mL FBS (heat inactivated), 4 mL 7.5% Sodium Bicarbonate, 1 mL 2% DEAE-Dextran in Hanks BSS, 0.5 mL 100X EBM Vitamin Solution, 1 mL 50X EBM Amino Acids. The final mixture was returned to the water-bath until the overlay was complete.

3. Infection of cells. The 12 well plates containing a confluent monolayer of Vero cells were labeled to identify which samples were represented, and the medium was removed. 200 µL of each dilution sample in the dilution series was added to the respective well. The plates were rocked to gently cover the cells with the virus and the plates were incubated at 28°C for 1 hour, and rocked gently every 5-10 minutes.

4. Adding of Overlay. After the hour incubation, 2 mL of the overlay mixture were added to each well and the plates were gently swirled to combine the virus dilutions with the agar/nutrient mixture. The agar solution was prepared so that it reached the correct temperature of 44°C by the time the hour incubation was over.

5. Incubation. The plates were allowed to set at room temperature for 30 minutes to an hour. Once solidified, the plates were flipped upside down and incubated at 28°C for 5 days.

6. Assay of plaques. The plates were flipped right side up, and 200 µL of an MTT Solution (150 mg Thiazolyl Blue Tetrazolium Bromide (USB Corp.) in 50 mL Millipore

filtered water) was added to each well. The plates were rocked gently to ensure the solution covered the surface of the agar. The plates were then incubated at 37°C for 4-6 hours until plaques were easily visible. Plaques were counted, and the PFU/mL was calculated using the following equation:

$$PFU/mL = \# \text{ Plaques} \times 5^* \times \text{Dilution in Series}$$

Where: 5 represents the dilution number to account for the fact that only 0.2 mL of each virus dilution was added to each well, and in order to obtain the PFU/mL, we need to multiply by 5.

IV. PREPARATION OF RNA SUBSTRATES AND RNA PROBES

Unlabeled genomic RNA used in the electroporation of BHK-21 cells to generate virus was prepared by *in vitro* transcription from the linearized pToto viral clones described above. The reaction consisted of 2 µg template DNA, 1X Sp6 Transcription buffer (New England Biolabs), 1 mM rNTPs, 1 mM m⁷G(5)ppp(5')G Cap Analog, 1U RNase Inhibitor (1U/µL), 20U Sp6 RNA Polymerase (20U/µL), increasing the volume to 50 µL with RNase-free H₂O. The reaction was incubated at 37°C for 2 hours, treated with DNase I to remove the DNA template, followed by phenol/chloroform extraction and ethanol precipitation to recover the RNA. The RNA was resuspended in 50 µL H₂O. Slightly labeled genomic RNA used in the standard curve for the total and genomic qRT-PCR primers (described below) was made in a similar reaction with minor modifications in that no cap analog was used, and 1 µL of a 1/100 dilution of ³²P-labeled α-UTP (800

$\mu\text{Ci/mMol}$) was added in order to calculate the *fmol* in the final reaction based on the counts/minute.

Internally-labeled substrate and probe RNAs were prepared by *in vitro* transcription from linearized plasmid DNA templates and gel purified as previously described (Wilusz & Shenk, 1988). The deadenylated marker for the reporter RNA was transcribed from the pGem-4 plasmid (Promega) linearized with Hind III. A matched reporter RNA containing a poly(A) tail was kindly provided by Dr. Carol Wilusz. It was generated by inserting a 60 base adenylate stretch downstream of the Hind III site of pGem-4. Cleavage of the plasmid with NsiI and transcription using SP6 RNA polymerase generates a reporter RNA that contains a 60 base adenylate tract precisely at its 3' end.

A template for generating the SinV-3' UTR RNA was obtained by inserting a 319 nucleotide fragment representing the Sindbis viral 3' UTR between the Eco RI and PstI sites of reporter RNA described above. The insert was generated by PCR from a DNA clone containing the entire MRE-16 Sindbis virus genome (accession # U90536) obtained from Dr. Carol Blair (Colorado State University) using the primers 5' CGG AAT TCC CGC TAC GCC CCA ATG ACC CG and 5' GAA ATA TTA AAA ACA AAA TTA CTG CAG TTT. Cleavage of the plasmid with NsiI generated a template to create SinV-3' UTR RNA that contained a poly(A) tail.

A number of studies were performed using an isolated Sindbis virus RSE along with a series of mutant derivatives. Templates to generate the Sindbis virus RSE 3' sequence were obtained by annealing two DNA oligomers, 5' AAA ACT CAA TGT ATT TCT GAG GAA GCG TGG TGC AGA ATG CCA CGC and 5'-GCG TGG CAT TAT GCA CCA CGC TTC CTC AGA AAT ACA TTG AGT TTT and inserting the

fragment into the EcoRI - PstI sites of pGemA60. The six RSE 3 mutants were constructed in a similar fashion using the following oligonucleotides, the primer listed first is the upper portion of the construct and the primer listed second represents the lower portion of the construct (mutated bases are underlined):

Stemloop1: 5'-CTC AAT GTA TTT CTG AG
5'-CTC AGA AAT ACA TTG AG

mLoop1: 5' AAA ACT CAT ACA TAA ACT GAG GAA GCG TGG TGC AGA
ATG CCA CGC
5'-GCG TGG CAT TAT GCA CCA CGC TTC CTC AGT TTA TGT
ATG AGT TTT

mLoop2: 5' AAA ACT CAA TGT ATT TCT GAG GAA GCG TGG TCG TAT
TAG CCA CGC
5'-GCG TGG CTA ATA CGA CCA CGC TTC CTC AGA AAT ACA
TTG AGT TTT

mRegion1: 5'-AAA AGT GAA TGT ATT TCT GAG GAA GCG TGG TGC AGA
ATG CCA CGC
5'-GCG TGG CAT TAT GCA CCA CGC TTC CTC AGA AAT ACA
TTC ACT TTT

mRegion2: 5' AAA ACT CAA TGT ATT TCT CAC GAA GCG TGG TGC AGA
ATG CCA CGC
5'-GCG TGG CAT TAT GCA CCA CGC TTC GTG AGA AAT ACA
TTG AGT TTT

Rescue: 5'-AAA AGT GAA TGT ATT TCT CAC GAA GCG TGG TGC AGA
ATG CCA CGC
5'-GCG TGG CAT TAT GCA CCA CGC TTC GTG AGA AAT ACA
TTC ACT TTT

To generate a probe to detect Sindbis viral RNAs in the ribonuclease protection assay (RPA), the primers 5'-ATA GGA TCC CCG TGA CGA CCC GGT ATG AGG TAG A and 5'-CAT AAG CTT TTT GAG AAG CCA GCC CGT TGC G were used to amplify a DNA fragment that spanned the genomic/subgenomic junction of Sindbis virus. PCR products were cloned into the Bam HI – Hind III sites of pGem-4. Plasmids were linearized with BsrGI and transcribed using T7 RNA polymerase. To generate a probe for detecting the ribosomal protein S5 (RPS5) mRNA in RPA assays, the primers 5'-ATT ACA TCG CCG TCA AGG AG and 5'-TCT TGA TGG CGT ACG AGT TG were used to amplify cDNA obtained from C6/36 cells and inserted into the pGEM T-Easy vector (Promega). Plasmid DNA was cut with NcoI and transcribed using SP6 RNA polymerase to generate an RPS5-specific probe.

V. ONE-STEP VIRAL GROWTH CURVES

To measure viral fitness, one-step viral growth curves were used. Confluent monolayers were infected at a multiplicity of infection of 5 in complete growth medium. Following a 1 hour absorption at 28°C, the cells were washed twice with complete medium to remove any remaining extracellular virus, the plates were replenished with an exact amount of medium (1-5 mL depending on the plate size chosen), duplicate 35 µL aliquots were taken and stored at -80°C and the plates were incubated at 28°C for 2

hours. Following the 2 hour incubation, another round of 35 μ L aliquots were taken and stored, the cells were again washed twice with complete medium to remove extra-cellular virus, and replenished with the same volume of medium. This process was repeated such that aliquots were taken every 2 hours for 12 hours. The duplicate samples were then assayed in separate plaque titration to determine the amount of viable virus that was present at each time point, and the values were averaged. The growth curve was repeated a minimum of three times.

VI. *IN VIVO* VIRAL RNA DECAY ASSAY

To measure the *in vivo* half-lives of Sindbis viral RNAs, confluent monolayers were infected at a multiplicity of infection of 5 in complete growth medium. Following absorption at 28°C (1 hour), the cells were incubated at 28°C for 10 hours. Following the incubation, an equal volume (to original inoculum) of pre-warmed 52°C complete medium was added to each well. The cells were then shifted to the non-permissive temperature of 40°C and total RNA was extracted using the Trizol method (Invitrogen) at various time points following the shift to the non-permissive temperature. The quantity and identity of viral RNA in each time point was assayed using the methods below.

VII. ANALYSIS OF *IN VIVO* VIRAL RNA DECAY

1. Quantitative Reverse Transcription PCR (qRT-PCR). The qRT-PCR assay was used to detect the amount of viral RNA during infection in human cell lines. The total RNA sample was treated with DNase I (Fermentas) following the manufacturer's protocol. The RNA was then used in a reverse transcription reaction using ImProm-II

Reverse Transcriptase (Promega) following the manufacturer's instructions for the standard reverse transcription. Three separate cDNA preparations were made per sample in order to separately and specifically amplify the genomic RNA (G4R: 5' AAC CAC GCC TTT GTT TCA TC), the total RNA (5' CCT TTC ACG TGC AGA GGT TT) and random hexamer to amplify all RNA (used specifically as a template for the reference gene). Additional reactions were also set up in order to produce standard curves for each primer set. These reactions were made using uninfected total RNA, the primer of interest, and a known amount of *in vitro* transcribed genomic RNA described in part IV of this chapter.

The products from the reverse transcription of the total, genomic, and both the total and genomic standard curves were used as the template cDNAs in the following qRT-PCR assay: Mix 43.75 μ L iQ SYBR Green Supermix (Bio-Rad), 3.5 μ L upstream primer (2.5 μ M), 3.5 μ L downstream primer (2.5 μ M), and 29.75 μ L H₂O; Add 75 μ L of this mix to 6.7 μ L template cDNA. The reference gene control reaction was modified in that 29.75 μ L H₂O was used in the master-mix, and then 79.7 μ L of the mix was added to 2 μ L template cDNA. The reference standard curve reaction was modified in that 26.45 μ L H₂O was used in the master-mix, and then 71.7 μ L of the mix was added to 10 μ L template cDNA. Each sample (consisting of master-mix and template cDNA) was then aliquoted at 25 μ L per well in triplicate in a 96-well qRT-PCR plate. The negative control for each plate was a single reaction with cDNA from uninfected cells. All expression values were standardized by graphing the expression per sample to the standard curve of each primer set including the genomic (G4L: 5' CAT CGG TGA GAG ACC ACC TT; G4R: 5' AAC CAC GCC TTT GTT TCA TC; Product size 183 nucleotides), the total

RNA (T4L: 5'ACC AAA AAC GCA GGA GAA GA; T4R: 5'CCT TTC ACG TGC AGA GGT TT Product size 180 nucleotides) and the internal reference gene (Human GapDH R1: 5'AAT GAA GGG GTC ATT GAT GG; Human GapDH F1: 5'AAG GTG AAG GTC GGA GTC AA; Product size 108 nucleotides). In this way, the quantity of the subgenomic RNA was calculated by subtracting the quantity of the genomic RNA from the quantity of the total RNA. All values were normalized to the reference gene. The program for the qRT-PCR is: Step 1-95°C for 3 minutes, Step 2-95°C for 10 seconds, Step 3-60°C for 45 seconds (repeat to step 2 40x), Step 4-95°C for 1 minute, Step 5-60°C for 1 minute, Step 6-60°C for 10 seconds +0.5°C increments (repeat to step 5 80x), and all qRT-PCRs were completed using the Bio-Rad MyiQ iCycler and accompanying software.

2. RNase Protection Assay (RPA). The RPA was employed for the determination of the quantity of viral RNA in C6/36 and BHK-21 cells, using the Sindbis virus subgenomic junction RNA probe described in part IV of this chapter. Briefly, total RNA from each sample (0.1 µg and 5 µg for wild-type Sindbis viral RNA from infection in BHK-21 and C6/36 cells respectively, 2 µg for Δ3' UTR Sindbis viral RNA from infection in BHK-21 cells) was used in a hybridization reaction which included a 1X concentration of RPA Hybridization buffer (80% Deionized Formamide, 40 mM Pipes pH 6.4, 0.4 mM NaOAc, 1 mM EDTA pH 8.0), the radioactive probe (1,000,000 counts per minute for the Sindbis viral probe and 100,000 counts per minute for the loading controls), brought up to 10 µL with water. The mixture was subjected to the following protocol in a PCR machine that allows for a graded cooling: 95°C for 2 minutes, slow

cool at 1°C/second until the temperature of 45°C is reached; samples incubated at 45°C for a minimum of 6 hours. Following hybridization of the radioactive probes to the viral RNA and the internal loading control, the samples were treated with a combination of RNase T1 and RNase A to digest the single-stranded regions of the RNA-RNA hybrid. The digestion was carried out at 37°C for 1 hour in a 20 µL reaction that included 10 µg of tRNA and a concentration of 1X RPA Digestion buffer (10 mM Tris-HCL pH 7.5, 5 mM EDTA pH 8.0, and 200 mM NaOAc). Following digestion, the samples were phenol/chloroform treated and ethanol precipitated to recover the RNA. The protected RNAs were separated on a 5% polyacrylamide gel containing 7M urea and visualized using BioRad Molecular Imager FX or the GE Healthcare Typhoon Imager. RPS5 mRNA (for C6/36 cells) and 5S rRNA (for BHK-21 cells) were routinely detected to ensure the validity of all quantifications. Finally, RNA quantification was determined using BioRad Quantity One software or the GE Healthcare ImageQuant TL software, respectively.

3. Statistical Analysis of Viral RNA Half-Lives. To calculate the half-lives of viral RNAs, the slope of decay was determined from the equation of exponential trend line. To determine if differences in viral RNA half-lives were statistically significant, the Welch t-Test was employed to solve for the t value of the independent samples, and the Welch-Satterthwaite Equation was used to solve for the degrees of freedom of the samples. This information was used against the Student's t-distribution, and t values that exceeded the value listed for the solved degrees of freedom with a 95% confidence interval were considered significant.

a. Calculation of the half-life from the equation of the exponential trend line:

$$y = 100e^{-b}$$

Where:

$$y = 0.5 \text{ (50\% of the RNA remaining)}$$

b = the slope of the trend line

b. Welch's t-Test:

$$t = (X_1 - X_2) / \sqrt{[(s_1^2/n_1) + (s_2^2/n_2)]}$$

Where:

X_1 = Half-life under condition 1

X_2 = Half-life under condition 2

s_1 = Standard deviation of X_1 within sample size n_1

s_2 = Standard deviation of X_2 within sample size n_2

n_1 = Sample size for X_1

n_2 = Sample size for X_2

c. Welch-Satterthwaite Equation to solve for degrees of freedom (ν):

$$\nu = [(s_1^2/n_1) + (s_2^2/n_2)]^2 / [[(s_1^2/n_1)^2]/(n_1-1) + [(s_2^2/n_2)^2]/(n_2-1)]$$

Where:

s_1 = Standard deviation of X_1

s_2 = Standard deviation of X_2

n_1 = Sample size for X_1

n_2 = Sample size for X_2

VIII. ANALYSIS OF *IN VIVO* VIRAL POLY(A) TAIL LENGTHS

1. RNase H/Northern Blotting. This assay was used to assess the length of the poly(A) tails during infection and was performed as described by (Zangar *et al.*, 1995) with minor modifications. Briefly, total RNA samples from infected cell time courses described above were hybridized to a DNA oligonucleotide (5'- TAG TGT TGC TAT ATT GCC CGC) designed to anneal to the region of the Sindbis virus 3' UTR between RSE1 and RSE2 and treated with RNase H. The hybridization reaction was comprised of 1-10 μ g RNA, 1X RNase H buffer (supplied with enzyme, New England Biolabs), 0.5-1 μ g virus-specific oligo, 5-20U RNase H (New England Biolabs) and H₂O up to 10-20 μ L. The concentration of the components in the hybridization reaction depended on the cell line and the virus strain being examined. Additional reactions also included oligo(dT) to generate a marker for fully deadenylated viral RNAs, a sample without RNase H as an undigested control, uninfected RNA as negative control and *in vitro* transcribed genomic RNA as a positive control. Reaction products were separated on a 5% denaturing acrylamide gel. The resolved products were electro-blotted from the gel to a nitrocellulose membrane using 1X TBE (one hour, at the constant Amp of 1, in a cold room of the temperature 4°C) The membrane was then pre-hybridized for 30 minutes in pre-hybridization buffer (2.5 mL 100X Denhardt's Solution (20g Polyvinyl Pyrrolidone, 20g Ficoll, 20g Bovine Serum Albumin in 1L of H₂O), 7 mL H₂O, 25 mL Formamide, 12.5 mL 20X SSC (3.0 M Sodium Chloride and 0.3 M Sodium Citrate), 2.5 mL 20% Sodium Dodecyl Sulfate (SDS), and 0.5 mL MB grade ssDNA (10 mg/mL- Roche)). The membrane was then probed with a Sindbis virus-specific probe as described in part IV of this chapter. Following three washes at 60°C which included two 50 mL less stringent

washes (45.5 mL H₂O, 5 mL 20X SSC and 0.25 mL 20% SDS), and one 50 mL stringent wash (49.25 mL H₂O, 0.5 mL 20X SSC and 0.25 mL 20X SDS), the RNA was visualized using the GE Healthcare Typhoon Imager, and poly(A) tail length was determined using the GE Healthcare ImageQuant TL software.

2. Linker Ligation-Mediated Poly(A) Tail Assay. This assay assesses the length of the poly(A) tail by ligation of a modified linker to the 3' end of all mRNAs within a total RNA sample, employing specific reverse transcription based on the linker, and finally using PCR amplification with a RNA-specific upstream primer and a linker-specific downstream primer. There are several steps to this assay, all of which are described in detail here.

To make an A₀ marker, 1 µg RNA (at 1 µg/µL) was combined with 1 µL 10X RNase H Digestion Buffer (supplied with enzyme-New England Biolabs), 2 µL oligo dT₂₆, 2 µL RNase H (5,000 U/mL, New England Biolabs), and H₂O up to 10 µL. The reaction was incubated for 45 minutes at 37°C, the volume was brought up to 100 µL with water, and then the digested product was recovered by phenol/chloroform extraction and ethanol precipitation. The A₀ marker RNA pellet (not easily visible) was resuspended in linker/ligation mixture described below replacing the 1µg RNA with a 1 µL volume of water.

To ligate the linker to the RNA samples or to resuspend the A₀ marker, 1 µg RNA (at 1 µg/µL) or 1 µL H₂O for the A₀ marker was combined with 1 µL of the 5'adenylated and 3'dideoxy C Linker-3 RNA (5'rApp-TTT AAC CGC GAA TTC CAG-ddC, Integrated DNA Technologies, stock 10 µM), 1 µL 10X Ligase buffer (50 mM Tris-Cl

pH 7.5, 10 mM MgCl₂, 20 mM DTT, 0.1 mg/ml BSA), 1 μL T4 RNA Ligase (20,000 U/mL, New England Biolabs), 1 μL RNase Inhibitor (40 U/ μL) and H₂O up to 10 μL. The reactions were incubated at 16°C for at least 2 hours. Following incubation, the volume of each reaction was brought up to 100 μL with H₂O, the samples were phenol/chloroform treated and ethanol precipitated (using 1 μL glycogen per reaction aided in the precipitation and the visualization of the subsequent RNA pellet).

To reverse transcribe the samples, the RNA pellets were resuspended in a mix of 1 μL (50uM stock) linker-specific primer (PAT-RT: 5' CTG GAA TTC GCG GGT) and 4 μL H₂O, and then reverse transcribed using Promega ImProm-II, as per manufacturers protocol. The resulting cDNA was then used as a template for PCR amplification using an upstream primer specific the viral strain (listed below) and a linker-specific downstream primer in a 50 μL reaction. The program used was as follows: Step 1- 95°C for 2 minutes, Step 2- 95°C for 30 seconds, Step 3- 45°C for 30 seconds, Step 4- 72°C for 30 seconds, Repeat to Step 2- 20X, 4°C hold. The products (10 μL) were run on a 5% native gel (1.5 mm thick) and visualized by soaking the gel in running buffer (1X TBE) and SYBR Green (at a dilution of 1 μL/10 mL for 10 minutes at room temperature and then scanning using the florescence setting (Blue Laser 520, 400 PMT) on the GE Healthcare Typhoon imager. Poly(A) tail length analysis was performed using the GE Healthcare ImageQuant TL software.

Primer for pToto/1101/ts6: GGA CTT ATG ATT TTT GCT TGC AG

Primer for pToto/1101/ts6/Δ3' UTR: GAA AGG AGC GGT GAC AGT CA

IX. ANALYSIS OF *IN VITRO* DEADENYLATION

Deadenylation assays using C6/36 and HeLa extracts were performed as described previously with minor modifications (Opyrchal *et al.*, 2005). A typical 27 μ L reaction mixture contained 100,000 CPM (5-40 fmol) of internally labeled RNA, 2.4% polyvinyl alcohol, 17.5 mM phosphocreatine, 0.7 mM ATP, 25 ng/ μ L poly(A) (Sigma), 20U RNase Inhibitor and 60% S100 C6/36 or HeLa cell cytoplasmic extracts. Reaction mixtures were incubated at 28°C (mosquito) and 37°C (mammalian) for the indicated times. Reaction products were recovered by phenol/chloroform extraction and ethanol precipitation, separated on a 5% polyacrylamide gel containing 7M urea, and visualized using a BioRad Molecular Imager FX or the GE Healthcare Typhoon Imager. Results were quantified by assessing the relative level of fully deadenylated RNA versus the total RNA in the sample using Quantity One software or the GE Healthcare ImageQuant TL software, respectively.

RESULTS

I. THE EFFICIENCY OF SINDBIS VIRUS REPLICATION IN HUMAN CELLS IS ASSOCIATED WITH RELATIVE VIRAL RNA STABILITY

Sindbis virus displays different replication rates in human cell lines.

Published studies on Sindbis virus replication in human cells are conflicting in their results. While the virus grows very well in the 293T human embryonic kidney cell line (Wahlfors *et al.*, 2000), it grows variably in the HeLa human cervical cancer cell line (Wahlfors *et al.*, 2000; Snyder & Sreevalsan, 1974; Buckley, 1964; Li *et al.*, 1997; Ohno *et al.*, 1997; Unno *et al.*, 2005; Rosemond & Sreevalsan, 1973; Buckley, 1964; Taylor *et al.*, 1955; Frothingham, 1955). To determine the efficiency of Sindbis virus replication in these two human cell lines in our hands, one-step viral growth curve analyses were performed. This assay requires an absorption period of one hour followed by a change of medium. A sample of the medium is then collected every subsequent two hours followed by a change of medium. The samples are then subjected to a plaque titration assay to determine the quantity of mature virions that are released from the infected cells over a twelve hour time course.

As seen in panel A of Figure 5, our data show that through the first eight hours post-infection the production of mature virions of Sindbis virus in both cell lines remained at base line. By ten hours post-infection however, there is almost a two log difference in growth, and it becomes clear the virus replicates much better in 293T cells compared to HeLa cells. To further exemplify this difference, Sindbis virus in 293T cells exhibited a ~51.5-fold increase over starting titer at twelve hours post-infection while

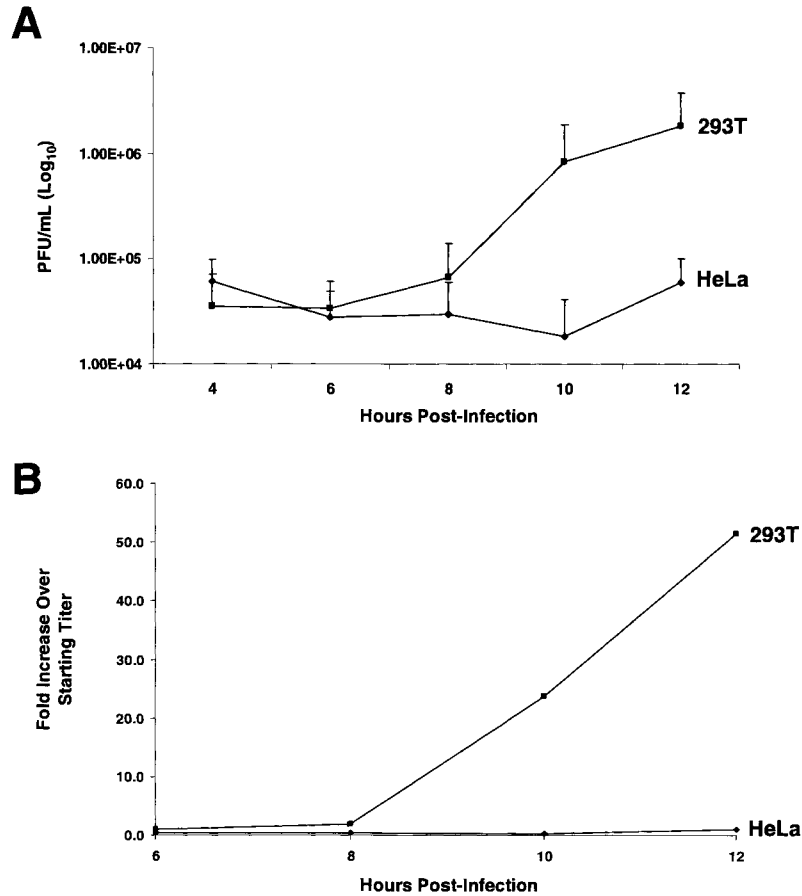


Figure 5 | Sindbis virus grows exponentially in 293T cells, but maintains only a basal level of infection in HeLa cells. A | In a one-step viral growth curve experiment, 293T cells and HeLa cells were inoculated with Sindbis virus and the production of mature virions, as measured by plaque titration on Vero cells, was plotted over the time course indicated. **B |** The titer of the sample at four hours post-infection was used as the starting titer to which the titers of subsequent time points were compared. Fold increases were graphically plotted over the time course indicated.

there was no appreciable increase in Sindbis virus production from the starting titer in the HeLa cells (Figure 5, panel B).

The results from Figure 5 demonstrate that the growth of Sindbis virus in 293T cells is consistent with that reported in the literature; 293T cells are exceptional hosts as Sindbis viral growth is exponential (Wahlfors *et al.*, 2000). Interestingly, in our hands HeLa cells only support a basal level of Sindbis virus infection, which is consistent with a selection of the published reports on HeLa cells (Rosemond & Sreevalsan, 1973; Frothingham, 1955; Taylor *et al.*, 1955). These results demonstrate that Sindbis virus replication in human cells depends on the cell type of the host, and that HeLa cells potentially contain host cell restriction factors which prevent successful Sindbis viral replication.

Development of an *in vivo* viral RNA decay assay.

Factors known to date to be responsible for host cell restriction against Sindbis virus include cell receptors, pH level, cholesterol content of host membranes, expression levels of the anti-apoptotic protein Bcl-2 and haplotype of the major histocompatibility complex I (Smit *et al.*, 1999; Wang *et al.*, 1991a; Lu *et al.*, 1999; Jan *et al.*, 1999; Ubol *et al.*, 1994; Hahn *et al.*, 1999). Despite this extensive knowledge, no one has examined the role of mRNA decay as a potential restriction mechanism, and furthermore, there are no reports on the mechanism of host cell restriction for Sindbis virus in HeLa cells.

Therefore, we were interested in determining if the difference in the one-step viral growth curve results presented in Figure 5 could be attributed to differences in viral RNA decay in 293T cells versus HeLa cells. Specifically, we hypothesized that the viral RNAs would

be targeted for decay in HeLa cells, but not in 293T cells, thus demonstrating a novel host cell restriction factor against Sindbis virus.

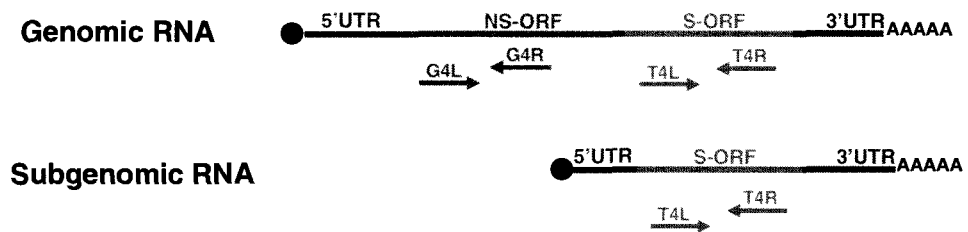
To address this question, an assay was required that would allow us to specifically monitor the rate of viral RNA decay during infection. To do this, viral RNA synthesis had to first be shut down—giving the assay a starting point for following viral RNA decay over time. Traditionally, universal transcription inhibitors are used to turn off RNA production to measure transcript stability (Ross, 1995), but these were undesirable to us for two reasons. First, we wanted to specifically turn off viral synthesis without affecting the host cell transcription machinery, thereby minimizing off-target effects of the assay. Second, inhibitors of DNA-dependent RNA polymerases have shown only variable efficacy on the Sindbis viral RNA-dependent RNA polymerases (Condreay *et al.*, 1988). Therefore, we chose instead to make use of the temperature-sensitive 6 Sindbis viral strain (ts6) that has a conditional lethal mutation in the nsP4 gene of the virus (the RNA-dependent RNA polymerase) (Bick *et al.*, 2003; Burge & Pfefferkorn, 1966; Hahn *et al.*, 1989a). When the cells infected by the ts6 strain of Sindbis virus are shifted to the non-permissive temperature, the nsP4 protein is unable to function and viral RNA synthesis ceases.

Therefore, we can infect host cells using the Sindbis virus ts6 strain and then confidently turn off viral RNA synthesis by shifting the cells from the permissive temperature of 28°C to the non-permissive temperature of 40°C. Following shutoff, total RNA samples are collected, and the half-life of the viral RNA is analyzed by quantitative Reverse Transcription PCR (qRT-PCR) or an RNase-Protection Assay (RPA). As development of the *in vivo* viral RNA decay assay progressed however, we came to a

critical obstacle in our analysis using both qRT-PCR and the RPA; We needed to differentiate between the genomic and subgenomic RNAs of Sindbis virus. The subgenomic RNA is identical to the 3' end of the genomic RNA. Therefore, any probe used to quantify the subgenomic would also detect the genomic. It was critical to distinguish between the viral RNA species as they have very different roles in the Sindbis viral lifecycle. While the subgenomic RNA is translated, the genomic RNA is involved in replication and packaging in addition to being a substrate of the translation machinery. This indicates that the mRNP structure of the genomic RNA is likely vastly different from that of the subgenomic RNA, which could affect the rate of viral RNA decay from one viral RNA species to the next.

For the qRT-PCR analysis (Figure 6, panel B), we transcribed three separate cDNA pools for each sample, using three separate primers; The G4R primer which is specific only to the genomic RNA, the T4R primer that would bind both the genomic and the subgenomic RNA, and finally the third pool was primed using random hexamer in order to detect the internal reference gene GapDH. These independent cDNAs were then used as templates for amplification in the qRT-PCR reaction. Importantly, each set was amplified with a primer set specific to the cDNA made. For example the cDNA made from the genomic-only primer was then amplified with a complete primer set to only amplify the genomic RNA. By using standard dilutions of known *fmol* of viral RNA and also of cDNA which was primed by random hexamer, we could accurately calculate the exact quantity of the genomic RNA, of the total RNA (genomic plus subgenomic), and of the reference gene in each sample. A simple mathematical equation was then employed such that: Total RNA - Genomic RNA = Subgenomic RNA.

A Quantitative Reverse Transcription PCR



B RNase Protection Assay

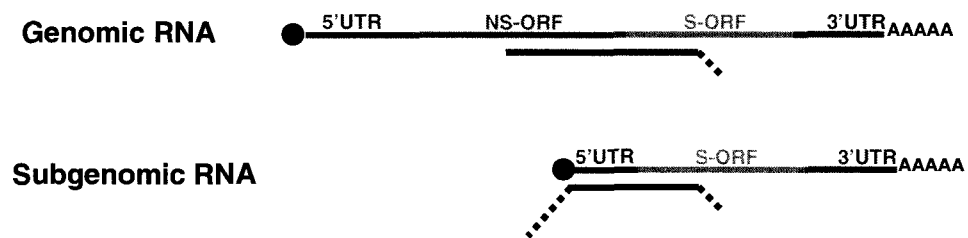


Figure 6 | Methods for distinguishing between the genomic and subgenomic RNAs of Sindbis virus. A | Quantitative Reverse Transcription PCR. A schematic representation of the viral RNAs is shown. The G4R primer is used to make a cDNA copy of the genomic RNA, and the T4R primer is used to make a cDNA copy of both the genomic and subgenomic RNAs. The cDNA pools are then amplified. Genomic cDNA is amplified using a primer set (orange) that binds only to the non-structural open reading frame (nsORF), and the subgenomic and genomic cDNA pool is amplified using a primer set (blue) that binds to the structural open reading frame (sORF). The total viral expression (T4 primer set) minus the genomic (G4 primer set) yields the quantity of the subgenomic RNA. B | RNase Protection Assay. A schematic representation of the viral RNAs and the radiolabeled probe which binds them (red). The probe is designed to bind at the genomic and subgenomic junction of the viral RNA. The genomic RNA protects a longer portion of the probe than the subgenomic RNA. The dotted line represents unprotected probe that is digested by the RNases.

Each sample was then normalized to the reference gene, and the quantity of viral RNA in time point zero was considered our starting amount. The amount of viral RNA in subsequent time points were divided the quantity measured at time point zero. Time point zero was set at 100% RNA remaining, and subsequent time point were then calculated as a percentage of that original 100%. The result was that we were able to accurately distinguish between the genomic and subgenomic viral RNA species in our calculation of the rate of viral RNA decay. To overcome this obstacle using RPA analysis, we designed a probe that bound to the genomic/subgenomic junction such that size of the protected RNA fragments would enable us to distinguish between the two RNAs following RNase digestion when using the RPA (Figure 6, panel B).

A caveat of this *in vivo* viral RNA decay assay is that the shutoff is very sensitive to temperature changes. At 37°C the shutoff is incomplete and viral RNA decay data will be inconclusive due to leaky RNA synthesis. Conversely, heating the cells to greater than 42°C will likely induce a heat shock response that could compromise the cellular processes such as mRNA turnover (Carvalho & Freitas, 1988). We found that 40°C is the optimum temperature for maintaining cell integrity and effectively shutting down viral RNA synthesis.

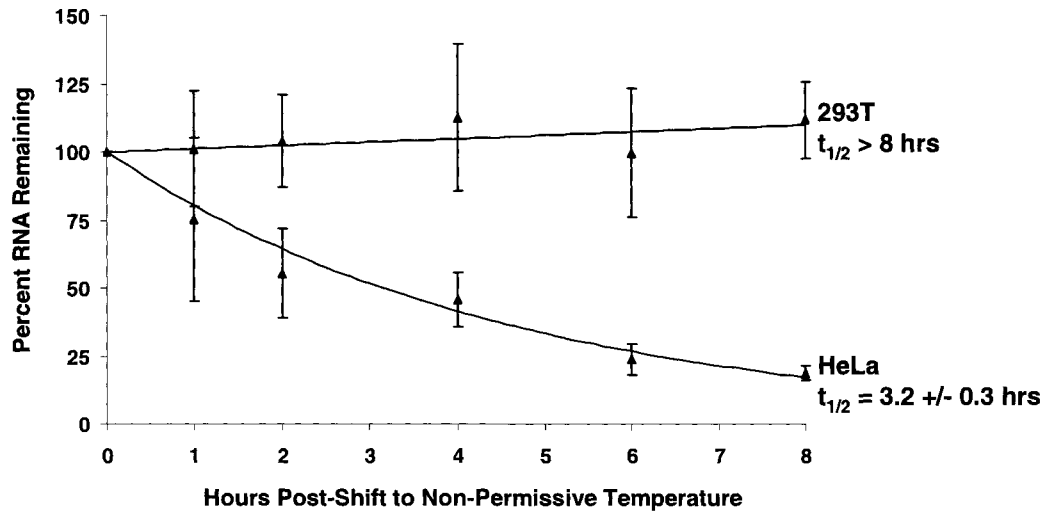
Finally, as will become evident, this assay was the cornerstone of the work presented in this dissertation. We were able to successfully use the *in vivo* viral RNA decay assay to determine the half-life of Sindbis viral RNAs in multiple cell types during infection, and to determine the contribution of prominent cellular mRNA decay factors to the viral RNA turnover.

Sindbis viral RNAs are exceptionally stable in 293T cells and are degraded very efficiently in HeLa cells.

The interface between viral RNAs and the host cell decay machinery could represent a novel host cell restriction mechanism if the viral RNAs are effectively targeted for decay in selected cell types. Therefore, we hypothesized that the decay rates of Sindbis viral RNAs would be significantly different during infection in HeLa cells versus infection in 293T cells. To address this hypothesis, we utilized the *in vivo* viral RNA decay assay described above and then analyzed the RNA samples by qRT-PCR.

As seen in Figure 7, panel A, the Sindbis viral genomic RNA was exceptionally stable in 293T cells, with a half-life that is much greater than 8 hours (the exact measurement was well beyond the time frame of these experiments). In strong contrast to the stability of the genomic RNA in 293T cells, is the rapid rate of genomic RNA turnover in HeLa cells with a calculated half-life of 3.2 +/- 0.3 hours (Figure 7, panel A). Similar to the genomic RNA half-life results, the results highlighted in Figure 7, panel B show the subgenomic RNA of Sindbis virus was also very stable in 293T cells and does not decay over the eight hour time course examined. Conversely, the rate of subgenomic viral RNA decay in HeLa cells was much faster, with a half-life of 2.3 +/- 0.2 hours. These results demonstrate that the RNA decay machinery in HeLa cells is able to target and degrade Sindbis viral RNAs at a much higher rate than the RNA decay machinery in 293T cells. When the biological differences in viral growth are taken into consideration (Figure 5), these data support a potential role for the rate of viral RNA decay in the ability of a virus to successfully replicate in host cells.

A Genomic RNA



B Subgenomic RNA

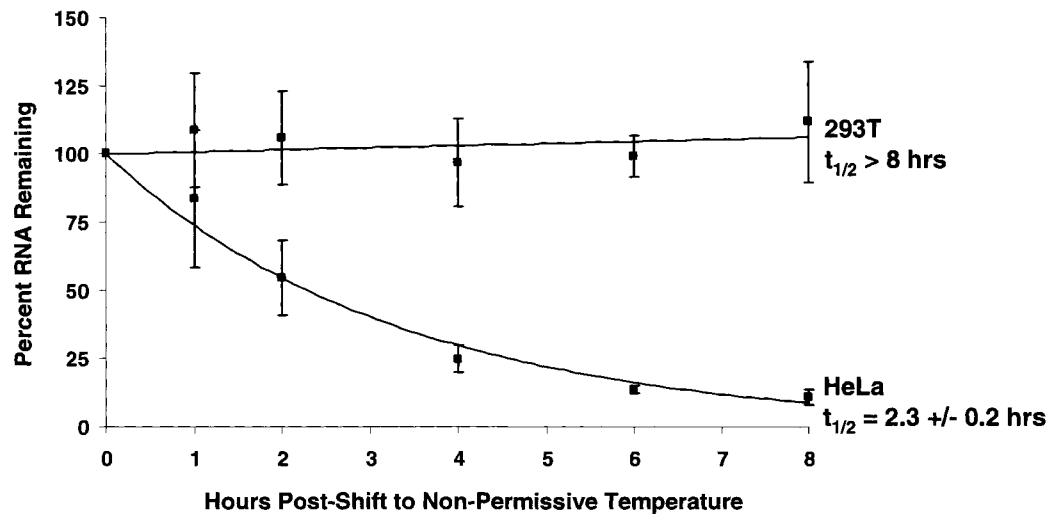


Figure 7 | Sindbis viral RNAs show dramatically different stabilities in the 293T versus HeLa human cell lines. Cells were inoculated with a temperature-sensitive strain of Sindbis virus (ts6), and at ten hours post-infection, cells were shifted to the non-permissive temperature of 40°C to shut off viral synthesis. Total RNA samples were taken at the time points indicated and the RNA was subjected to analysis by qRT-PCR. A | Analysis of Genomic RNA. B | Analysis of subgenomic RNA.

The Exo9 and Xrn1 proteins contribute to viral RNA turnover.

A thorough understanding of the interactions between Sindbis virus and the host cell is imperative to fully understanding the biology of the virus. The next logical step in the analysis of Sindbis viral RNA decay was to establish if the major RNA turnover pathway in mammalian cells—deadenylation-dependent decay—was responsible for the rapid degradation of the viral RNAs during infection in HeLa cells. The deadenylation-dependent decay pathway as depicted in panel A of Figure 8, depicts the four major steps in this process: deadenylation, decapping, 5' to 3' exonucleolytic decay, and 3' to 5' exonucleolytic decay. It is important to note the redundancy that is built into this cellular mRNA turnover pathway. This is exemplified by the existence of multiple deadenylases in the cell, including PARN, Ccr4 and Caf1, and Pan2-Pan3 that are able to catalyze the first and rate-limiting step of the reaction, which is shortening of the poly(A) tail.

In order to evaluate the enzymatic activity of the proteins that work within this pathway, siRNAs were used to transiently target the mRNAs of selected enzymes that contribute to the four major steps in this decay process as listed above (Δ denotes knock down). As highlighted in panel A of Figure B, deadenylation was addressed by silencing PARN, one of the major deadenylases of the cell. The 3' to 5' exonucleolytic decay was targeted by knocking down the expression of exosome component 9 (Exo9), a protein that is part of the core of the multi-component complex the exosome. The decapping process was targeted by silencing expression of the decapping protein 2 (Dcp2), which represents the enzymatic protein responsible for decapping. Finally 5' to 3' exonucleolytic decay was addressed by knocking down the major cytoplasmic 5' to 3' exonuclease Xrn1.

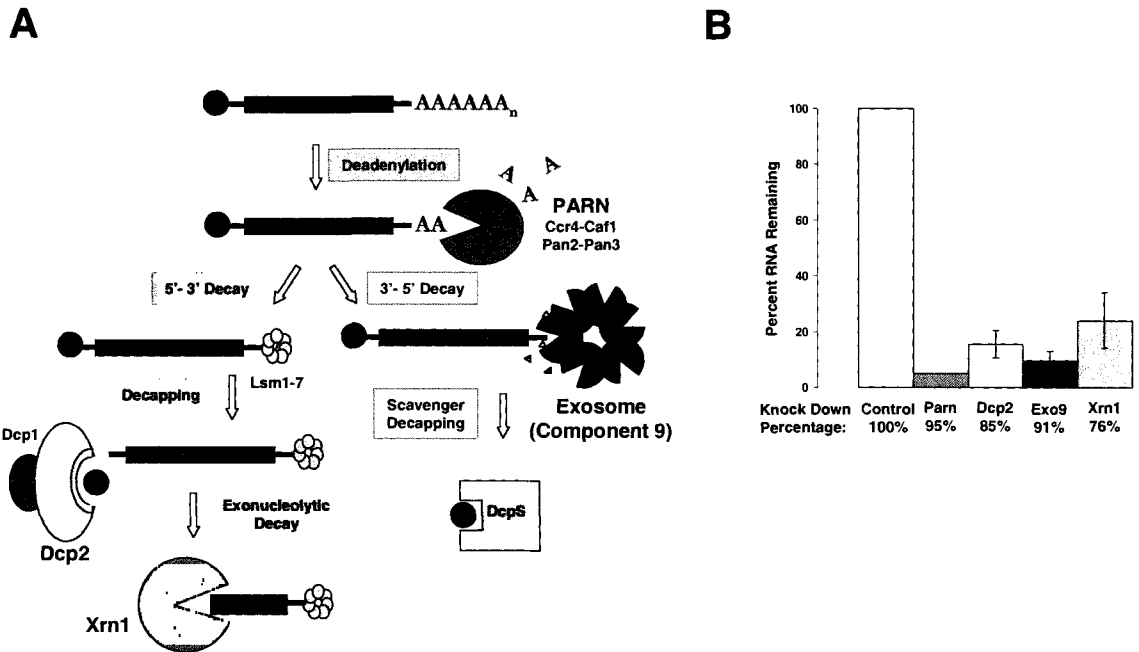


Figure 8 | Knock down of mRNA turnover enzymes within the deadenylation-dependent pathway. A | A schematic representation of the deadenylation-dependent mRNA decay pathway highlights the key proteins that were targeted for siRNA knockdown. B | Graphical representation of the expression following siRNA knock down of PARN, Dcp2, Exo9 or Xrn1. HeLa cells were transfected with siRNA constructs against PARN, Dcp2, Exo9 or Xrn1, total RNA was sampled at 48 hours post-transfection and analyzed by qRT-PCR. The expression of each mRNA is calculated as a percentage of the expression of the mRNA in control cells.

As seen in panel B of Figure 8, expression of the PARN mRNA was knocked down by 95%, Dcp2 was down by 85%, Exo9 was down by 91% and Xrn1 was knocked down by 76%. While these percentages are within the acceptable range, limitations still exist within the assay. For example, while the 95% knock down of the mRNA for the deadenylase PARN is exceptional, as mentioned above there is redundancy in enzymes that shorten the poly(A) tail that could cloud the viral decay data in these cells. Additionally, Exo9 is one of 9 components that comprise the exosome core and furthermore is not the catalytic subunit of the complex. Therefore it is difficult to precisely know the effect of knock down of Exo9 will have on the enzymatic activity of the exosome. In contrast however, Dcp2 and Xrn1 represent the major enzymes in decapping and 5' to 3' exonucleolytic decay respectively, and therefore the knock down results reported likely reflect direct repression of these steps in the turnover pathway.

Following transient knock down of PARN, Dcp2, Exo9 or Xrn1, cells were then infected with the ts6 strain of Sindbis virus and used in the *in vivo* viral RNA decay assay described in the above section. The half-lives of the genomic RNA and subgenomic RNA were analyzed by qRT-PCR and compared to cells that were treated with the transfection reagent as a control. The results from this analysis are shown in Figure 9 (genomic RNA) and Figure 10 (subgenomic RNA). It is important to note that the points were plotted using a Y-axis representing the percent RNA remaining, and that an exponential trend line best fit the plotted points as determined by the r^2 value of the line. The half-lives were solved using the equation of the trend line, as described in the Materials and Methods chapter.

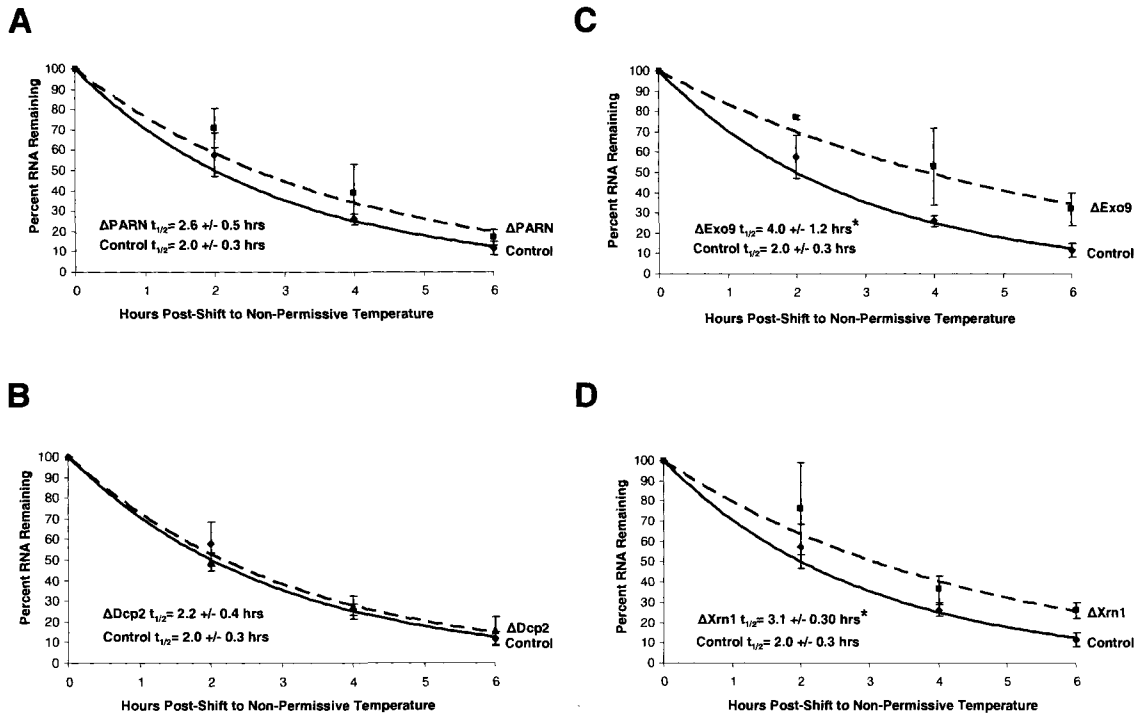


Figure 9 | Exo9 and Xrn1 contribute to the decay of the genomic RNA of Sindbis virus in HeLa cells. Cells were transfected with a siRNA construct A | Δ PARN. B | Δ Dcp2. C | Δ Exo9. D | Δ Xrn1. At 24 hours post-transfection, the cells were inoculated with a temperature-sensitive strain of Sindbis virus (ts6). At ten hours post-infection, cells were shifted to the non-permissive temperature of 40°C to shut off viral synthesis. Total RNA samples were taken at the time points indicated and the RNA was subjected to analysis by qRT-PCR.

As seen in panels C and D of Figure 9, there is an apparent trend of increasing stability of the genomic RNA in the Δ Exo9 and Δ Xrn1 cells compared to the control cells. In contrast, there was no appreciable change in the half-life of the genomic RNA in the Δ PARN cells (Figure 9, panel A), and no apparent change in the half-life of the genomic RNA in the Δ Dcp2 cells (Figure 9, panel B). To determine if these trends were statistically significant, the Welch t-Test was employed to solve for the t-value of the independent samples (to compare the half-lives), and the Welch-Satterthwaite Equation was used to solve for the degrees of freedom of the samples (both equations and a list of variables are detailed in section VII of the Materials and Methods chapter). This information was used against the Student's t-distribution and t-values that exceeded the value listed for the solved degrees of freedom with a 95% confidence interval were considered significant. With this analysis, the half-lives of the genomic RNA in the Δ PARN and Δ Dcp2 cell lines as suspected were not significant. However, the genomic RNA showed half-lives in both the Δ Exo9 and the Δ Xrn1 cell lines that were both found to be statistically significant.

Similar analysis was used to determine which enzymes significantly contributed to the decay of the subgenomic RNA during infection. The results depicted in panels C and D of Figure 10, show an apparent trend of increasing stability of the genomic RNA in the Δ Exo9 and Δ Xrn1 cells compared to the control cells. In contrast, there was no appreciable change in the half-life of the subgenomic RNA in the Δ Dcp2 cells (Figure 10, panels B) and there was no apparent change in the half-life of the subgenomic RNA in the Δ PARN cells (Figure 10, panels A). The half-life of the subgenomic RNA in the

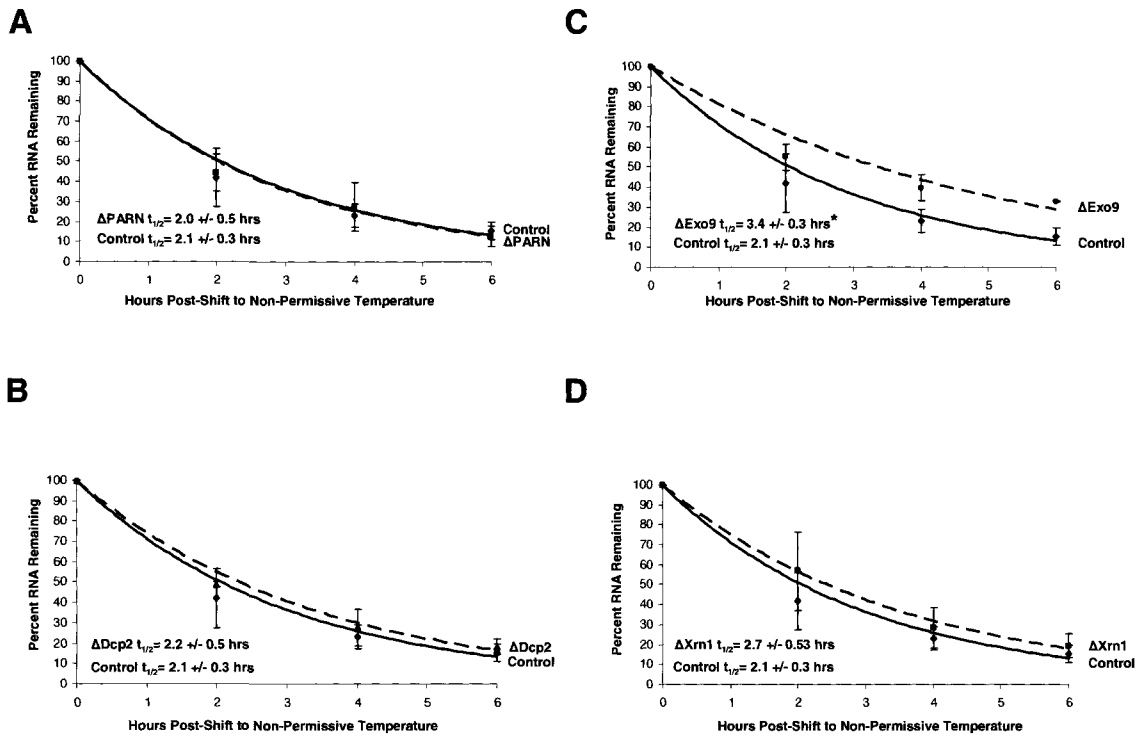


Figure 10 | Exo9 contributes to the decay of the subgenomic RNA of Sindbis virus in HeLa cells. Cells were transfected with the indicated siRNA construct A | Δ PARN. B | Δ Dcp2. C | Δ Exo9. D | Δ Xrn1. At 24 hours post-transfection, the cells were inoculated with a temperature-sensitive strain of Sindbis virus (ts6). At ten hours post-infection, cells were shifted to the non-permissive temperature of 40°C to shut off viral synthesis. Total RNA samples were taken at the time points indicated and the RNA was subjected to analysis by qRT-PCR.

Δ Exo9 cells was the only increase that proved to be statistically significant from half-life observed in the control cells with a confidence interval of 95%.

These results indicate that the Exo9, a core component of the 3' to 5' decay exosome complex, and Xrn1, the major 5' to 3' exonuclease, likely contribute to the targeting of viral RNAs during infection in HeLa cells. This is particularly significant as these enzymes are critical to the deadenylation-dependent decay pathway, but are also involved in other RNA turnover pathways in the cell. It is important to point out however, that these data do not fully rule out the role PARN may play in the decay of viral RNAs. As mentioned earlier and highlighted in Figure 8, panel A, and there is a significant amount of complexity in the first step of the deadenylation-dependent decay pathway, and many deadenylases can contribute to this function. This high level of redundancy could account for the statistically insignificant change in the half-life of the viral RNAs in the Δ PARN cells compared to the control cells. In addition, all the results could have been influenced by the small amount of functional protein left following knock down. Therefore, while we can not precisely conclude which cellular RNA decay pathway is accountable for the targeting of viral RNAs, the decay factors Exo9 and Xrn1 appear to be part of the mechanism responsible for the observed viral RNA degradation.

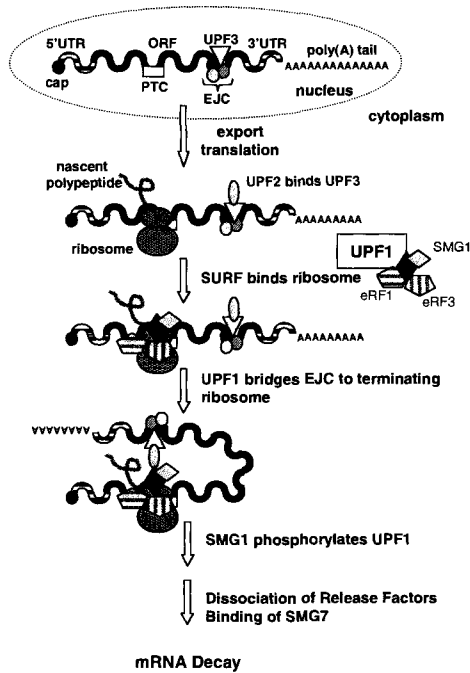
The endonuclease Dicer targets viral RNAs for decay.

The half-life results above (Figure 9 & 10) demonstrate that Exo9 and Xrn1 do contribute to the targeting of Sindbis viral RNAs for turnover. In addition to deadenylation-dependent RNA decay, we wanted to examine other, non-conventional, pathways of decay that require Exo9 and Xrn1 and may be contributing to the rapid

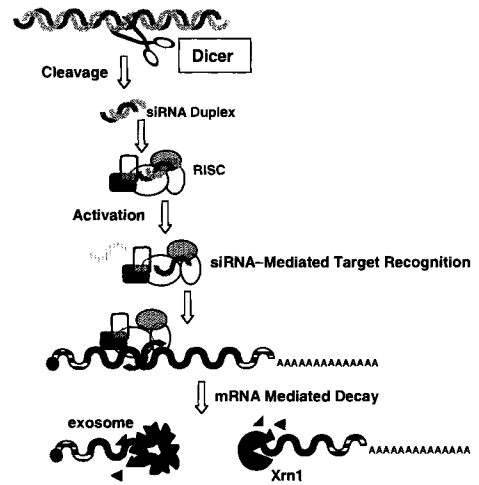
decay of viral RNAs in HeLa cells. Specialized, non-conventional decay pathways such as Nonsense-Mediated Decay (NMD) and RNA Interference (RNAi) are depicted in Figure 11, panels A and B. NMD is initiated by a premature termination codon, and RNAi is dependent on the recognition of double-stranded RNAs within the cell. Both these pathways cleave target RNAs by means of an endonuclease and then the body of the transcript is turned over by exonucleases such as Xrn1 and the multi-protein exosome complex which includes Exo9. It is of interest to note that the genomic RNA of Sindbis virus contains two open reading frames, and thus could be considered to possess a premature termination codon following the first open reading frame. Also, Sindbis virus replication likely produces double-stranded RNA intermediates which could induce RNAi. Therefore, Sindbis viral RNAs could be interfacing with either the NMD and/or RNAi pathways.

To examine the role of the NMD and RNAi pathways in Sindbis viral RNA degradation we used stable knocked down cell lines of Upf1 or Dicer (denoted as Δ). These lines were previously made by Emily Chaskey in our laboratory using shRNAs in a lentivirus delivery system to target the mRNA for the major endonuclease of the RNAi pathway, Dicer, and also to target the critical protein of the NMD decay pathway, Upf1. The selected cells were analyzed for knock down expression using qRT-PCR analysis. As graphically depicted in panel C of Figure 11 the Δ Dicer cells showed a 77% knock down and the Δ Upf1 cells showed a 70% knock down. These cells were then infected and used in the *in vivo* viral RNA decay assay to determine if the loss of either enzyme would significantly increase the stability of the viral RNAs.

A Nonsense-Mediated Decay



B RNA Interference-Mediated Decay



C

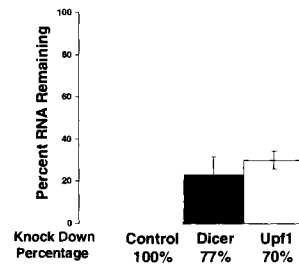


Figure 11 | Knock down of Upf1 and Dicer, two major proteins in non-conventional pathways of mRNA decay. A | To inhibit the nonsense-mediated decay pathway the Upf1 protein (boxed) was silenced using RNAi. B | To inhibit the RNA interference-mediated decay (RNAi) the endonuclease Dicer was silenced using RNAi. C | Expression following siRNA knock down of Upf1 or Dicer. HeLa cells were infected with lentiviruses carrying an shRNA construct against either Upf1 or Dicer. Stable cell lines were selected and total RNA was analyzed by qRT-PCR. The expression of each mRNA is calculated as a percentage of the expression of the mRNA in control cells.

As seen in Figure 12, the half-lives of the genomic RNA and the subgenomic RNA during infection in the Δ Dicer cells are increased over the half-lives in the control cells. Following statistical analysis identical to that employed for half-lives in the transient knock down cells, it was found that the increase in half-life for both the genomic and the subgenomic viral RNAs were statistically significant in the Δ Dicer cells with a 95% confidence interval. Conversely, there appeared to be no appreciable change in half-lives of the Sindbis viral RNAs in the Δ Upf1 cells compared to the control cells (Figure 13, panels A and B). Accordingly, there was no significant difference in these half-lives using Welch's t-test and the Welch-Satterwaithe Equation for degrees of freedom. These data suggest that the specialized RNAi-mediated decay pathway contributes to the turnover of the Sindbis viral RNA in HeLa cells, and that the NMD pathway is not involved.

Collectively, the results from section I demonstrate that the rate of viral RNA decay during infection can be correlated to the productivity of that infection as measured by viral growth and mature virion production. Furthermore, it puts forth evidence that mRNA decay represents a novel host cell restriction function against viruses, and it is the first demonstration of a mechanism of host cell restriction against Sindbis virus in HeLa cells. Finally, Exo9, Xrn1 and the endonuclease Dicer are important in Sindbis viral RNA turnover. This suggests that the RNAi-mediated RNA decay pathway is likely contributing to the viral RNA degradation observed during infection, and furthermore puts forth compelling evidence that RNAi could potentially act as a potent antiviral mechanism in mammalian cells.

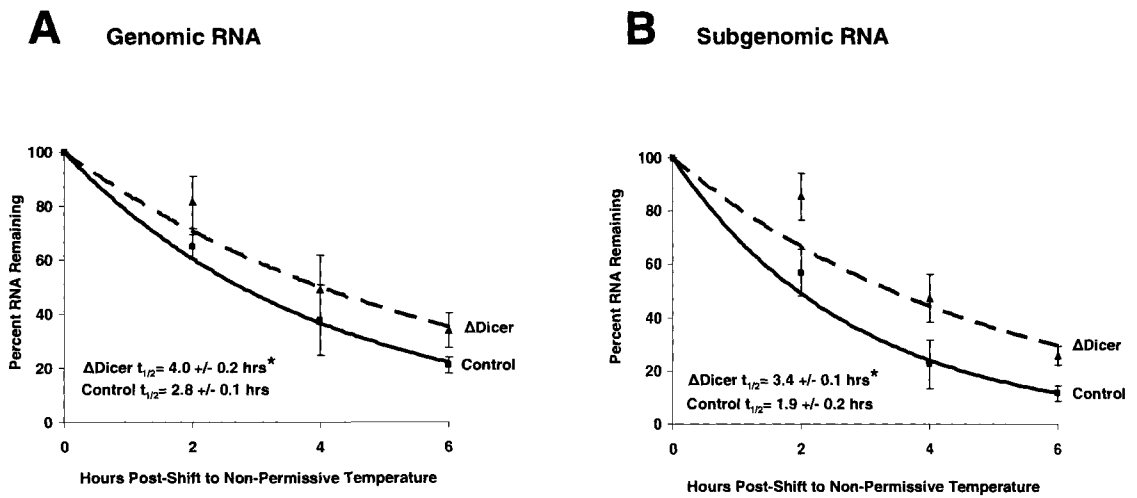


Figure 12 | The endonuclease Dicer contributes to the decay of the Sindbis viral RNA in HeLa cells. Stably knocked down Dicer cells (Δ Dicer) were inoculated with a temperature-sensitive strain of Sindbis virus (ts6). At ten hours post-infection, cells were shifted to the non-permissive temperature of 40°C to shut off viral synthesis. Total RNA samples were taken at the time points indicated and the RNA was subjected to analysis by qRT-PCR. Results for the genomic and subgenomic RNAs are shown in panels A and B, respectively.

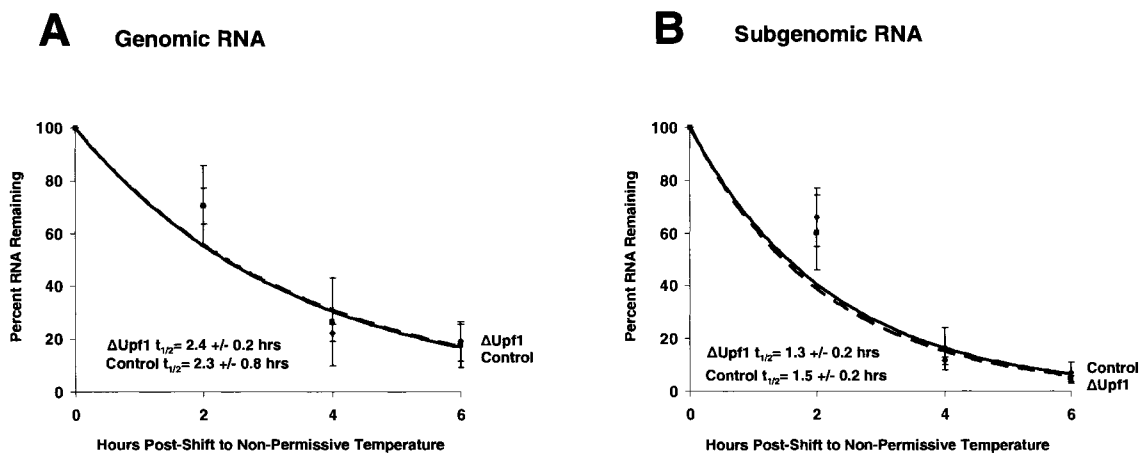


Figure 13 | The nonsense-mediated decay factor Upf1 does not contribute to the decay of the Sindbis viral RNA in HeLa cells. Stably knocked down Upf1 cells (Δ Upf1) were inoculated with a temperature-sensitive strain of Sindbis virus (ts6). At ten hours post-infection, cells were shifted to the non-permissive temperature of 40°C to shut off viral synthesis. Total RNA samples were taken at the time points indicated and the RNA was subjected to analysis by qRT-PCR. Results for the genomic and subgenomic RNAs are shown in panels A and B, respectively.

RESULTS

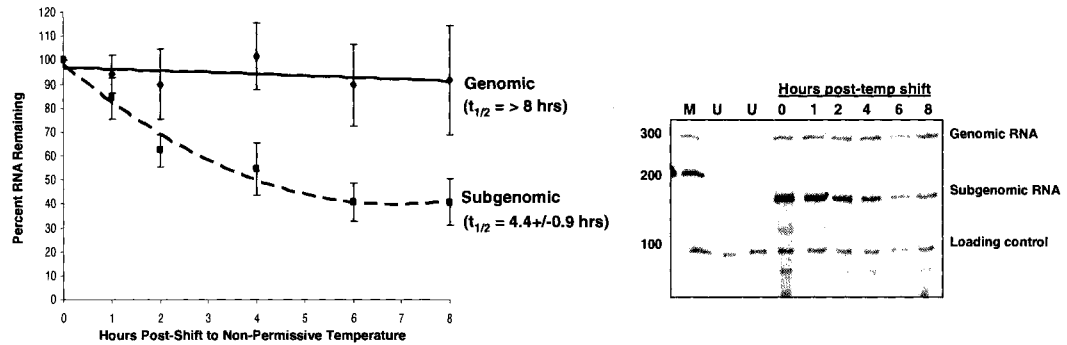
II. SINDBIS VIRUS STABILITY IS A FUNCTION OF THE VIRAL 3' UTR

Sindbis viral RNAs are subject to RNA decay in mosquito cells.

Sindbis virus is an arthropod-borne virus that is transmitted to the vertebrate host by the mosquito vector. In order to examine the phenomenon of viral RNA decay in both of these host cell types, we elected to study a representative mammalian (non-human) cell line and a mosquito cell line concurrently (baby hamster kidney- BHK-21, and *Aedes albopictus* mosquito larval cells-C6/36 respectively). These selections were made based on literature demonstrating the ability of both these cell lines to support robust viral growth (Kuhn *et al.*, 1990; Renz & Brown, 1976). From these two cell lines we were interested in determining what, if any, interaction occurred between the host cell decay machinery and the Sindbis viral RNAs. The *in vivo* viral RNA decay assay, as described in Results Section I, was again used. The viral RNAs were then quantified using the RNase Protection assay (RPA), and the data from multiple experiments were analyzed.

As seen in the left panel of Figure 14A, graphical analyses show that the genomic RNA is exceptionally stable in the BHK-21 cell line with a half-life greater than 8 hours, and that the subgenomic RNA has a measurable half-life of 4.4 +/- 0.9 hours. The subgenomic data were plotted with a second order polynomial trend line, which was found to best represent the data points. This suggests a potential biphasic pattern of decay of the subgenomic RNA that may be reflective of possible changes in the cellular mRNA decay machinery over the time course assessed.

A BHK-21



B C6/36

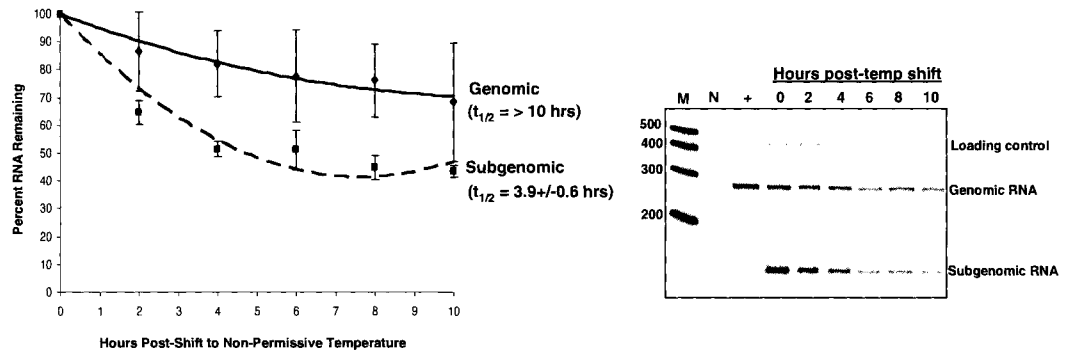


Figure 14 | Sindbis viral RNAs are subject to decay in mosquito cells. **A** | BHK-21 (mammalian-non human) cells were infected with a Sindbis virus variant containing a temperature-sensitive mutation in its RNA polymerase gene. At 10 hours post infection, cells were shifted to the non-permissive temperature of 40°C to shut off viral synthesis, total RNA samples were taken at the indicated times and probed for viral specific transcripts by RNase protection (RPA). The level of the ribosomal RNA 5S was detected concurrently to allow normalization of all samples for accurate quantification. Reaction products were separated on a 5% acrylamide gel containing 7M urea and visualized by phosphorimaging. The lane labeled “N” represents the results obtained when total cellular RNA from uninfected cells was added to the reaction, and the lane labeled + represents an RPA performed on *in vitro* transcribed Sindbis virus genomic RNA. Representative RPA is shown in the right panel. Graphical representation of multiple experiments is shown in the left panel. **B** | C6/36 mosquito cells were infected with ts6 virus At 10 hours post infection, cells were shifted to 40°C to shut off viral transcription, total RNA samples were taken at the indicated times and probed for viral specific transcripts by RNase protection (RPA). The level of the mRNA for ribosomal protein S5 was detected concurrently to allow normalization of all samples for accurate quantification. Reaction products were separated on a 5% acrylamide gel containing 7M urea and visualized by phosphorimaging. The lanes labeled “U” represents the results obtained when total cellular RNA from uninfected cells was added to the reaction. Representative RPA is shown in the right panel. Graphical representation of multiple experiments is shown in the left panel.

The right panel in Figure 14A depicts a representative RPA, which clearly highlights the stability of the genomic RNA, the turnover of the subgenomic RNA, and band representing the 5S ribosomal RNA which was used as an internal loading control for the analysis. Finally, uninfected cells (U) were used as a negative control to ensure the probes were specific for the viral RNA.

In the left panel of Figure 14B, a graphical representation of the data shows that the Sindbis viral genomic RNA is also very stable in the C6/36 mosquito cells, with a half-life greater than 10 hours. The half-life of the subgenomic RNA during infection in the C6/36 was found to 3.9 +/- 0.6 hours. The representative RPA shown in the right panel of Figure 14B depicts the relative stability of the genomic RNA in mosquito cells, the clear degradation of the subgenomic RNA, and the band representing the mRNA encoding the ribosomal small protein 5 which was used as an internal loading control for analysis. Also included is a negative control (N-no RNA) and *in vitro* transcribed genomic RNA as a positive control (+) for the assay.

The observation that the Sindbis viral genomic RNA was so stable in both the BHK-21 mammalian cells and the C6/36 mosquito cells could be reflective of the fact that the genomic RNA is subject to replication and packaging in addition to being translated. This is in contrast to the subgenomic RNA which is solely translated, and accordingly is much less stable than the genomic RNA in BHK-21. Another interesting observation is that the half-life of the subgenomic RNAs in the C6/36 mosquito cell line is greater than the average class of mRNAs in these cells as previously reported in our laboratory (Opyrchal *et al.*, 2005). This suggests that Sindbis virus may employ a means for protecting its viral RNAs from decay in this cell type. Furthermore, these findings

confirm that the phenomenon of viral RNA decay is not solely restricted to mammalian cell lines and can be found in other host cell lines, including the mosquito vector.

Wild-type Sindbis viral RNAs decay in a deadenylation-independent manner.

The deadenylation-dependent mRNA turnover pathway is the major pathway of degradation for cellular mRNAs in mammalian cells (Chen & Shyu, 2003; Conrad *et al.*, 2006; Yamashita *et al.*, 2005). Although mRNA decay pathways in mosquitoes are much less understood than they are in mammalian cells, it is clear that *Aedes albopictus* mosquitoes contain homologues to all the critical mammalian mRNA decay enzymes (Opyrchal *et al.*, 2005). Furthermore, mosquito mRNAs, like mammalian mRNAs, decay in a predominantly deadenylation-dependent manner (Opyrchal *et al.*, 2005). We were interested in determining if Sindbis viral RNAs were substrates for the major mRNA degradation pathway and were therefore deadenylated prior to decay in the human, hamster and mosquito cells we had previously studied. To examine this we used an RNase H/northern blot technique (as described in section VIII of the Materials and Methods chapter). This technique allowed us to visualize and assess the length of the viral poly(A) tail over the time course examined.

As seen in panel A of Figure 15, the band representing the viral poly(A) tail does not migrate towards the A₀ marker (representing a fully deadenylated transcript). Therefore, the viral RNAs are not deadenylated over the course of the *in vivo* viral RNA assay in BHK-21 cells. The poly(A) tail of the viral RNA was similarly maintained during turnover in the C6/36 mosquito cell line (Figure 15, panel B) as well as in the human HeLa cell line (Figure 15, panel C).

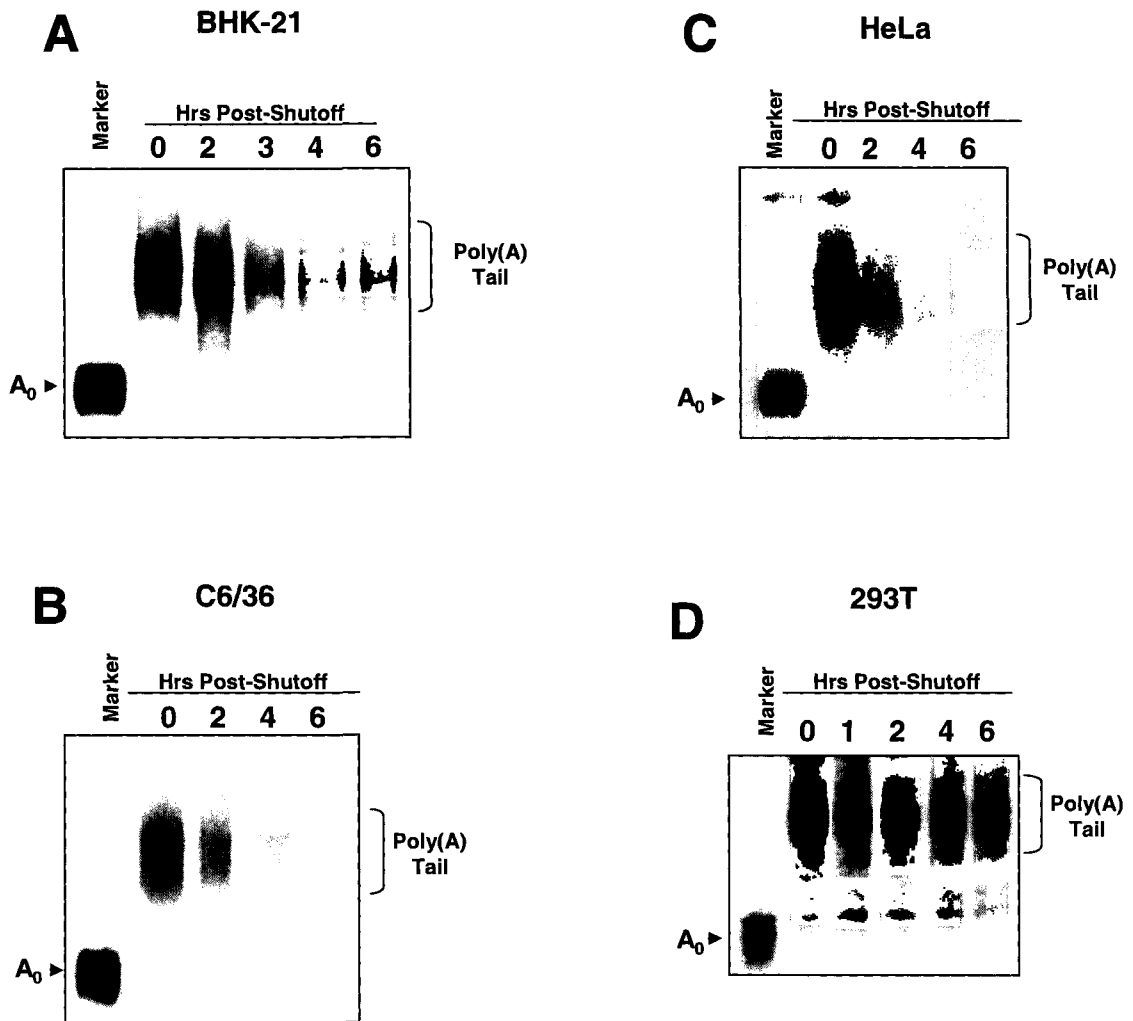


Figure 15 | Sindbis virus RNAs decay in a deadenylation-independent fashion. BHK-21 (panel A), C6/36 (panel B), HeLa (panel C) and 293T (panel D) cells were infected with a Sindbis virus variant containing a temperature sensitive mutation in its RNA polymerase gene. At 10 hours post infection, cells were shifted to 40°C to shut off viral transcription and total RNA samples were isolated at the indicated times. RNAs were hybridized to a DNA oligo designed to bind to the region of the Sindbis virus 3'UTR and treated with RNase H. Samples for the lane labeled "Marker" were also hybridized to oligo(dT) prior to RNase H treatment to generate a marker for fully deadenylated viral mRNAs. Reaction products were separated on a 5% acrylamide gel, electro-blotted to Hybond N membranes and probed with Sindbis virus-specific probes. Results were visualized by phosphorimaging.

The lack of deadenylation was also apparent in the 293T cell line (Figure 15, panel D), but as the viral RNAs were previously demonstrated to be very stable in this cell line (refer to Figure 7), this result was expected.

In summary, the poly(A) tail did not appreciably shorten during decay of the viral RNAs in BHK-21, C6/36 and in HeLa cells. These data indicate that the Sindbis viral RNAs, unlike endogenous mRNAs in the cytoplasm, are not acted upon by the cellular deadenylases and may help to explain the lack of function the PARN deadenylase was shown to have on the half-lives of the viral RNAs in HeLa cells (panel A of Figures 9 & 10). Therefore, we conclude that Sindbis viral RNAs appear to be refractory to deadenylation. We hypothesize that the virus likely contains a means for protecting itself against the very potent cellular deadenylases.

The 3' UTR represses deadenylation during infection of BHK-21 cells.

Features that are known to protect RNAs from decay include the presence of stabilizer elements within the 3' UTR, strong RNA structures and *trans*-acting proteins (Conrad *et al.*, 2006; Harris *et al.*, 2006; Ford & Wilusz, 1999b; Weil & Beemon, 2006). Sindbis virus contains a well defined 3' UTR composed of distinct elements outlined in Figure 16. These elements include the three Repeat Sequence Elements (RSE), the U-Rich Element (URE) and the Conserved Sequence Element (CSE). We hypothesized that the viral 3' UTR and its elements, like cellular 3' UTRs and accompanying elements, could be responsible for protecting viral transcripts from cellular deadenylases.

A Sindbis virus 3'UTR RNA Sequence

```

CCGCUACGCCCCAAUGAUCCGACCAGCAAAACUCGAUGUACUCCGAGGAACUGAUGUG
CAUAAUGCAUCAGGCUGGUACAUAUAGAUCGCCCGCUUACCGCGGGCAAUAUAGCAACACU
AAAAACUCGAUGUACUCCGAGGAAGCGCAGUGCAUAAUGCUGCGCAGUGUUGCCACAU
AACCACUAUAUUAACCAUUUAUCUAGCGGACGCCAAAAACUCAAAUGUAUUUCUGAGGAA
GCGUGGUGCAUAAUGCCACGCAGCGUCUGCAUAACUUUUUAUUUUUUUUUUUAUUAUCA
ACAAAAUUUUGUUUUUAACAUUUC
  
```

```

RSE 1- AAAACUCGAUGUACUCCGAGGAACUGAUGUGCAUAAUGC
RSE 2- AAAACUCGAUGUACUCCGAGGAAGCGCAGUGCAUAAUGC
RSE 3- AAAACUCAAAUGUAUUUCUGAGGAAGCGUGGUGCAUAAUGC
URE   - GUCUGCAUAACUUUUUAUUUUUUUUUAUUUAUCAACAAA
CSE   - AUUUUGUUUUUAACAUUUC
  
```

B

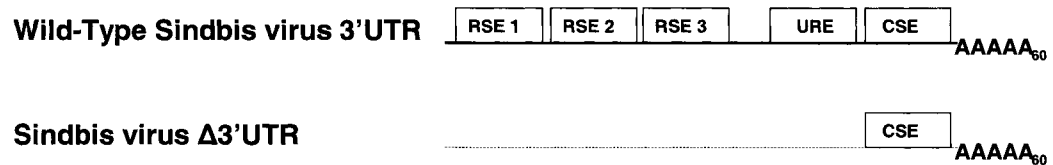


Figure 16 | Sequence and organization of the Sindbis virus 3'UTR. A | The highlighted sequences represent the characterized 3'UTR elements of Sindbis virus which are also individually depicted directly beneath the full 3'UTR sequence. The repeat sequence element 1, 2 and 3 (RSE 1, 2, 3) are located in the 5' section of the 3'UTR. The U-rich element (URE) and the conserved sequence elements are located at the very 3' of the 3'UTR. B | The diagrammatic organization of the wild-type Sindbis virus 3'UTR is represented in the top panel. The 3'UTR deletion construct is shown in the bottom panel and depicts a gross deletion of 300 nucleotides from the 5' end of the 3'UTR. The only remaining sequence is the CSE.

To address this hypothesis, we created a virus with as much of the 3' UTR as possible deleted, thereby removing any potential protective elements. The temperature-sensitive 6 (ts6) strain of Sindbis virus was used as the backbone for constructing a gross deletion of the viral 3' UTR (Figure 16, panel B). The Sindbis Δ 3' UTR viral construct lacked the entire 3' UTR with the exception of the CSE, a required replication element (Kuhn *et al.*, 1990; Levis *et al.*, 1986). Using the Sindbis ts6 Δ 3' UTR virus, BHK-21 cells were infected, viral RNA synthesis was turned off by shifting the cell to the non-permissive temperature, and total RNA was collected over time. Again, RNase H/northern blot analysis was employed to visualize the status of the poly(A) tail.

As seen in panel A of Figure 17, the wild-type viral RNA, as was previously demonstrated in Figure 16, does not undergo deadenylation. However, as shown in panel B, deleting the 3' UTR from that same viral RNA results in a progressive shortening of the poly(A) tail over the time course. This is best exemplified at four hours post-shutoff of viral RNA synthesis where the average length of the poly(A) tail has decreased from the length demonstrated at time point zero, and is approaching the marker that represents the fully deadenylated viral RNA transcript band in this assay.

In addition, it is of note to mention that in order to visualize the Δ 3' UTR deletion viral RNA in the RNase H/northern blot analysis, 20X the amount of total RNA was required to visualize the poly(A) tail of the Δ 3' UTR RNA than was required for the wild-type viral RNA. This emphasizes the poor accumulation of the Δ 3' UTR viral RNA in BHK-21 mammalian cells as compared to the wild-type virus.

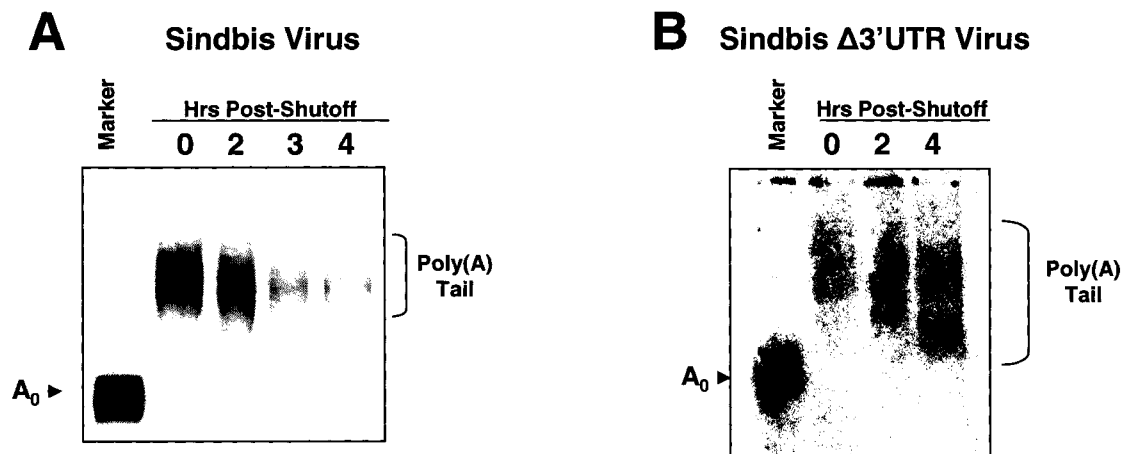


Figure 17 | The 3'UTR of Sindbis virus represses deadenylation during infection in BHK-21 cells. BHK-21 cells were infected with either a wild-type (panel A) or a $\Delta 3'$ UTR Sindbis virus (panel B), each containing a temperature sensitive mutation in its RNA polymerase gene. At 10 hours post infection, cells were shifted to 40°C to shut off viral transcription and total RNA samples were isolated at the indicated times. RNAs were hybridized to a DNA oligo designed to bind to the region of the Sindbis virus 3'UTR and treated with RNase H. Samples for the lane labeled "Marker" were also hybridized to oligo(dT) prior to RNase H treatment to generate a marker for fully deadenylated viral mRNAs. Reaction products were separated on a 5% acrylamide gel, electro-blotted to Hybond N membranes and probed with Sindbis virus-specific probes. Results were visualized by phosphorimaging.

These data suggest that the viral 3' UTR is in fact a protective feature of the virus that represses cellular deadenylases from shortening the poly(A) tail, therefore preventing the major pathway of RNA decay from acting on the viral RNA.

Development of the linker ligation-mediated poly(A) tail assay (LLM-PAT).

We were also interested in examining the status of the poly(A) tail on Sindbis virus RNAs during infection in mosquito cells. Unfortunately, we were unable to successfully use the RNase H/northern technique described above due to the poor growth of the virus in this cell type. Therefore, we needed to develop a method for visualizing the poly(A) tail of low concentration RNAs within a total RNA sample.

To accomplish this, we adapted the PCR-based technique for poly(A) tail length assessment called the ligation-mediated poly(A) tail assay (LM-PAT) (Salles *et al.*, 1999). Our method, diagramed in Figure 18, is sensitive to small changes in the poly(A) tail due to the use of a modified oligonucleotide (Linker-3, Integrated DNA Technologies; Pfeffer *et al.*, 2005). The modifications of the Linker-3 include a 3' terminal dideoxy-C and a 5' adenylation. These modifications prevent self-ligation and pre-activated the linker for ligation in an ATP-independent fashion. Thus, the reaction will neither result in self-ligation nor in RNA circularization or inappropriate ligation of multiple RNAs.

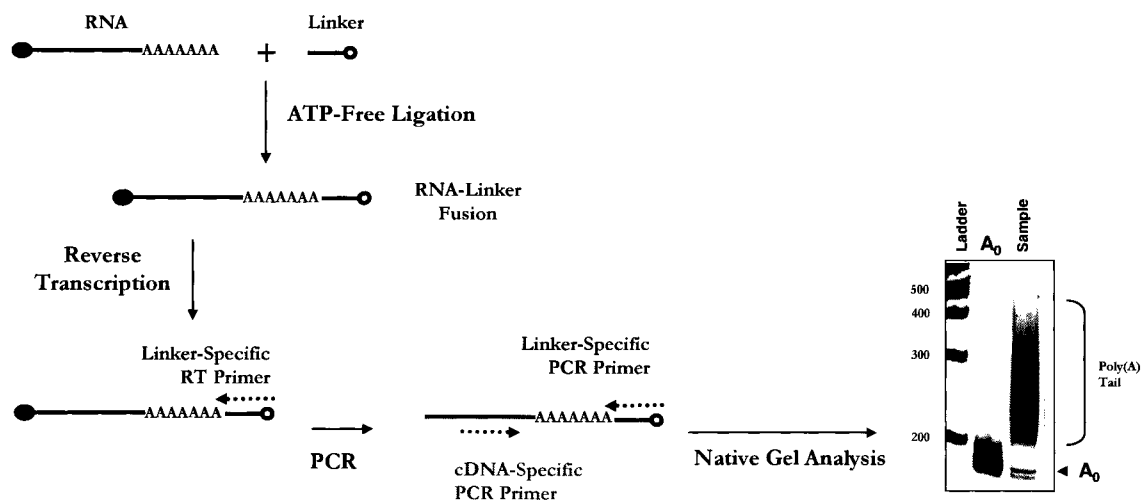


Figure 18 | Linker-ligation mediated poly(A) tail assay (LLM-PAT). The LLM-PAT assay begins with ligation of a modified oligo linker to the 3' end of the RNA. The ligated RNA is then reverse transcribed using a primer specific to the linker. The cDNA is used as a template for a PCR reaction using a primer specific to the linker and a primer specific to the target RNA. The PCR product is then resolved on a 5% native polyacrylamide gel, and the state of the poly(A) tail can be visualized by staining the gel with a nucleic acid dye and imaging. A representative result from an LLM-PAT assay is shown in the gel on the right. The “A₀” lane represents the amplification product from RNA samples that were pretreated with oligo dT/RNase H to remove the poly(A) tail. This serves as a marker for a fully deadenylated target RNA in this assay. Adapted from Garneau *et al.*, 2009.

Following ligation, the RNA is reverse transcribed using a primer specific to the linker. The resulting cDNA is used in a PCR reaction with a downstream PCR primer specific to the linker and an upstream primer specific to the viral RNA. Importantly, the amount of cDNA used in this reaction can be adjusted to compensate for a low concentration of the RNA of interest in the total RNA sample. Finally, the PCR product is visualized on a 5% native polyacrylamide gel using both a DNA ladder and a poly(A)⁻ product as a marker.

The 3' UTR represses deadenylation in C6/36 mosquito cells.

With the establishment of the LLM-PAT assay, we now had a very sensitive tool to analyze poly(A) tail lengths from very low concentrations of viral RNA. Therefore, we were very interested in establishing if the block in deadenylation of the Sindbis viral RNAs due to the 3' UTR was a phenomenon found only in the mammalian host, or if it could also be observed in the mosquito host.

As seen in Figure 19, using the LLM-PAT assay we found that the poly(A) tail length of the wild-type viral RNA was maintained over the time course examined in C6/36 mosquito cells. By contrast, Sindbis viral RNA lacking its 3' UTR was no longer able to protect the poly(A) tail from deadenylation, and a progressive shortening of the poly(A) tail was observed. The lane labeled “Uninfected” represents LLM-PAT analysis completed with RNA from uninfected cells as a negative control. As shown by the asterisk (*) in Figure 19, a non-specific band of 140 nucleotides is detected in RNA samples of both uninfected and the infected cells using the primer set to detect viral RNAs with a wild-type 3' UTR.

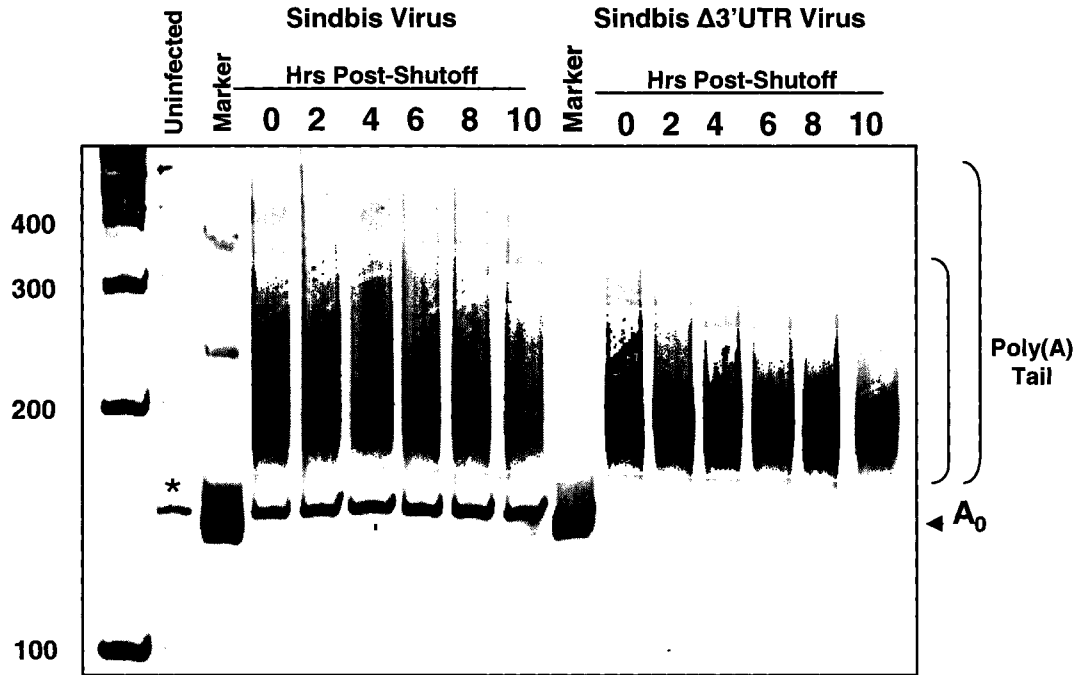


Figure 19 | The 3'UTR of Sindbis virus represses deadenylation during infection in C6/36 cells. C6/36 mosquito cells were infected with either a wild-type or a $\Delta 3'$ UTR Sindbis virus, each containing a temperature-sensitive mutation in its RNA polymerase gene. At 10 hours post infection, cells were shifted to 40°C to shut off viral transcription and total RNA samples were isolated at the indicated times. The poly(A) tail length was assessed using the PCR-based LLM-PAT assay described in Figure 16, and products were analyzed by agarose gel electrophoresis. RNAs were hybridized to oligo (dT) (lanes marked dT) and digested with RNase H prior to LLM-PAT analysis. The uninfected lane shows the products of an LLM-PAT assay done on total RNA from uninfected C6/36 cells using a primer set to detect Sindbis virus transcripts with a wild-type 3'UTR. The positions of the molecular size markers are shown on the left. Brackets on the right indicate the migration of PCR products derived from the poly(A⁺) RNAs.

Unfortunately, this non-specific band is the same size as a fully deadenylated transcript, and although numerous digestion enzymes (with no known restriction sites in the cDNA made from Sindbis viral RNA) were employed, regrettably none of them were able to digest away this inconvenient band.

In summary, these data emphasize the importance of the Sindbis viral 3' UTR to protect against cellular deadenylases. Furthermore, it is evidence that the block in deadenylation due to the viral 3' UTR is found in both the mammalian and the mosquito cell types and may represent a conserved mechanism of protecting viral RNA from the dominant, deadenylation-dependent decay pathway.

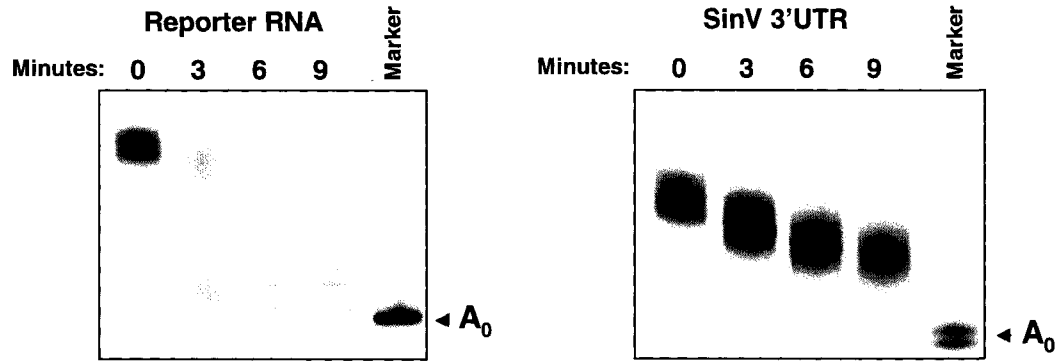
The 3' UTR of Sindbis virus blocks deadenylation in an *in vitro* C6/36 mosquito cell cytoplasmic extract system.

An *in vitro* deadenylation system has been established in our laboratory using both HeLa cell and C6/36 mosquito cell cytoplasmic extracts, and has proven to be a useful tool for identifying RNA stability elements and delineating mechanisms of RNA decay (Opyrchal *et al.*, 2005; Ford & Wilusz, 1999a). Using this system, a reporter RNA which is transcribed from the multiple cloning site of the plasmid pGEM-4 has been shown to deadenylate very rapidly. Interestingly, our lab has also previously observed that the 3'UTR of Sindbis blocks deadenylation in C6/36 mosquito cell extracts, but not in HeLa cell cytoplasmic extracts (Garneau *et al.*, 2008; Opyrchal, 2005). We wanted to utilize this assay to address whether the protection we observed *in vivo* could be recapitulated *in vitro*. This additional tool would enable a more detailed analysis of the role the viral 3' UTR plays in repressing the shortening of the poly(A) tail.

As seen in the left panel of Figure 20A, the pGem-4 reporter RNA that contains no stability elements shows rapid deadenylation of its poly(A) tail in mosquito cell cytoplasmic extracts. By three minutes, there is an accumulation of fully deadenylated transcript, and by six minutes virtually all of the RNA used in the assay has been deadenylated. Conversely, as seen in the right panel of Figure 20A, the insertion of the Sindbis virus 3' UTR into the same reporter RNA now represses the process of deadenylation in mosquito cell cytoplasmic extracts. In fact, the 3' UTR effectively blocks complete deadenylation of the RNA from occurring over the time frame examined, as there is no accumulation of fully deadenylated transcripts by nine minutes. When the same reporter RNA was exposed to human HeLa cell cytoplasmic extracts, we found that fully deadenylated transcripts began to accumulate by ten minutes, and that shortening of the poly(A) tail was complete by twenty minutes (Figure 20B, left panel). In contrast to the data in the mosquito cell extracts, we found that insertion of the Sindbis viral 3' UTR into the reporter RNA did not appreciably protect the transcript from the cellular deadenylases. As shown in the right panel of Figure 20B, the pattern and rate of deadenylation of the Sindbis viral 3' UTR RNA is identical to the reporter RNA, accumulation of poly(A)⁻ RNA begins around ten minutes, and deadenylation is complete by twenty minutes post-exposure to the HeLa cytoplasmic extracts.

While the C6/36 mosquito cell extracts dependably recapitulate the ability of the viral RNA to block its deadenylation of as was observed *in vivo*, this regulation is not reproduced in HeLa cell cytoplasmic extracts. Importantly though, the C6/36 mosquito cell extract system can be further used to delineate the potential protective role of the elements within the viral 3' UTR.

A C6/36



B HeLa

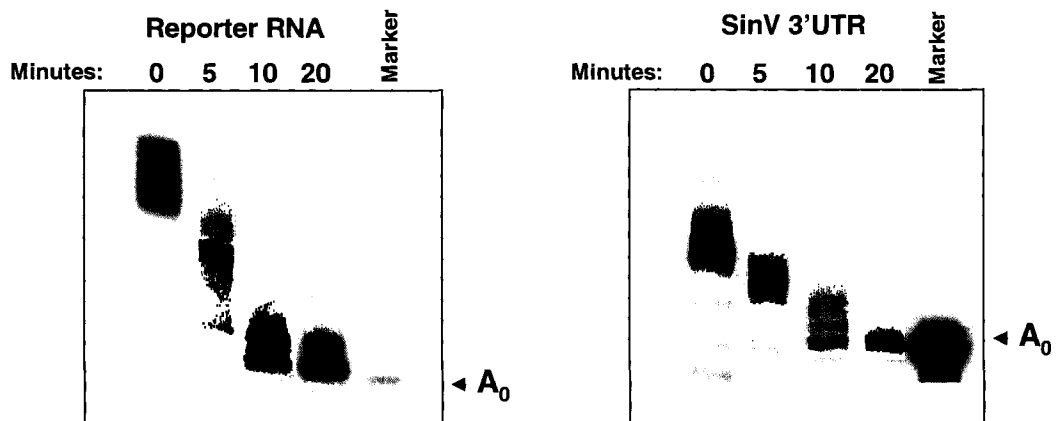


Figure 20 | The 3' UTR of Sindbis virus represses deadenylation in C6/36 cytoplasmic extracts. A polyadenylated reporter RNA (left panel) or a variant containing the 3' UTR of Sindbis virus (right panel) were incubated in an *in vitro* RNA deadenylation/decay system derived from either C6/36 (panel A) or HeLa S100 (panel B) cytoplasmic extracts for the indicated times. Reaction products were analyzed on a 5% acrylamide gel containing 7M urea and visualized by phosphorimaging. The marker lane denotes fully deadenylated versions of the input transcript, as indicated by the A₀ arrow.

Repeat Sequence Element 3 of the Sindbis viral 3' UTR contributes to the regulation of deadenylation *in vitro*.

There are three repeat sequence elements (RSE) in the 3' UTR of Sindbis virus. These elements share 82.5% sequence homology to one another (Figure 16, panel A). Additionally, although the sequence itself is not well conserved, RSEs of various compositions and sizes are found in all alphaviruses (Pfeffer *et al.*, 1998; Ou *et al.*, 1981). Despite this conservation, their function has yet to be identified. As many 3' UTR elements within cellular transcripts regulate mRNA degradation, we were very interested in the possibility that the RSEs could represent a *cis*-acting stabilization element of the poly(A) tail of the Sindbis viral RNA.

To assess the role of the RSEs in repressing deadenylation, we chose to examine the sequence of just one RSE (RSE 3, plus 5 downstream nucleotides = 45 nucleotides total) in the context of our *in vitro* deadenylation assay. This decision was made due to the high sequence homology of the three Sindbis viral RSEs, and the reality that working with one RSE over three sequential RSEs (which would have amounted to 220 nucleotides) would enable us to easily identify which aspects of the conserved sequence were potentially important to the stability of the viral poly(A) tail.

As seen in the left panel of Figure 21A, the pGem-4 reporter RNA shows rapid deadenylation of the poly(A) tail, with the majority of the accumulation of deadenylated transcript occurring by nine minutes post-exposure to mosquito cell cytoplasmic extract. In support of our hypothesis we found that the sequence of the RSE 3, when inserted into the reporter construct, was able to prevent this high level of accumulation of completely deadenylated transcripts (Figure 21A, right panel).

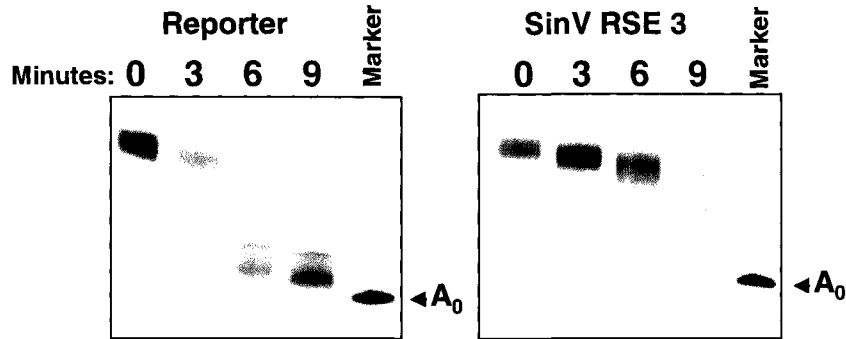
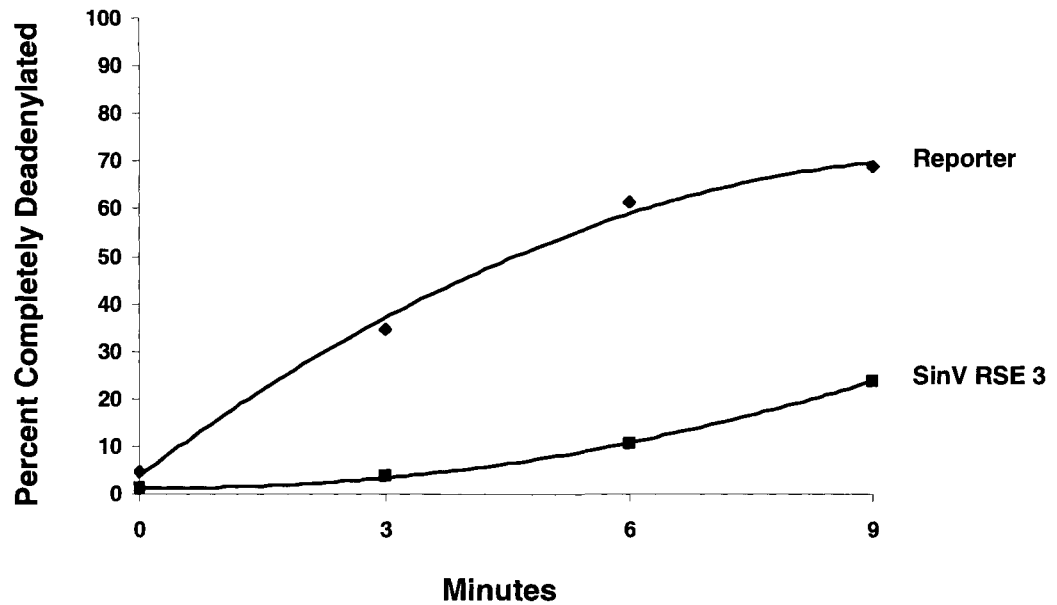
A**B**

Figure 21 | Repeat Sequence Element 3 (RSE 3) of Sindbis virus represses deadenylation in C6/36 cytoplasmic extracts. A | The polyadenylated reporter RNA (left panel) or a variant containing the RSE of Sindbis virus (right panel) were incubated in an *in vitro* RNA deadenylation/decay system derived from C6/36 S100 cytoplasmic extracts for the indicated times. Reaction products were analyzed on a 5% acrylamide gel containing 7M urea and visualized by phosphorimaging. The marker lane denotes fully deadenylated versions of the input transcript, as indicated by the A_0 arrow. B | Graphical representation of the data presented in panel A.

In fact, the pattern of repressed deadenylation from the RSE 3 sequence was identical to the pattern of repressed deadenylation we saw for the full Sindbis viral 3' UTR (Figure 20A, right panel). Graphical representations of the block in deadenylation by the RSE 3 are reported in Figure 21, panel B. Here it is clear that by nine minutes, the majority of the starting reporter RNA is completely deadenylated, in contrast to small percentage of RSE 3 RNA that is completely deadenylated at this time. This is the first evidence that an RSE as a conserved element exhibits a function, and these data demonstrate that the function of RSE 3 of Sindbis virus is likely to be in the regulation of deadenylation of the viral RNA.

Nucleotides 5-17 of Sindbis viral 3' UTR element RSE 3 contribute to the regulation of deadenylation *in vitro*.

As seen in panel A of Figure 22, the structure of RSE 3 as predicted by the computer program Mfold suggests that the element is composed of two stem-loops connected by a linker region (Zuker, 2003). From this prediction, we were interested in determining two things. First, if either the primary sequence or the predicted secondary structure of the RSE 3 was responsible for the action of blocking deadenylation. Second, we wanted to determine the minimal sequence of the stabilization element within the RSE 3 responsible for blocking the shortening of the poly(A) tail.

To address these questions, we created mutations in the sequence of the RSE 3 based on the predicted structure (all mutations are diagramed beneath the wild-type sequence of RSE 3 in Figure 22, panel B). The mutations we examined included

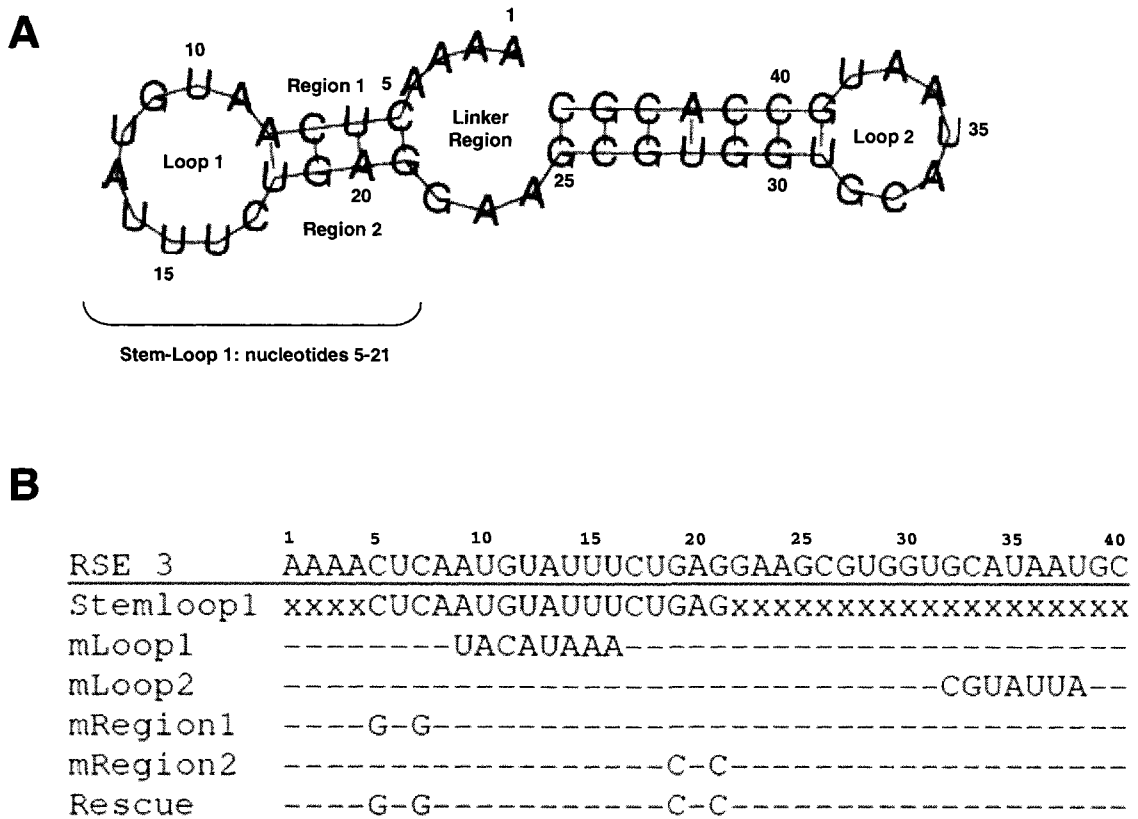


Figure 22 | Predicted secondary structure, primary sequence and mutant constructs of the Sindbis virus RSE 3. A | The structure of the Sindbis virus RSE 3 as computed using the thermodynamic stability prediction program Mfold. The nucleotides are numbered from the 5' to the 3' end, sections of interest are labeled. B | The sequence of RSE 3 is shown underlined at the top of this panel. Nucleotides are numbered in a 5' to 3' manner. The mutant constructs are listed below the RSE 3 wild-type sequence. Mutations are indicated with a change of nucleotide. A dashed line indicates that the nucleotides are identical to that in the top line. Stretches of xxx indicate deleted nucleotides.

mLoop1 and mLoop2 in which the wild-type nucleotides of each loop are mutated to the Watson and Crick complementary nucleotides. We also constructed mRegion1 and mRegion2 include mutations from the wild-type nucleotides of each region to the Watson and Crick complementary nucleotides. A gross deletion of all nucleotides, save 5-21, yielded Stem-Loop 1. Finally, the mutant termed Rescue contains the complementary mutations made in mRegion1 and mRegion2, such that the predicted Stem-Loop 1 structure will be restored. To identify the role of each of these sections of the RSE 3, the mutated constructs were examined in our C6/36 mosquito cell extract *in vitro* deadenylation assay.

As seen in the left panel of Figure 23A, the poly(A) tail of the mLoop1 RNA was rapidly shortened when the RNA was exposed to mosquito cytoplasmic extracts. Over 30% of this RNA was completely deadenylated at three minutes and was nearly completely deadenylated by nine minutes (Figure 23, panel B). In contrast, the poly(A) tail of the mLoop2 RNA was not appreciably shortened, and only a small amount of the RNA was completely deadenylated over the time course of the experiment (Figure 23, panel B). These data indicated that Loop 1, represented by nucleotides 9 through 17, and not Loop 2, was important in the regulation of deadenylation of Sindbis viral RNAs.

Based on the data that nucleotides 9-17 represented a critical sequence to the regulation of deadenylation (Figure 23), we wanted to determine if the full Stem-Loop 1, which included this loop sequence as well as the adjacent stem, would be able to repress deadenylation to the extent that the full RSE 3 did. As seen in the right panel of Figure 24A, the shortening of the poly(A) tail of Stem-Loop 1 is greatly slowed. Less than

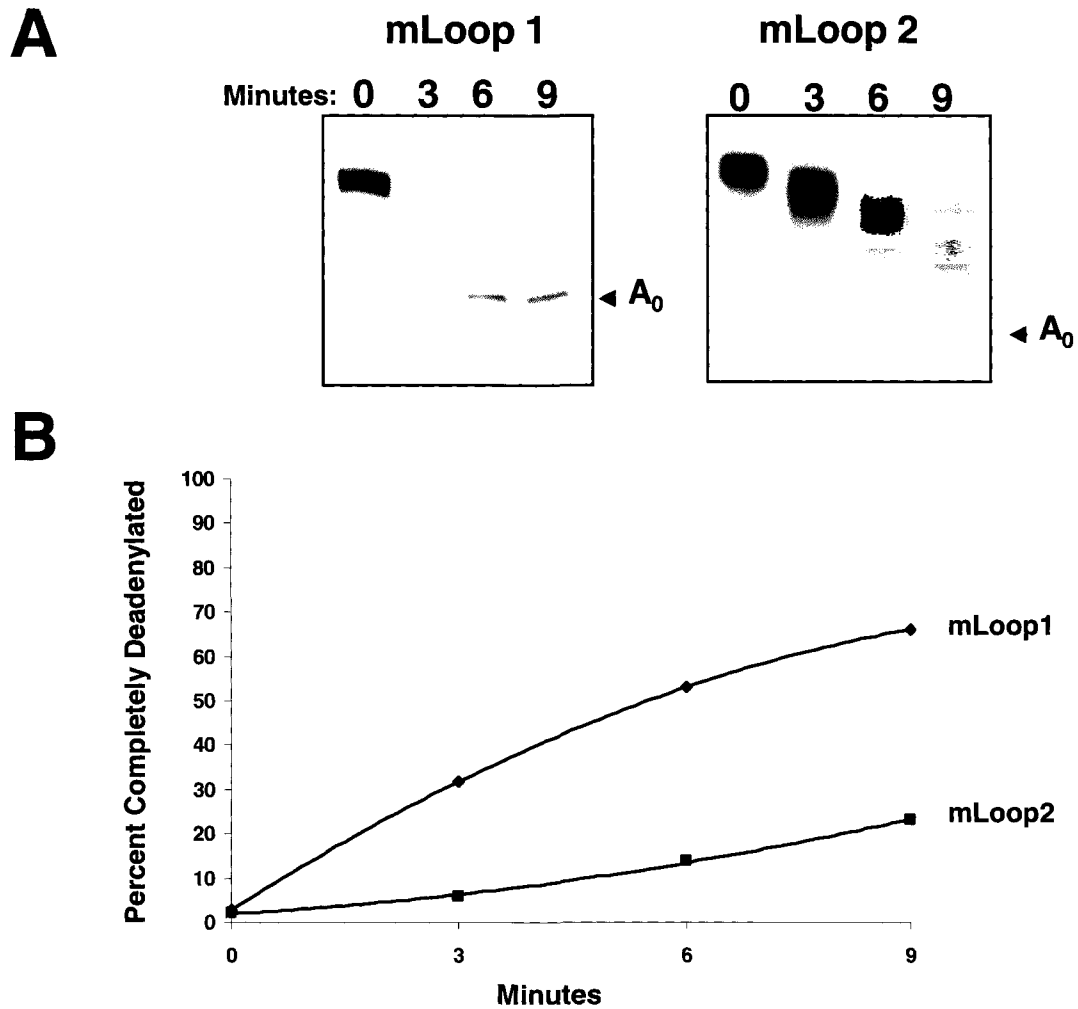


Figure 23 | Sequences in Loop 1 of RSE 3 of Sindbis virus contribute to the repression of deadenylation in C6/36 cytoplasmic extracts. A | The mLoop1 RNA (left panel) or the mLoop2 RNA (right panel) were incubated in an *in vitro* RNA deadenylation/decay system derived from C6/36 S100 cytoplasmic extracts for the indicated times. Reaction products were analyzed on a 5% acrylamide gel containing 7M urea and visualized by phosphorimaging. The marker lane denotes fully deadenylated versions of the input transcript, as indicated by the A_0 arrow. B | Graphical representation of the data presented in panel A.

30% of the RNA is completely deadenylated over the time course of the experiment (Figure 24, panel B). Furthermore, the pattern of deadenylation is similar to the pattern of deadenylation of the full RSE 3 RNA (Figure 24A, left panel). From these data, we chose to focus our efforts on further delineating the critical sequence for stabilization of the viral poly(A) tail within the context of Stem-Loop 1.

To address the importance of structure of the RSE 3 in modulating repression of deadenylation, we were interested in examining the role of Region 1 and Region 2. These regions are predicted to base pair forming the “stem” section of Stem-Loop 1. If structure was indeed critical to the stabilization of the poly(A) tail, then mutating one region of the stem or the other would impair the ability of the stem-loop to form and would consequently then have detrimental effects on regulation of deadenylation. The mutations of Region 1 and Region 2 (outlined in Figure 22) were examined in the context of our C6/36 mosquito cell cytoplasmic extract *in vitro* deadenylation assay.

As seen in the left panel of Figure 25A, the mutation of Region 1 (mRegion1) in the context of the full RSE 3 allowed deadenylation to readily occur on the RNA. In contrast, mutation of Region 2 (mRegion2) in the context of the full RSE 3 had no effect on the RSE 3 function of regulating deadenylation (Figure 25A, middle panel). These data suggested that either the predicted secondary structure was incorrect or that the primary sequence, and not the structure, is important to the function of RSE 3. To examine this further, a double mutant termed Rescue was made in the context of the full RSE 3 that contained both the original Region 1 and Region 2 mutations, thus reconstituting the “stem” portion of the predicted Stem-Loop 1.

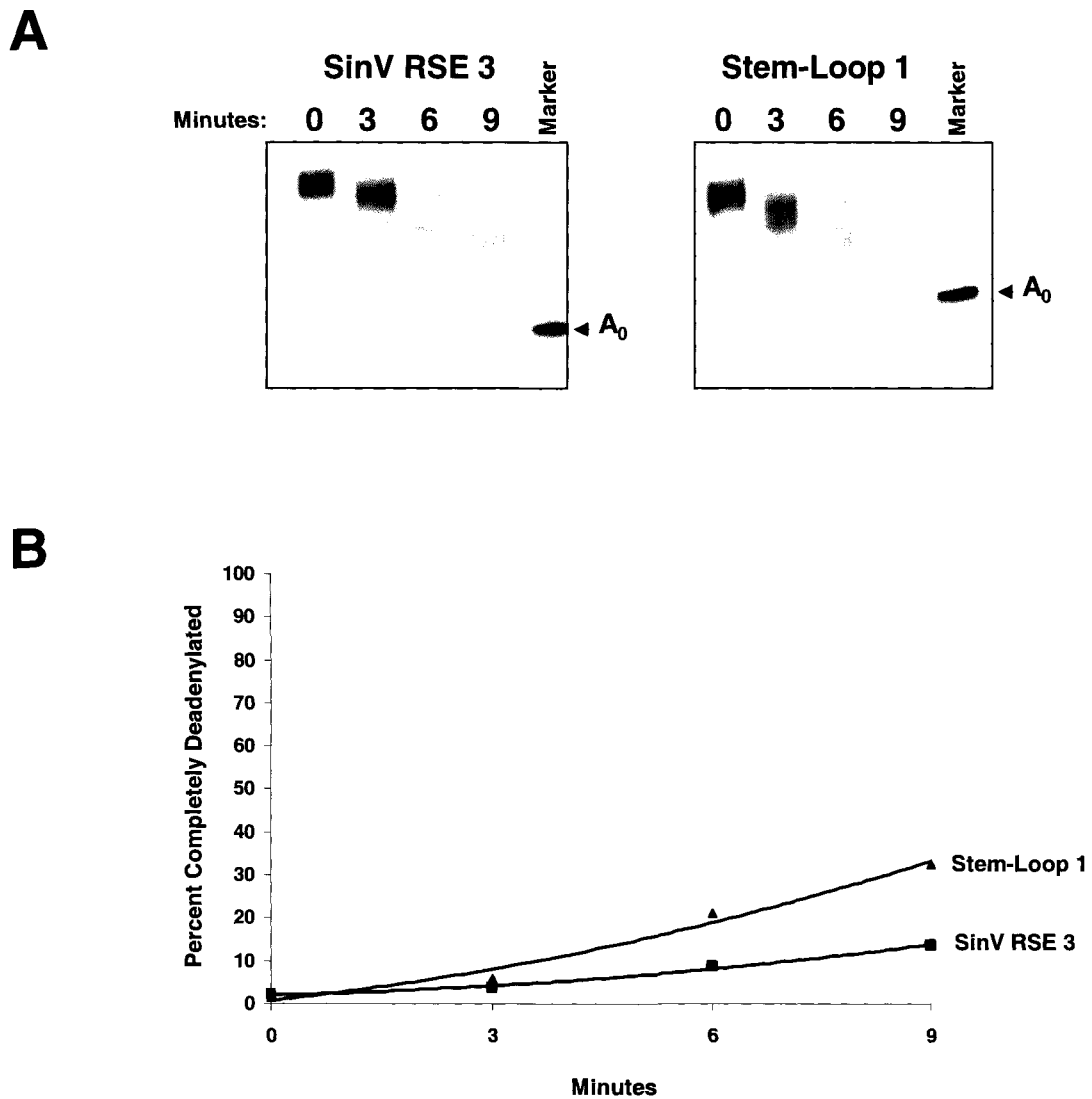


Figure 24 | Stem-Loop 1 of RSE 3 alone represses deadenylation in C6/36 cytoplasmic extracts. A | The polyadenylated reporter RNA (left panel), a variant containing the RSE of Sindbis virus (middle panel) or a variant containing just the Stem-Loop1 of the RSE 3 of Sindbis virus (right panel) were incubated in an *in vitro* RNA deadenylation/decay system derived from C6/36 S100 cytoplasmic extracts for the indicated times. Reaction products were analyzed on a 5% acrylamide gel containing 7M urea and visualized by phosphorimaging. The marker lane denotes fully deadenylated versions of the input transcript, as indicated by the A_0 arrow. B | Graphical representation of the data presented in panel A.

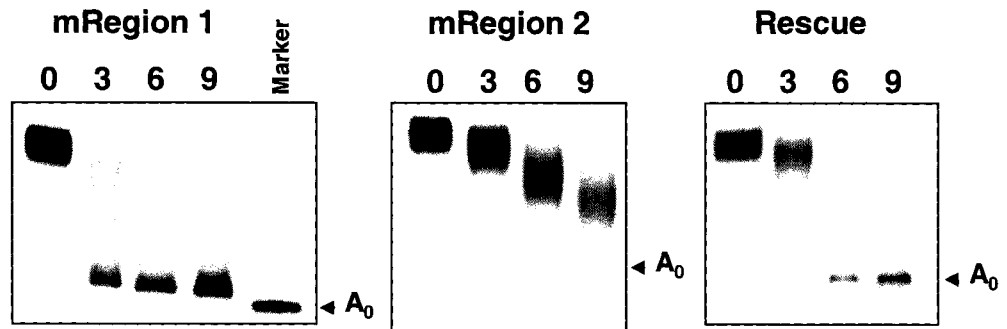
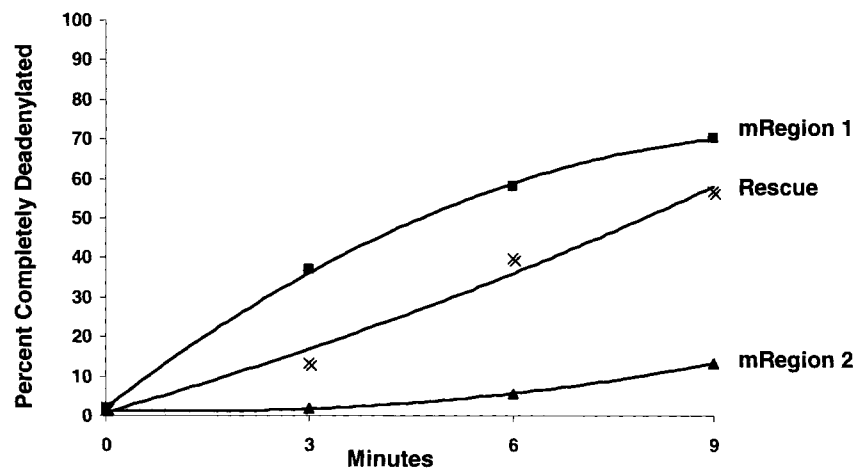
A**B**

Figure 25 | Region 1 of RSE 3 contributes to the repression of deadenylation in C6/36 cytoplasmic extracts. A | The mRegion1 RNA (left panel), the mRegion2 RNA (middle panel) or the Rescue RNA (right panel) were incubated in an *in vitro* RNA deadenylation/decay system derived from C6/36 S100 cytoplasmic extracts for the indicated times. Reaction products were analyzed on a 5% acrylamide gel containing 7M urea and visualized by phosphorimaging. The marker lane denotes fully deadenylated versions of the input transcript, as indicated by the A_0 arrow. B | Graphical representation of the data presented in panel A.

Using the *in vitro* deadenylation assay to assess the status of the poly(A) tail on this final RNA, we found that the Rescue RNA was still readily deadenylated (Figure 25A, right panel). A graphical depiction of these data is represented in panel B of Figure 25.

We conclude from these data that the RSE 3 function in regulation of deadenylation was not restored with the reconstitution of the predicted structure. Therefore, the predicted secondary structure of RSE 3 is likely not correct. However, we cannot exclude the possibility that the primary sequence, and not the secondary structure, represents the protective feature of the RSE 3. Importantly, nucleotides 5- 17 (as outlined in Figure 22) contribute to the function of the Sindbis viral 3' UTR element RSE 3 to regulate repression of deadenylation.

In summary, the results from section II demonstrate that the phenomenon of viral RNA decay is not limited to human cells, but is also observed in other mammalian cells and in mosquito cells. Furthermore, in each cell type examined, we found that the viral RNA is able to repress the action of cellular deadenylases from shortening the viral poly(A) tail during infection. This block of deadenylation was found to be a function of the 3' UTR of the viral RNA as investigated *in vivo* in both mammalian and mosquito cells and *in vitro* in mosquito cell cytoplasmic extracts. Finally, the Repeat Sequence Element 3, and in particular nucleotides 5-17, was found to contribute to repression of deadenylation, thus representing the first evidence for function for this conserved viral RNA 3' UTR element.

DISCUSSION

I. THE DEVELOPMENT OF AN *IN VIVO* VIRAL RNA DECAY ASSAY

This dissertation evolved from an interest in determining what, if any, interaction between viral RNAs and cellular mRNA decay machinery existed in host cells during infection. Published reports on nearly every characterized eukaryotic virus offer insight into viral lifecycles, host cell tropism and immune responses, and counter measures employed by the virus, but nothing concerning the potential role of mRNA decay in viral biology. The prospect of venturing into uncharted waters was very exciting, and so it began.

We chose to work with Sindbis virus for two reasons. First, a cDNA clone which contained a temperature-sensitive mutation in the RNA-dependent RNA polymerase was readily available. This would enable us to both utilize the ts6 mutation to turn off viral RNA synthesis and also gave us a means for easily mutating additional viral sequences for our studies. Second, the virus can safely be worked with under biosafety level 2 conditions. This was advantageous as we could conduct our experiments using a biosafety cabinet within our laboratory. Therefore, Sindbis virus afforded an easy to manipulate and convenient system with which to examine viral RNA decay.

To examine Sindbis viral RNA turnover during infection, we developed an assay that allowed us to shut off viral RNA synthesis with minimal off-target effects on the host cell. Using the aforementioned ts6 strain of Sindbis virus, the assay began with a one hour inoculation of the cells, the infection was then allowed to progress for an additional ten hours. Viral RNA synthesis was inhibited by shifting the infected cells to the non-permissive temperature for a period of one hour. It is of interest to point out that to aid in

the temperature shift, pre-heated medium was added to each individual well prior to the plates being switched to 40°C. By assaying the viral RNA over a short interval time course, we found that this method did not immediately shut off viral RNA synthesis, but took approximately one hour at 40°C for the viral polymerase to cease functioning. This could possibly be due a number of items. First, the temperature-sensitive mutation is due to a point mutation which causes a change in the amino acid sequence of the viral RNA polymerase. It may be that this mutation did not immediately inactivate the protein when the cells were shifted to the non-permissive temperature. Second, the plates that were used in this assay may retain ambient temperature for a period of time. Finally, the delay in inactivity of the viral RNA polymerase could be due to the fact that heated air does not rapidly transfer heat, and that any time the incubator was opened and closed, the incubator would need to recover from the loss of temperature.

From there, the sampling of viral RNAs occurs over the specified time course. At each time point cells are collected in Trizol reagent (Invitrogen) and total RNA is extracted. Following RNA purification, the viral RNA can be assayed by a number of procedures; for our analysis we used both the RNase Protection Assay and qRT-PCR.

While the RNase Protection Assay, like a northern blot, allows for the actual visualization of the size and integrity of the RNA that is in question, qRT-PCR reigns supreme over this traditional method for three reasons. First, results can be assessed in hours as opposed to days. Second, it does not require radiolabeled probes and instead relies on fluorescence detection. Finally, the most important benefit, particularly to this project, is that qRT-PCR only requires a small amount of RNA for effective analysis and

thus demonstrates increased sensitivity. For these reasons, qRT-PCR was favored over the RPA, although both methods were employed in our studies.

Although this assay was originally designed with Sindbis virus in mind, it can be very easily adapted to examine the half-lives of other positive-sense viral RNAs during infection in cultured host cells. For example, temperature-sensitive mutations in the viral RNA synthesis machinery have been characterized for influenza A, Sendai, vesicular stomatitis, polio and dengue viruses. As influenza A and dengue viruses contribute to a high degree of morbidity and mortality world-wide, it would be particularly beneficial to examine these viruses in the context of viral RNA stability as it could potentially lead to much needed therapeutics.

II. SINDBIS VIRAL RNA STABILITY IS CORRELATED TO VIRAL GROWTH EFFICIENCY IN HOST CELLS

The development of the *in vivo* viral RNA decay assay gave us a precise tool for determining the rate of viral RNA turnover during infection in many different host cell types. We chose to work with two very well known Sindbis host cell lines, the mammalian BHK-21 and the mosquito C6/36, as well as two less frequently used human cell lines, HeLa and 293T cells. Interestingly, the genomic and subgenomic RNAs showed variably levels of stability depending on infected cell type. A measurable half-life of the genomic RNA was observed only in the HeLa cell line. In contrast, subgenomic RNA decay was evident in the C6/36 mosquito cells, the BHK-21 mammalian cells, as well as in the HeLa human cells.

The variably decay rates of the Sindbis viral RNAs suggest three main points. First, the genomic and the subgenomic RNAs are not decayed equally during infection.

This was not a surprising find. The subgenomic RNA is only translated during infection, whereas the genomic RNA replicated and packaged. The RNAs likely have very different mRNP structures which could explain why the genomic RNA is uniformly more stable than the subgenomic RNA during infection in the C6/36, the BHK-21 and the HeLa cell line.

Second, the turnover rates of the viral RNAs in the human 293T cells were minimal during the time course assessed and thus we could not accurately calculate the half-lives. This could be due to inherent differences in the RNA decay machinery from cell line to cell line, even within the same host cell type. For example, it has been observed that cytoplasmic extracts made from 293T cells do not exhibit deadenylation activity unless the additional factor TTP is added. It may be that the concentration of deadenylase accessory proteins is very low in 293T cells, or perhaps such factors are localized to the nucleus, thus preventing deadenylation activity in 293T cytoplasmic extracts.

Finally, the rate of Sindbis viral RNA decay we observed during infection in the HeLa and 293T cell lines correlate with the efficiency of viral replication as determined by a one-step viral growth curve. Specifically, the viral RNAs were decayed rapidly in HeLa cells, and accordingly the virus replicated very poorly in this cell type. In contrast, there was no observed decay of the viral RNAs in 293T cells, and interestingly, the virus replicates very well in this cell type. This correlation suggests that viral RNA decay may be a novel factor of viral biology. Furthermore, these data offer the first evidence that mRNA decay potentially functions as a host cell restriction factor against a virus, and more specifically that a mechanism of host cell restriction against Sindbis virus in the HeLa cell line may include viral RNA decay.

It's important to discuss the reasons we chose to specifically focus on Sindbis viral replication in HeLa cells compared to the 293T cells. First, these two cell lines displayed the greatest difference in Sindbis viral RNA stability, as compared to the results in BHK-21 and C6/36 cell lines. Additionally, the growth curves of the virus in the BHK-21 and C6/36 cell lines are already well-established in the literature. Second, published reports in HeLa cells are inconclusive as to the ability of the cell to support viral growth, while the 293T cell line was shown to support robust viral growth. Finally, the study of RNA decay as a novel mechanism for host cell restriction is most beneficial in human cells. In this way the basic research conducted here could potentially be used in the development of small molecule drugs that could specifically target alphaviral RNAs for decay, and thus prevent further replication and virion production. This type of novel antiviral therapeutic would ultimately prevent infection from progressing and spreading.

It is well accepted that Sindbis virus replicates in a wide range of cultured cells. Therefore, future studies could aim to examine the half-life of the viral RNAs in other host cell types, such as chicken embryo fibroblasts. These cells, which are used frequently in Sindbis studies, might yield additional information for two reasons. First, they are a primary cell line and so accurately represent the host cell than do propagated cell lines. Second, these cells represent the avian and thus non-mammalian vertebrate host of the virus. Finally, the study of viral RNA stability for other viruses, particularly ones of importance to human health and disease, may give better insight into the biology of these viruses and could open the door to novel treatments.

III. CELLULAR mRNA DECAY ENZYMES CONTRIBUTE TO THE TURNOVER OF SINDBIS VIRAL RNAS

With the evidence that viruses interact with cellular mRNA decay machinery during infection, and that the interaction contributed to the virus growth potential, we began to work towards understanding the pathway of RNA decay that was responsible for the targeting of the viral RNA. Cellular mRNA decay is vast and intricate process. It contains multiple pathways designed to deal with a wide range of RNA substrates, and is complicated by cross-talk between pathways and redundancy among enzymes with the same or similar functions. Therefore we aimed to systematically analyze the role of major RNA decay factors in the turnover of viral RNAs.

The major pathway of decay in eukaryotes is deadenylation-dependent. Therefore, we chose to first examine the role of representative proteins for each major step in this dominant mammalian mRNA turnover mechanism. siRNAs were used in HeLa cells to target the proteins PARN, Dcp2, Exo9 or Xrn1, which represent the steps of deadenylation, decapping, 3' to 5' exonucleolytic decay, and 5' to 3' exonucleolytic decay. We found that an increased stability of the genomic RNA was apparent and statistically significant in the Δ Exo9 and Δ Xrn1 cells, but not in either the Δ Dcp2 or the Δ PARN cells. Interestingly, only the Δ Exo9 cells exhibited a statistical increase in the stability of the subgenomic RNA.

While these data suggest an important role for the mammalian exonucleases in the turnover of Sindbis viral RNAs, alone they do not offer insight into the actual pathway of viral RNA decay. This is because exonucleases play vital roles in many pathways in addition to the deadenylation-dependent RNA decay pathway. In addition, while the expression of each protein was significantly knocked down (76-95%), it is difficult to

assess the impact of the remainder of the mRNA that was not silenced, and which could have played a role in the Δ PARN and perhaps the Δ Dcp2 cells. Finally, the redundancy within the cellular mRNA decay pathways may have complicated our analysis. Specifically, the knock down of the expression of PARN was very high at 95%, but deadenylation activity could still be maintained by the other mammalian deadenylases including the Ccr4-Caf1 or Pan2-Pan3 complexes. However, as will be discussed further, deadenylases were subsequently shown to not act on Sindbis viral RNAs, and so this result was subsequently expected.

To continue our systematic analysis of decay factors, we chose to examine alternative RNA decay pathways that require exonucleases. Both RNAi and Nonsense-Mediated Decay (NMD) have the potential to interact with the Sindbis viral RNAs and rely on the activity of Xrn1 and the exosome. Therefore, we stably knocked down expression of a major protein in RNAi and also in NMD, Dicer and Upf1 respectively. When Dicer was knocked down, both the genomic and subgenomic RNAs of Sindbis virus exhibited increased stability when compared to a control cell line. When Upf1 was knocked down, there appeared to be no change in the half-life of the viral RNAs compared to the control cells. The increase in the half-life of the viral RNAs in the Δ Dicer cells was statistically significant with a confidence interval of 95%, but the half-lives in Δ Upf1 cells were not did not change significantly from the control cell line.

It could be that as Sindbis viral RNAs do not have a nuclear experience, they may in fact be immune to NMD. However, these results by no means suggest that other viruses do not interface with the NMD factors. NMD likely plays a role in the stability retroviral RNA during infection of mammalian cells. For example, HIV-1 produces

transcripts which remain unspliced during export from the nucleus to the cytoplasm. In order to ward off recognition as an aberrant mRNA to the NMD proteins, the virus might employ a means for tricking the cell into believing it is not merely a faulty cellular transcript. In this manner, it could be advantageous to examine the stability of HIV-1 transcripts.

As with the siRNA transient knock down cells, the knock down efficiencies of Dicer and Upf1 were acceptable (77% & 70% respectively), but significant activity likely remained. Additionally, it is difficult to obtain high knock down rates of essential factors in stable cell lines as the knock down may compromise growth. To study the role of these proteins further it would be advantageous to transiently knock down expression, or perhaps use an inducible system. In this way, high knock down percentages could be obtained and likely tolerated. A re-examination of the role of both Upf1 and Dicer in the *in vivo* viral RNA decay assay may prove a more pronounced role for Dicer, and potentially a role for Upf1 may be shown to exist.

These data acquired from the stably knocked down cell lines nicely complemented what was observed in the transient knock down cell lines. Exo9, Xrn1 and Dicer are all active in the pathway of RNAi, and thus the data point to effective mammalian RNAi as an antiviral mechanism. It is well accepted that RNAi is an important antiviral pathway in insect cells, although its importance in mammalian cells, where Dicer is most readily associated with the processing of microRNAs, is unclear. Therefore, the discovery that mammalian RNAi is functional as an antiviral was very exciting. More evidence will be required to confirm the role of RNAi as an antiviral mechanism during infection. This can be accomplished with a variety of experiments.

First, knocking down expression of other RNAi proteins would be necessary. A possible candidate would be Argonaute 2 which represents the major catalytic enzyme of the RNAi pathway. Second, examining the decay of viral RNAs in the absence of infection may offer insight into RNAi. Specifically, cells could be transfected with *in vitro* transcribed viral RNA with or without an siRNA. The half-life from such experimentation could be compared to the half-life of the viral RNA in cells that also receive a modified complimentary oligo to bind up the siRNA and prevent it from its incorporation into the RISC. Finally, concurrently knocking down the expression of multiple enzymes within a given pathway at once would be valuable. It would be useful to transiently knock down Exo9 and Xrn1 in the context of the Dicer stable knock down cell line, or to knock down both the catalytic proteins of the RNAi machinery (Dicer and Ago2) to highlight a more direct role of this decay pathway in the stability of the viral RNA. This would ensure that the experimental limitations in knock down efficiency and enzymatic redundancy would be far less of a concern, enabling straightforward analysis of the half-life data.

To take our experimentation with RNA decay enzymes one step further, transiently over-expressing the exonuclease Xrn1, the exosome, or Dicer in the 293T cell line could perhaps alter the stability of the viral RNAs in this cell type by inducing decay. If this was found to be the case, it might be possible to target viral RNAs specifically for decay by expression of a viral capsid-RNA decay enzyme fusion protein within the host cell. Theoretically, the fusion protein could selectively target the viral RNA for decay without negatively affecting the host cell. If this can be shown to work effectively, it could become the basis for novel treatments of alphaviral diseases.

To conclude this section, it will be important in future studies to further demonstrate the role of mRNA decay enzymes and pathways on functional viral biology. This could be assessed using extended time courses to evaluate the effect of specific decay enzymes on viral growth. And as a final note, while our data point to the role of the exonucleases Exo9 and Xrn1 in viral RNA decay in HeLa cells, it could be that different cell lines employ different mechanisms for viral RNA turnover. Thus, it will be important to examine these enzymes and pathways in other host cell types as well.

IV. DEVELOPMENT OF THE LINKER LIGATION-MEDIATED POLY(A) TAIL ASSAY

RNase H/northern blotting is a well-established method for visualizing poly(A) tail lengths. This technique works especially well for abundant RNAs, but the drawback is that it requires micrograms of total RNA and it is labor and time intensive. In our analysis, we found that the Sindbis $\Delta 3'$ UTR virus did not replicate nearly as well as the wild-type virus in either the mammalian or the mosquito cell lines examined, consistent with published literature (Kuhn *et al.*, 1990). Consequently, the poly(A) tail of the $\Delta 3'$ UTR viral RNA collected from the *in vivo* viral RNA assay was difficult to assess using the RNase H/northern blot assay. In order to properly evaluate the length of the poly(A) tail of the mutated virus in BHK-21 cells we had to use 20X the concentration of RNA as compared to wild-type Sindbis virus RNA. Furthermore, we were unable to successfully use the RNase H/northern blot to visualize changes in the poly(A) tail of the mutated viral RNA from mosquito cells. Therefore, we developed a method that would be

sensitive enough to resolve` changes in the poly(A) tail in such low concentration samples.

A described PCR-based technique in the LM-PAT method was adapted for use in our assay (Salles *et al.*, 1999). We selected this technique because the amplification step allows for visualization of the RNA of interest in even low concentration samples. The remainder of the LM-PAT assay however, which centers on the binding of oligo(dT) to the poly(A) tail to be assessed was unsuitable for measuring short poly(A) tails. To formulate our method, we made use of a modified RNA oligonucleotide, termed Linker-3, rather than oligo(dT). The Linker-3 oligo contains a 3' terminal dideoxy-C and is 5' adenylated, and thus is immune to self-ligation and is pre-activated for ligation under ATP-free conditions. Ligation conditions that do not include ATP are advantageous in that it prevents circularization of RNAs or inappropriate ligation of individual RNA to each other.

A useful aspect of the ligation method is that it can be modified to accommodate the investigation of any RNA of interest, making the implications of this assay wide ranging. Specifically, it is very useful for the analysis of samples with a low concentration of the RNA of interest. Efforts to take this assay further could result in the utilization of modified linkers and PCR-based amplifications to design similar assays, which would trap RNA decay intermediates. This would be useful for providing a visual means for identifying RNAs that are degraded in a 5' to 3' manner or those which are degraded via endonucleolytic decay.

In summary, the LLM-PAT method is highly sensitive to even small changes in poly(A) tail dynamics. The use of Linker-3 matched with the PCR-based amplification

technique allows the assay to accommodate even low concentrations of target RNAs. Finally, the LLM-PAT is useful to assess the poly(A) tail of different RNAs, and therefore is generally applicable for studies within a wide range of disciplines.

V. SINDBIS VIRUS REPRESSES DEADENYLATION OF ITS RNAs DUE TO A NOVEL FUNCTION OF THE VIRAL 3' UTR

Deadenylation of cellular transcripts is often regulated by the 3' UTR of the RNA, and more specifically by 3' UTR *cis*-elements. Sindbis viral RNAs function like cellular mRNAs in that they are translated and subject to RNA decay. The viral RNAs are also capped at the 5' terminus, contain a 5' and 3' UTR, and a poly(A) tail. These characteristics are important in the regulation of both translation and RNA decay for mammalian mRNAs, which led to our interest in determining if the mechanism of viral RNA decay was the same as cellular mRNA decay, in that it was deadenylation-dependent. Although our Δ PARN cell lines showed the change in the half-lives of the viral RNAs to be statistically insignificant, we could not confidently state that the deadenylation function was completely knocked out due to enzymatic redundancy. Therefore, we were interested in directly assessing the status of the viral poly(A) tail during infection.

The RNA samples collected from the *in vivo* viral RNA decay assay during infection with wild-type Sindbis virus in HeLa, 293T, BHK-21 and C6/36 cell lines, were all subjected to RNase H/northern blotting and analyzed. We found that the wild-type virus was able to effectively block shortening of the poly(A) tail in all four host cell types examined. While the data were very strong, it was difficult to determine the meaning of

the repression of deadenylation. Was it that the virus truly was not a substrate of the major pathway of cellular mRNA decay? Or perhaps was it that virus employed a means of protecting its viral RNA from deadenylation?

To address these questions we stripped the virus of the 3' UTR. Based on cellular mRNA decay studies we hypothesized that the viral 3' UTR, like cellular 3' UTRs, to be the means of protection. We were very pleased to find that using the RNase H/northern blot technique, the Δ 3' UTR viral RNA collected during infection of BHK-21 cells exhibited deadenylation, and furthermore, using the newly developed LLM-PAT assay, the same results were found for the Δ 3' UTR virus in C6/36 mosquito cells. In addition, the repression of deadenylation was then recapitulated using our *in vitro* mosquito cell cytoplasmic extract deadenylation assay, allowing us a supplementary tool for studying this phenomenon.

These data effectively defined a novel role of the viral 3' UTR as a stability element and demonstrated that the interface between the viral RNAs and the host cell decay machinery is dynamic. Interestingly, they also confirmed that PARN, or any deadenylase for that matter, did not function to shorten the poly(A) tail of wild-type Sindbis. Therefore, the wild-type Sindbis viral RNAs were not subject to the deadenylation-dependent RNA decay pathway—the major decay pathway of the cell—and rather exhibited a pattern of decay that is vastly different to the pattern found for the majority of cellular mRNAs.

The 3' UTR of the Sindbis viral RNA could be blocking deadenylation due to the function of *cis*-elements, cellular *trans*-factors, or likely a combination of these features. To this end, our lab has begun to identify the binding of mosquito cellular factors in

relation to regulation of deadenylation. Published and unpublished data demonstrates that the mosquito homolog of HuR (termed ELAV) binds to the URE of the 3'UTR of Sindbis virus and may contribute to the block in deadenylation observed *in vitro* (K. Sokoloski, Personal Communication).

Interestingly, the absence of the 3'UTR permitted deadenylases to act on the viral RNA, but it did not clearly result in a change of stability. Due to poor replication efficiencies, we were unable to accurately measure the half-life of the Δ 3'UTR virus using the RPA. However, based on our experience working with this strain and from one-step viral growth curves within the published literature, it is apparent that the 3'UTR is required for efficient replication. So perhaps the ability of the 3'UTR to protect against deadenylation is not to protect against the major RNA decay pathway, as we hypothesized originally, but to ensure the poly(A) tail remains intact for efficient translation. This speculation is supported in part by the discovery that RNAi is likely the pathway responsible for Sindbis viral RNA decay. In this pathway, the presence or absence of the 3'UTR would not necessarily affect the ability of the pathway to target the viral RNA for endonucleolytic cleavage, and so the 3'UTR would not function as a major stability factor against RNA decay.

The ability of the 3'UTR to repress deadenylation was novel, and merited experimentation that would reveal which regions of the 3'UTR sequence were required to effectively produce this result. Therefore, we shifted our studies from *in vivo* to *in vitro*. Our laboratory has previously described two cytoplasmic extract systems, HeLa and C6/36 mosquito which faithfully recapitulate the activity of cellular deadenylases. Using these described systems, we examined the ability of the 3' UTR to block deadenylation.

As was previously shown in our lab (Opyrchal, 2005), we confirmed that the C6/36 mosquito cell extracts dependably recapitulated the ability of the viral 3' UTR to block deadenylation observed *in vivo*, and that this regulation was not reproduced in HeLa cell cytoplasmic extracts. Perhaps altering reaction conditions or extraction methods could be used to overcome these technical limitations of our current HeLa cell *in vitro* RNA decay system, but these were not pursued in this project. We did pursue the observation that the mosquito cell extract system could be used to easily study the contribution of specific regions of the Sindbis viral 3' UTR to repression of deadenylation.

In conclusion, Sindbis virus RNA is able to deflect the activity of the major cellular deadenylases. This fine-tuned active repression of deadenylation is due to the presence of the 3' UTR on the viral RNA. It is difficult to consider that Sindbis virus is the only virus that has evolved a means for protecting its viral RNAs from decay. Likely, other positive-strand RNA viruses employ similar means. To this end, there are positive-strand RNA viruses, like flaviviruses, which do not contain poly(A) tails. There are also viruses, like polio, which do not contain 5' cap structures. Without these defining mRNA stability features, it is curious that such viruses survive in host cells if they do not possess a means to protect their viral RNAs during infection.

VI. THE REPEAT SEQUENCE ELEMENT OF SINDBIS VIRUS CONTRIBUTES TO THE REPRESSION OF DEADENYLATION *IN VITRO*

The Sindbis viral 3' UTR is a potent regulator of deadenylation during infection and also as demonstrated *in vitro*. Similar to cellular 3' UTRs, which each contain

specific elements, the 3' UTR of Sindbis virus can be defined by its elements. These include a conserved sequence element (CSE) which is composed of 19 nucleotides, is located immediately before the poly(A) tail and has been shown to be critical to viral replication. There is also a U-rich element (URE) which is directly upstream of the CSE and consists of 40 nucleotides. Finally, the repeated sequence elements (RSEs) are each 40 nucleotides in length and are separated from one another by approximately 50 nucleotides. RSEs of various compositions are found in every alphavirus species, yet the function has remained elusive. We were interested in examining the role of the RSE in the ability of the 3' UTR to block deadenylation.

Using the mosquito cell *in vitro* deadenylation system, we found a single RSE was able to repress shortening of the poly(A) tail to same extent as the full Sindbis viral 3' UTR. This provided the first evidence that the repeat sequence elements within the Sindbis viral 3' UTR exhibited a function. Further studies to delineate the precise sequence required for this repression were also completed, and the minimal sequence necessary to uphold the function of the RSE was found to be 13 nucleotides. It is of interest to note that while our mutational analysis of the RSE 3 was based on the predicted secondary structure of the element, mutations that abolished the predicted structure did not affect the ability of the RSE 3 to block deadenylation. Thus the predicted structure could be inaccurate, although an alternative explanation is that the primary structure plays the predominant role in the function to repress deadenylation. Collectively, these data provide evidence that the Sindbis virus RSE within the viral 3' UTR influences the efficiency of deadenylation on viral RNAs, and that the sequence in the 5' portion of the element appears to be necessary for the observed repression.

Although we only examined RSE 3 in detail, RSE 1 and RSE 2 likely exhibit the same function. This speculation is based on the fact that the specific nucleotide stretch from 5 to 17 within RSE 3 that was observed to contribute to the block in deadenylation is 92% identical to the corresponding nucleotide compositions of RSEs 1 and 2. The exception to this conservation is that nucleotide 8 is represented by a G in RSEs 1 and 2, while it is an A in RSE 3 (Figure 16, panel A). Interestingly however, a closer examination of the sequence and the predicted structure does demonstrate that nucleotide 8 (A) of RSE 3 likely base pairs to nucleotide 18 (U). Accordingly, the compensatory nucleotide 18 (C) of the primary sequence of RSEs 1 and 2 indicate that this binding is conserved, even if the primary sequence at these nucleotides is not. Therefore, determining the actual structure of RSEs 1, 2, and 3 using RNase digestion or chemical modification studies, would likely confirm or refute the role of secondary structure as a conserved feature of these elements and potentially as a factor to repress deadenylation. Additionally, to better understand the role of the RSE 3 within context of the other viral 3' UTR elements, it would be important to examine different combinations of elements in the *in vitro* deadenylation system. From these data, elements that show potential for exhibiting a role in repression of deadenylation could be studied in the context of the full viral sequence either as a deletion mutation or as an add back element to the Δ 3' UTR virus used in this study.

As mentioned above, the *in vitro* system is an excellent way to quickly assess the role of an arboviral 3' UTR in the regulation of deadenylation. From there, it would also be very easy then to examine elements in the 3' UTRs of other viruses, such as the RSEs in other alphaviruses. This information could help to determine if the ability of the

Sindbis viral 3' UTR to repress deadenylation is conserved among all viruses that have lifecycles maintained between mosquitoes and mammals. This could also help to determine if viral 3' UTR elements like the RSE are actually conserved in function across a genus, or even across a family.

CONCLUSIONS

The work presented here demonstrates the existence of an active interface between the viral RNAs in the lifecycle of Sindbis virus and the mRNA decay enzymes within the host cell. First, with the development of the *in vivo* viral RNA decay assay, we were able to accurately assess the rate of alphavirus RNA decay during infection in multiple cell types. This method fills a gap that existed for tools to readily study the stability of viral RNAs during infection. Second, using this assay we identified a correlation between Sindbis viral RNA stability and viral replication efficiency. This is the first demonstration of mRNA decay functioning as a host cell restriction factor against any virus, and furthermore is the first evidence to correlate the mechanism of HeLa host cell restriction against Sindbis virus.

With the establishment that Sindbis viral RNAs are in fact targeted for decay during infection, it was important to begin studying the mechanism of both the cellular and viral contribution to the interface. The third major finding of this dissertation was the result demonstrating that the 5' to 3' exonuclease Xrn1, component 9 of the exosome (Exo9), and the endonuclease Dicer all contribute to Sindbis viral RNA decay. Therefore, the RNAi pathway likely plays an important role in the decay of Sindbis viral RNAs during infection of HeLa cells. These data will undoubtedly be valuable in further studies to delineate the exact mechanism of viral RNA decay.

To continue our effort to understand the mechanism of viral RNA decay, we wanted to accurately examine the status of the viral RNA poly(A) tail during infection. As growth of the mutated virus yielded low concentrations of viral RNAs, we developed the LLM-PAT method. This assay, as the fourth achievement of this dissertation,

provided a more sensitive manner in which to study poly(A) tail dynamics, and is generally applicable for studies within a wide range of disciplines. The fifth major discovery of this dissertation was the importance of the viral 3' UTR to the repression of the action of cellular deadenylases on the viral poly(A) tail *in vitro* in mosquito cell extracts and also *in vivo* during infection of the HeLa, 293T, BHK-21, and C6/36 cell lines. This point is particularly significant as it demonstrates that the Sindbis viral RNAs are not subject to the major decay pathway of the cell, and rather exhibit a pattern of decay which is vastly different from that found for the majority of cellular mRNAs. Finally we have shown that the third of three Repeat Sequence Elements within the Sindbis viral 3' UTR contributes to the regulation of deadenylation of viral RNAs, providing the first evidence for function of this conserved alphaviral element.

In conclusion, Sindbis viral RNAs interact with the host cell RNA decay machinery and the virus protects its RNAs to ensure a productive infection. We are reminded that a complete understanding of viral biology must include a comprehensive knowledge of all aspects virus-host interactions. The work presented in this dissertation provides evidence that a comprehensive knowledge of virus-host interactions is incomplete without defining the role of mRNA decay in viral RNA stability and growth. With a better understanding of viruses comes more advanced ways to deal with infections, and with more advanced treatments, we can minimize the impact viruses have on veterinary and human health.

LITERATURE CITED

- Ahola,T. & Kaariainen,L. (1995). Reaction in alphavirus mRNA capping: formation of a covalent complex of nonstructural protein nsP1 with 7-methyl-GMP. *Proc.Natl.Acad.Sci.U.S.A*, 92(2), 507-511.
- Albert,T.K., Lemaire,M., van Berkum,N.L., Gentz,R., Collart,M.A., & Timmers,H.T. (2000). Isolation and characterization of human orthologs of yeast CCR4-NOT complex subunits. *Nucleic Acids Res.*, 28(3), 809-817.
- Alexopoulou,L., Holt,A.C., Medzhitov,R., & Flavell,R.A. (2001). Recognition of double-stranded RNA and activation of NF-kappaB by Toll-like receptor 3. *Nature*, 413(6857), 732-738.
- Aliperti,G. & Schlesinger,M.J. (1978). Evidence for an autoprotease activity of sindbis virus capsid protein. *Virology*, 90(2), 366-369.
- Allmang,C., Petfalski,E., Podtelejnikov,A., Mann,M., Tollervey,D., & Mitchell,P. (1999). The yeast exosome and human PM-Scl are related complexes of 3' --> 5' exonucleases. *Genes Dev.*, 13(16), 2148-2158.
- Bakheet,T., Williams,B.R., & Khabar,K.S. (2006). ARED 3.0: the large and diverse AU-rich transcriptome. *Nucleic Acids Res.*, 34(Database issue), D111-D114.
- Baltimore,D. (1971). Expression of animal virus genomes. *Bacteriol.Rev.*, 35(3), 235-241.
- Belloc,E., Pique,M., & Mendez,R. (2008). Sequential waves of polyadenylation and deadenylation define a translation circuit that drives meiotic progression. *Biochem.Soc.Trans.*, 36(Pt 4), 665-670.
- Beloso,A., Martinez,C., Valcarcel,J., Santaren,J.F., & Ortin,J. (1992). Degradation of cellular mRNA during influenza virus infection: its possible role in protein synthesis shutoff. *J.Gen.Virol.*, 73 (Pt 3), 575-581.
- Bergman,N., Moraes,K.C., Anderson,J.R., Zaric,B., Kambach,C., Schneider,R.J., Wilusz,C.J., & Wilusz,J. (2007). Lsm proteins bind and stabilize RNAs containing 5' poly(A) tracts. *Nat.Struct.Mol.Biol.*, 14(9), 824-831.
- Bernstein,E., Caudy,A.A., Hammond,S.M., & Hannon,G.J. (2001). Role for a bidentate ribonuclease in the initiation step of RNA interference. *Nature*, 409(6818), 363-366.
- Berthomme,H., Jacquemont,B., & Epstein,A. (1993). The pseudorabies virus host-shutoff homolog gene: nucleotide sequence and comparison with alphaherpesvirus protein counterparts. *Virology*, 193(2), 1028-1032.

- Bessman,M.J., Frick,D.N., & O'Handley,S.F. (1996). The MutT proteins or "Nudix" hydrolases, a family of versatile, widely distributed, "housecleaning" enzymes. *J.Biol Chem.*, 271(41), 25059-25062.
- Bick,M.J., Carroll,J.W., Gao,G., Goff,S.P., Rice,C.M., & MacDonald,M.R. (2003). Expression of the zinc-finger antiviral protein inhibits alphavirus replication. *J.Virol.*, 77(21), 11555-11562.
- Brewer,G. & Ross,J. (1988). Poly(A) shortening and degradation of the 3' A+U-rich sequences of human c-myc mRNA in a cell-free system. *Mol.Cell Biol.*, 8(4), 1697-1708.
- Brouwer,R., Allmang,C., Raijmakers,R., Van Aarssen,Y., Vree,E.W., Petfalski,E., Van Venrooij,W.J., Tollervy,D., & Pruijn,G.J. (2000). Three novel components of the human exosome. *J Biol.Chem.*
- Brown,C.E., Tarun,S.Z., Jr., Boeck,R., & Sachs,A.B. (1996). PAN3 encodes a subunit of the Pab1p-dependent poly(A) nuclease in *Saccharomyces cerevisiae*. *Mol Cell Biol*, 16(10), 5744-5753.
- Buckley,S. (1964). Applicability of the HeLa (Gey) Strain of Human Malignant Epithelial Cells to the Propagation of Arboviruses. *Proc.Soc.Exp.Biol.Med.*, 116, 354-358.
- Buhler,M., Steiner,S., Mohn,F., Paillusson,A., & Muhlemann,O. (2006). EJC-independent degradation of nonsense immunoglobulin-mu mRNA depends on 3' UTR length. *Nat.Struct.Mol.Biol.*, 13(5), 462-464.
- Burge,B.W. & Pfefferkorn,E.R. (1966). Isolation and characterization of conditional-lethal mutants of Sindbis virus. *Virology*, 30(2), 204-213.
- Busslinger,M., Portmann,R., & Birnstiel,M.L. (1979). A regulatory sequence near the 3' end of sea urchin histone genes. *Nucleic Acids Res.*, 6(9), 2997-3008.
- Carvalho,M.G. & Freitas,M.S. (1988). Effect of continuous heat stress on cell growth and protein synthesis in *Aedes albopictus*. *J.Cell Physiol*, 137(3), 455-461.
- Castelli,J.C., Hassel,B.A., Maran,A., Paranjape,J., Hewitt,J.A., Li,X.L., Hsu,Y.T., Silverman,R.H., & Youle,R.J. (1998). The role of 2'-5' oligoadenylate-activated ribonuclease L in apoptosis. *Cell Death.Differ.*, 5(4), 313-320.
- Chamieh,H., Ballut,L., Bonneau,F., & Le,H.H. (2008). NMD factors UPF2 and UPF3 bridge UPF1 to the exon junction complex and stimulate its RNA helicase activity. *Nat.Struct.Mol.Biol.*, 15(1), 85-93.
- Chao,J.A., Lee,J.H., Chapados,B.R., Debler,E.W., Schneemann,A., & Williamson,J.R. (2005). Dual modes of RNA-silencing suppression by Flock House virus protein B2. *Nat.Struct.Mol.Biol.*, 12(11), 952-957.

- Cheadle,C., Fan,J., Cho-Chung,Y.S., Werner,T., Ray,J., Do,L., Gorospe,M., & Becker,K.G. (2005a). Control of gene expression during T cell activation: alternate regulation of mRNA transcription and mRNA stability. *BMC.Genomics*, 6(1), 75.
- Cheadle,C., Fan,J., Cho-Chung,Y.S., Werner,T., Ray,J., Do,L., Gorospe,M., & Becker,K.G. (2005b). Stability regulation of mRNA and the control of gene expression. *Ann.N.Y.Acad.Sci.*, 1058, 196-204.
- Chen,C.Y., Gherzi,R., Ong,S.E., Chan,E.L., Raijmakers,R., Pruijn,G.J., Stoecklin,G., Moroni,C., Mann,M., & Karin,M. (2001). AU Binding Proteins Recruit the Exosome to Degrade ARE-Containing mRNAs. *Cell*, 107(4), 451-464.
- Chen,C.Y. & Shyu,A.B. (2003). Rapid deadenylation triggered by a nonsense codon precedes decay of the RNA body in a mammalian cytoplasmic nonsense-mediated decay pathway. *Mol.Cell Biol.*, 23(14), 4805-4813.
- Chen,C.Y. & Shyu,A.B. (1995). AU-rich elements: characterization and importance in mRNA degradation. *Trends Biochem Sci*, 20(11), 465-470.
- Chen,C.Y., Xu,N., & Shyu,A.B. (2002). Highly Selective Actions of HuR in Antagonizing AU-Rich Element-Mediated mRNA Destabilization. *Mol.Cell Biol.*, 22(20), 7268-7278.
- Chen,G., Guo,X., Lv,F., Xu,Y., & Gao,G. (2008). p72 DEAD box RNA helicase is required for optimal function of the zinc-finger antiviral protein. *Proc.Natl.Acad.Sci.U.S.A*, 105(11), 4352-4357.
- Chendrimada,T.P., Gregory,R.I., Kumaraswamy,E., Norman,J., Cooch,N., Nishikura,K., & Shiekhattar,R. (2005). TRBP recruits the Dicer complex to Ago2 for microRNA processing and gene silencing. *Nature*, 436(7051), 740-744.
- Cho,H., Kim,K.M., & Kim,Y.K. (2009). Human proline-rich nuclear receptor coregulatory protein 2 mediates an interaction between mRNA surveillance machinery and decapping complex. *Mol.Cell*, 33(1), 75-86.
- Condreay,L.D., Adams,R.H., Edwards,J., & Brown,D.T. (1988). Effect of actinomycin D and cycloheximide on replication of Sindbis virus in *Aedes albopictus* (mosquito) cells. *J.Virol.*, 62(8), 2629-2635.
- Conrad,N.K., Mili,S., Marshall,E.L., Shu,M.D., & Steitz,J.A. (2006). Identification of a rapid mammalian deadenylation-dependent decay pathway and its inhibition by a viral RNA element. *Mol.Cell*, 24(6), 943-953.
- Cougot,N., Babajko,S., & Seraphin,B. (2004). Cytoplasmic foci are sites of mRNA decay in human cells. *J.Cell Biol.*, 165(1), 31-40.
- de Groot,R.J., Hardy,W.R., Shirako,Y., & Strauss,J.H. (1990). Cleavage-site preferences of Sindbis virus polyproteins containing the non-structural proteinase. Evidence for

- temporal regulation of polyprotein processing in vivo. *The EMBO Journal*, 9(8), 2631-2638.
- De, I., Fata-Hartley, C., Sawicki, S.G., & Sawicki, D.L. (2003). Functional analysis of nsP3 phosphoprotein mutants of Sindbis virus. *J. Virol.*, 77(24), 13106-13116.
- Dehlin, E., Wormington, M., Korner, C.G., & Wahle, E. (2000). Cap-dependent deadenylation of mRNA. *EMBO J*, 19(5), 1079-1086.
- Ding, M.X. & Schlesinger, M.J. (1989). Evidence that Sindbis virus NSP2 is an autoprotease which processes the virus nonstructural polyprotein. *Virology*, 171(1), 280-284.
- Doench, J.G., Petersen, C.P., & Sharp, P.A. (2003). siRNAs can function as miRNAs. *Genes Dev.*, 17(4), 438-442.
- Doepker, R.C., Hsu, W.L., Saffran, H.A., & Smiley, J.R. (2004). Herpes simplex virus virion host shutoff protein is stimulated by translation initiation factors eIF4B and eIF4H. *J. Virol.*, 78(9), 4684-4699.
- Dohm, D.J., Logan, T.M., Barth, J.F., & Turell, M.J. (1995). Laboratory transmission of Sindbis virus by *Aedes albopictus*, *Ae. aegypti*, and *Culex pipiens* (Diptera: Culicidae). *J. Med. Entomol.*, 32(6), 818-821.
- Doma, M.K. & Parker, R. (2006). Endonucleolytic cleavage of eukaryotic mRNAs with stalls in translation elongation. *Nature*, 440(7083), 561-564.
- Dunckley, T. & Parker, R. (1999). The DCP2 protein is required for mRNA decapping in *Saccharomyces cerevisiae* and contains a functional MutT motif. *EMBO J*, 18(19), 5411-5422.
- Dziembowski, A., Lorentzen, E., Conti, E., & Seraphin, B. (2007). A single subunit, Dis3, is essentially responsible for yeast exosome core activity. *Nat. Struct. Mol. Biol.*, 14(1), 15-22.
- Eberle, A.B., Lykke-Andersen, S., Muhlemann, O., & Jensen, T.H. (2009). SMG6 promotes endonucleolytic cleavage of nonsense mRNA in human cells. *Nat. Struct. Mol. Biol.*, 16(1), 49-55.
- Elbashir, S.M., Harborth, J., Lendeckel, W., Yalcin, A., Weber, K., & Tuschl, T. (2001). Duplexes of 21-nucleotide RNAs mediate RNA interference in cultured mammalian cells. *Nature*, 411(6836), 494-498.
- Emara, M.M. & Brinton, M.A. (2007). Interaction of TIA-1/TIAR with West Nile and dengue virus products in infected cells interferes with stress granule formation and processing body assembly. *Proc. Natl. Acad. Sci. U.S.A*, 104(21), 9041-9046.

- Espert,L., Degols,G., Gongora,C., Blondel,D., Williams,B.R., Silverman,R.H., & Mechti,N. (2003). ISG20, a new interferon-induced RNase specific for single-stranded RNA, defines an alternative antiviral pathway against RNA genomic viruses. *J.Biol.Chem.*, 278(18), 16151-16158.
- Espert,L., Degols,G., Lin,Y.L., Vincent,T., Benkirane,M., & Mechti,N. (2005). Interferon-induced exonuclease ISG20 exhibits an antiviral activity against human immunodeficiency virus type 1. *J.Gen.Virol.*, 86(Pt 8), 2221-2229.
- Eulalio,A., Behm-Ansmant,I., & Izaurralde,E. (2007). P bodies: at the crossroads of post-transcriptional pathways. *Nat.Rev.Mol.Cell Biol.*, 8(1), 9-22.
- Fenger-Gron,M., Fillman,C., Norrild,B., & Lykke-Andersen,J. (2005). Multiple processing body factors and the ARE binding protein TTP activate mRNA decapping. *Mol.Cell*, 20(6), 905-915.
- Fire,A., Xu,S., Montgomery,M.K., Kostas,S.A., Driver,S.E., & Mello,C.C. (1998). Potent and specific genetic interference by double-stranded RNA in *Caenorhabditis elegans*. *Nature*, 391(6669), 806-811.
- Floyd-Smith,G., Slattery,E., & Lengyel,P. (1981). Interferon action: RNA cleavage pattern of a (2'-5')oligoadenylate--dependent endonuclease. *Science*, 212(4498), 1030-1032.
- Ford,L.P. & Wilusz,J. (1999b). 3'-Terminal RNA structures and poly(U) tracts inhibit initiation by a 3'-->5' exonuclease in vitro. *Nucleic Acids Res.*, 27(4), 1159-1167.
- Ford,L.P. & Wilusz,J. (1999a). An in vitro system using HeLa cytoplasmic extracts that reproduces regulated mRNA stability. *Methods*, 17(1), 21-27.
- Fred,R.G., Tillmar,L., & Welsh,N. (2006). The role of PTB in insulin mRNA stability control. *Curr.Diabetes Rev.*, 2(3), 363-366.
- Fred,R.G. & Welsh,N. (2005). Increased expression of polypyrimidine tract binding protein results in higher insulin mRNA levels. *Biochem.Biophys.Res.Comm.*, 328(1), 38-42.
- Fred,R.G. & Welsh,N. (2009). The importance of RNA binding proteins in preproinsulin mRNA stability. *Mol.Cell Endocrinol.*, 297(1-2), 28-33.
- Frischmeyer,P.A., van Hoof,A., O'Donnell,K., Guerrerio,A.L., Parker,R., & Dietz,H.C. (2002). An mRNA surveillance mechanism that eliminates transcripts lacking termination codons. *Science*, 295(5563), 2258-2261.
- Frolova,E., Gorchakov,R., Garmashova,N., Atasheva,S., Vergara,L.A., & Frolov,I. (2006). Formation of nsP3-specific protein complexes during Sindbis virus replication. *J.Virol.*, 80(8), 4122-4134.

- Frothingham, T.E. (1955). Tissue Culture Applied to the Study of Sindbis Virus. *Am J Trop Med Hyg.*, 4(5), 863-871.
- Fukuhara, N., Ebert, J., Unterholzner, L., Lindner, D., Izaurralde, E., & Conti, E. (2005). SMG7 is a 14-3-3-like adaptor in the nonsense-mediated mRNA decay pathway. *Mol. Cell*, 17(4), 537-547.
- Gamarnik, A.V. & Andino, R. (1997). Two functional complexes formed by KH domain containing proteins with the 5' noncoding region of poliovirus RNA. *RNA*, 3(8), 882-892.
- Gandhi, R., Manzoor, M., & Hudak, K.A. (2008). Depurination of Brome mosaic virus RNA3 in vivo results in translation-dependent accelerated degradation of the viral RNA. *J. Biol. Chem.*, 283(47), 32218-32228.
- Gao, M., Fritz, D.T., Ford, L.P., & Wilusz, J. (2000). Interaction between a poly(A)-specific ribonuclease and the 5' cap influences mRNA deadenylation rates in vitro. *Mol. Cell*, 5(3), 479-488.
- Garcia-Martinez, J., Aranda, A., & Perez-Ortin, J.E. (2004). Genomic run-on evaluates transcription rates for all yeast genes and identifies gene regulatory mechanisms. *Mol Cell*, 15(2), 303-313.
- Garneau, N.L., Sokoloski, K.J., Opyrchal, M., Neff, C.P., Wilusz, C.J., & Wilusz, J. (2008). The 3' Untranslated Region of Sindbis Virus Represses the Deadenylation of Viral Transcripts in Mosquito and Mammalian Cells. *J. Virol.*
- Garneau, N.L., Wilusz, C.J., & Wilusz, J. (2009). Chapter 5. In vivo analysis of the decay of transcripts generated by cytoplasmic RNA viruses. *Methods Enzymol.*, 449, 97-123.
- Garneau, N.L., Wilusz, J., & Wilusz, C.J. (2007). The highways and byways of mRNA decay. *Nat. Rev. Mol. Cell Biol.*, 8(2), 113-126.
- Gavin, A.C., Bosche, M., Krause, R., Grandi, P., Marzioch, M., Bauer, A., Schultz, J., Rick, J.M., Michon, A.M., Cruciat, C.M., Remor, M., Hofert, C., Schelder, M., Brajenovic, M., Ruffner, H., Merino, A., Klein, K., Hudak, M., Dickson, D., Rudi, T., Gnau, V., Bauch, A., Bastuck, S., Huhse, B., Leutwein, C., Heurtier, M.A., Copley, R.R., Edelmann, A., Querfurth, E., Rybin, V., Drewes, G., Raida, M., Bouwmeester, T., Bork, P., Seraphin, B., Kuster, B., Neubauer, G., & Superti-Furga, G. (2002). Functional organization of the yeast proteome by systematic analysis of protein complexes. *Nature*, 415(6868), 141-147.
- Ge, Q., McManus, M.T., Nguyen, T., Shen, C.H., Sharp, P.A., Eisen, H.N., & Chen, J. (2003). RNA interference of influenza virus production by directly targeting mRNA for degradation and indirectly inhibiting all viral RNA transcription. *Proc. Natl. Acad. Sci. U.S.A.*, 100(5), 2718-2723.

- Geigenmuller-Gnirke,U., Nitschko,H., & Schlesinger,S. (1993). Deletion analysis of the capsid protein of Sindbis virus: identification of the RNA binding region. *J.Virol.*, 67(3), 1620-1626.
- Gilks,N., Kedersha,N., Ayodele,M., Shen,L., Stoecklin,G., Dember,L.M., & Anderson,P. (2004). Stress granule assembly is mediated by prion-like aggregation of TIA-1. *Mol.Biol.Cell*, 15(12), 5383-5398.
- Gitlin,L., Karelsky,S., & Andino,R. (2002). Short interfering RNA confers intracellular antiviral immunity in human cells. *Nature*, 418(6896), 430-434.
- Glaunsinger,B., Chavez,L., & Ganem,D. (2005). The exonuclease and host shutoff functions of the SOX protein of Kaposi's sarcoma-associated herpesvirus are genetically separable. *J.Virol.*, 79(12), 7396-7401.
- Glavan,F., Behm-Ansmant,I., Izaurralde,E., & Conti,E. (2006). Structures of the PIN domains of SMG6 and SMG5 reveal a nuclease within the mRNA surveillance complex. *The EMBO Journal*, 25(21), 5117-5125.
- Gongora,C., David,G., Pintard,L., Tissot,C., Hua,T.D., Dejean,A., & Mechti,N. (1997). Molecular cloning of a new interferon-induced PML nuclear body-associated protein. *J.Biol.Chem.*, 272(31), 19457-19463.
- Gorbalenya,A.E., Koonin,E.V., Donchenko,A.P., & Blinov,V.M. (1988). A novel superfamily of nucleoside triphosphate-binding motif containing proteins which are probably involved in duplex unwinding in DNA and RNA replication and recombination. *FEBS Lett.*, 235(1-2), 16-24.
- Gorchakov,R., Frolova,E., Sawicki,S., Atasheva,S., Sawicki,D., & Frolov,I. (2008a). A new role for ns polyprotein cleavage in Sindbis virus replication. *J.Virol.*, 82(13), 6218-6231.
- Gorchakov,R., Garmashova,N., Frolova,E., & Frolov,I. (2008b). Different types of nsP3-containing protein complexes in Sindbis virus-infected cells. *J.Virol.*
- Graves,R.A. & Marzluff,W.F. (1984). Rapid reversible changes in the rate of histone gene transcription and histone mRNA levels in mouse myeloma cells. *Mol.Cell Biol.*, 4(2), 351-357.
- Graves,R.A., Pandey,N.B., Chodchoy,N., & Marzluff,W.F. (1987). Translation is required for regulation of histone mRNA degradation. *Cell*, 48(4), 615-626.
- Griffin,D.E. (2001). Alphaviruses. In D.M.Knipe & Howley P.M. (Eds.), *Fields Virology* (pp. 917-962). Philadelphia, PA: Lippincott Williams & Wilkins.
- Guo,X., Carroll,J.W., MacDonald,M.R., Goff,S.P., & Gao,G. (2004). The zinc finger antiviral protein directly binds to specific viral mRNAs through the CCCH zinc finger motifs. *J.Virol.*, 78(23), 12781-12787.

- Guo,X., Ma,J., Sun,J., & Gao,G. (2007). The zinc-finger antiviral protein recruits the RNA processing exosome to degrade the target mRNA. *Proc.Natl.Acad.Sci. U.S.A*, 104(1), 151-156.
- Haase,A.D., Jaskiewicz,L., Zhang,H., Laine,S., Sack,R., Gatignol,A., & Filipowicz,W. (2005). TRBP, a regulator of cellular PKR and HIV-1 virus expression, interacts with Dicer and functions in RNA silencing. *EMBO Rep.*, 6(10), 961-967.
- Hahn,C.S., Strauss,E.G., & Strauss,J.H. (1985). Sequence analysis of three Sindbis virus mutants temperature-sensitive in the capsid protein autoprotease. *Proc.Natl.Acad.Sci. U.S.A*, 82(14), 4648-4652.
- Hahn,Y.S., Grakoui,A., Rice,C.M., Strauss,E.G., & Strauss,J.H. (1989a). Mapping of RNA- temperature-sensitive mutants of Sindbis virus: complementation group F mutants have lesions in nsP4. *J.Virol.*, 63(3), 1194-1202.
- Hahn,Y.S., Guanzon,A., Rice,C.M., & Hahn,C.S. (1999). Class I MHC molecule-mediated inhibition of Sindbis virus replication. *J Immunol.*, 162(1), 69-77.
- Hahn,Y.S., Strauss,E.G., & Strauss,J.H. (1989b). Mapping of RNA- temperature-sensitive mutants of Sindbis virus: assignment of complementation groups A, B, and G to nonstructural proteins. *J.Virol.*, 63(7), 3142-3150.
- Hardy,R.W. & Rice,C.M. (2005). Requirements at the 3' end of the Sindbis virus genome for efficient synthesis of minus-strand RNA. *J.Virol.*, 79(8), 4630-4639.
- Hardy,W.R., Hahn,Y.S., de Groot,R.J., Strauss,E.G., & Strauss,J.H. (1990). Synthesis and processing of the nonstructural polyproteins of several temperature-sensitive mutants of Sindbis virus. *Virology*, 177(1), 199-208.
- Hardy,W.R. & Strauss,J.H. (1988). Processing the nonstructural polyproteins of Sindbis virus: study of the kinetics in vivo by using monospecific antibodies. *J.Virol.*, 62(3), 998-1007.
- Hardy,W.R. & Strauss,J.H. (1989). Processing the nonstructural polyproteins of sindbis virus: nonstructural proteinase is in the C-terminal half of nsP2 and functions both in cis and in trans. *J.Virol.*, 63(11), 4653-4664.
- Harris,D., Zhang,Z., Chaubey,B., & Pandey,V.N. (2006). Identification of cellular factors associated with the 3'-nontranslated region of the hepatitis C virus genome. *Mol.Cell Proteomics.*, 5(6), 1006-1018.
- Hatfield,L., Beelman,C.A., Stevens,A., & Parker,R. (1996). Mutations in trans-acting factors affecting mRNA decapping in *Saccharomyces cerevisiae*. *Mol Cell Biol*, 16(10), 5830-5838.

- Hau,H.H., Walsh,R.J., Ogilvie,R.L., Williams,D.A., Reilly,C.S., & Bohjanen,P.R. (2007). Tristetraprolin recruits functional mRNA decay complexes to ARE sequences. *J.Cell Biochem.*, 100(6), 1477-1492.
- He,F., Li,X., Spatrick,P., Casillo,R., Dong,S., & Jacobson,A. (2003). Genome-wide analysis of mRNAs regulated by the nonsense-mediated and 5' to 3' mRNA decay pathways in yeast. *Mol.Cell*, 12(6), 1439-1452.
- Hernandez,H., Dziembowski,A., Taverner,T., Seraphin,B., & Robinson,C.V. (2006). Subunit architecture of multimeric complexes isolated directly from cells. *EMBO Rep.*, 7(6), 605-610.
- Hovanessian,A.G., Brown,R.E., & Kerr,I.M. (1977). Synthesis of low molecular weight inhibitor of protein synthesis with enzyme from interferon-treated cells. *Nature*, 268(5620), 537-540.
- Hui,E.K., Yap,E.M., An,D.S., Chen,I.S., & Nayak,D.P. (2004). Inhibition of influenza virus matrix (M1) protein expression and virus replication by U6 promoter-driven and lentivirus-mediated delivery of siRNA. *J Gen.Virol.*, 85(Pt 7), 1877-1884.
- Igarashi,A. (1978). Isolation of a Singh's *Aedes albopictus* cell clone sensitive to Dengue and Chikungunya viruses. *J.Gen.Virol.*, 40(3), 531-544.
- Inada,T. & Aiba,H. (2005). Translation of aberrant mRNAs lacking a termination codon or with a shortened 3'-UTR is repressed after initiation in yeast. *The EMBO Journal*, 24(8), 1584-1595.
- Ingelfinger,D., rmdt-Jovin,D.J., Luhrmann,R., & Achsel,T. (2002). The human LSm1-7 proteins colocalize with the mRNA-degrading enzymes Dcp1/2 and Xrn1 in distinct cytoplasmic foci. *RNA.*, 8(12), 1489-1501.
- Jackson,A.C., Bowen,J.C., & Downe,A.E. (1993). Experimental infection of *Aedes aegypti* (Diptera: Culicidae) by the oral route with Sindbis virus. *J.Med.Entomol.*, 30(2), 332-337.
- Jan,J.T., Byrnes,A.P., & Griffin,D.E. (1999). Characterization of a Chinese hamster ovary cell line developed by retroviral insertional mutagenesis that is resistant to Sindbis virus infection. *J.Virol.*, 73(6), 4919-4924.
- Jiang,D., Guo,H., Xu,C., Chang,J., Gu,B., Wang,L., Block,T.M., & Guo,J.T. (2008). Identification of three interferon-inducible cellular enzymes that inhibit the replication of hepatitis C virus. *J.Virol.*, 82(4), 1665-1678.
- Johnson,K.L., Price,B.D., Eckerle,L.D., & Ball,L.A. (2004). Nodamura virus nonstructural protein B2 can enhance viral RNA accumulation in both mammalian and insect cells. *J.Virol.*, 78(12), 6698-6704.

- Kahana,R., Kuznetzova,L., Rogel,A., Shemesh,M., Hai,D., Yadin,H., & Stram,Y. (2004). Inhibition of foot-and-mouth disease virus replication by small interfering RNA. *J Gen. Virol.*, 85(Pt 11), 3213-3217.
- Kamer,G. & Argos,P. (1984). Primary structural comparison of RNA-dependent polymerases from plant, animal and bacterial viruses. *Nucleic Acids Res.*, 12(18), 7269-7282.
- Kamitani,W., Narayanan,K., Huang,C., Lokugamage,K., Ikegami,T., Ito,N., Kubo,H., & Makino,S. (2006). Severe acute respiratory syndrome coronavirus nsp1 protein suppresses host gene expression by promoting host mRNA degradation. *Proc.Natl.Acad.Sci.U.S.A*, 103(34), 12885-12890.
- Kang,D.C., Gopalkrishnan,R.V., Wu,Q., Jankowsky,E., Pyle,A.M., & Fisher,P.B. (2002). mda-5: An interferon-inducible putative RNA helicase with double-stranded RNA-dependent ATPase activity and melanoma growth-suppressive properties. *Proc.Natl.Acad.Sci.U.S.A*, 99(2), 637-642.
- Karpf,A.R. & Brown,D.T. (1998). Comparison of Sindbis virus-induced pathology in mosquito and vertebrate cell cultures. *Virology*, 240(2), 193-201.
- Kashima,I., Yamashita,A., Izumi,N., Kataoka,N., Morishita,R., Hoshino,S., Ohno,M., Dreyfuss,G., & Ohno,S. (2006). Binding of a novel SMG-1-Upf1-eRF1-eRF3 complex (SURF) to the exon junction complex triggers Upf1 phosphorylation and nonsense-mediated mRNA decay. *Genes Dev.*, 20(3), 355-367.
- Kato,H., Takeuchi,O., Sato,S., Yoneyama,M., Yamamoto,M., Matsui,K., Uematsu,S., Jung,A., Kawai,T., Ishii,K.J., Yamaguchi,O., Otsu,K., Tsujimura,T., Koh,C.S., Reis e Sousa, Matsuura,Y., Fujita,T., & Akira,S. (2006). Differential roles of MDA5 and RIG-I helicases in the recognition of RNA viruses. *Nature*, 441(7089), 101-105.
- Kaygun,H. & Marzluff,W.F. (2005). Regulated degradation of replication-dependent histone mRNAs requires both ATR and Upf1. *Nat.Struct.Mol.Biol.*, 12(9), 794-800.
- Kebaara,B.W. & Atkin,A.L. (2009). Long 3'-UTRs target wild-type mRNAs for nonsense-mediated mRNA decay in *Saccharomyces cerevisiae*. *Nucleic Acids Res.*
- Kedersha,N. & Anderson,P. (2002). Stress granules: sites of mRNA triage that regulate mRNA stability and translatability. *Biochem.Soc.Trans.*, 30(Pt 6), 963-969.
- Kedersha,N., Stoecklin,G., Ayodele,M., Yacono,P., Lykke-Andersen,J., Fitzler,M.J., Scheuner,D., Kaufman,R.J., Golan,D.E., & Anderson,P. (2005). Stress granules and processing bodies are dynamically linked sites of mRNP remodeling. *J.Cell Biol.*, 169(6), 871-884.
- Kedersha,N.L., Gupta,M., Li,W., Miller,I., & Anderson,P. (1999). RNA-binding proteins TIA-1 and TIAR link the phosphorylation of eIF-2 alpha to the assembly of mammalian stress granules. *J Cell Biol.*, 147(7), 1431-1442.

- Kerr, I.M., Brown, R.E., & Hovanessian, A.G. (1977). Nature of inhibitor of cell-free protein synthesis formed in response to interferon and double-stranded RNA. *Nature*, 268(5620), 540-542.
- Kerr, I.M., Williams, B.R., Hovanessian, A.G., Brown, R.E., Martin, E.M., Gilbert, C.S., & Birdsall, N.J. (1979). Cell-free protein synthesis and interferon action: protein kinase(s) and an oligonucleotide effector, pppA₂'p5'A₂'p5'A. *Haematol. Blood Transfus.*, 23, 291-294.
- Khabar, K.S. (2005). The AU-rich transcriptome: more than interferons and cytokines, and its role in disease. *J. Interferon Cytokine Res.*, 25(1), 1-10.
- Kiledjian, M., Wang, X., & Liebhaber, S.A. (1995). Identification of two KH domain proteins in the alpha-globin mRNP stability complex. *EMBO J*, 14(17), 4357-4364.
- Kimball, S.R., Horetsky, R.L., Ron, D., Jefferson, L.S., & Harding, H.P. (2003). Mammalian stress granules represent sites of accumulation of stalled translation initiation complexes. *Am. J. Physiol Cell Physiol*, 284(2), C273-C284.
- Koonin, E.V. (1993). A highly conserved sequence motif defining the family of MutT-related proteins from eubacteria, eukaryotes and viruses. *Nucleic Acids Res.*, 21(20), 4847.
- Korner, C.G. & Wahle, E. (1997). Poly(A) tail shortening by a mammalian poly(A)-specific 3'-exoribonuclease. *J Biol Chem*, 272(16), 10448-10456.
- Kren, B.T. & Steer, C.J. (1996). Posttranscriptional regulation of gene expression in liver regeneration: role of mRNA stability. *FASEB J.*, 10(5), 559-573.
- Kubota, K., Nakahara, K., Ohtsuka, T., Yoshida, S., Kawaguchi, J., Fujita, Y., Ozeki, Y., Hara, A., Yoshimura, C., Furukawa, H., Haruyama, H., Ichikawa, K., Yamashita, M., Matsuoka, T., & Iijima, Y. (2004). Identification of 2'-phosphodiesterase, which plays a role in the 2-5A system regulated by interferon. *J. Biol. Chem.*, 279(36), 37832-37841.
- Kuhn, R.J., Hong, Z., & Strauss, J.H. (1990). Mutagenesis of the 3' nontranslated region of Sindbis virus RNA. *J. Virol.*, 64(4), 1465-1476.
- Kwong, A.D., Kruper, J.A., & Frenkel, N. (1988). Herpes simplex virus virion host shutoff function. *J. Virol.*, 62(3), 912-921.
- LaStarza, M.W., Grakoui, A., & Rice, C.M. (1994a). Deletion and duplication mutations in the C-terminal nonconserved region of Sindbis virus nsP3: effects on phosphorylation and on virus replication in vertebrate and invertebrate cells. *Virology*, 202(1), 224-232.
- LaStarza, M.W., Lemm, J.A., & Rice, C.M. (1994b). Genetic analysis of the nsP3 region of Sindbis virus: evidence for roles in minus-strand and subgenomic RNA synthesis. *J. Virol.*, 68(9), 5781-5791.

- Le Hir,H., Izaurrealde,E., Maquat,L.E., & Moore,M.J. (2000). The spliceosome deposits multiple proteins 20-24 nucleotides upstream of mRNA exon-exon junctions. *EMBO J*, 19(24), 6860-6869.
- LeBlanc,J.J. & Beemon,K.L. (2004). Unspliced Rous sarcoma virus genomic RNAs are translated and subjected to nonsense-mediated mRNA decay before packaging. *J.Virol.*, 78(10), 5139-5146.
- Lebreton,A., Tomecki,R., Dziembowski,A., & Seraphin,B. (2008). Endonucleolytic RNA cleavage by a eukaryotic exosome. *Nature*, 456(7224), 993-996.
- Lee,H.H., Kim,Y.S., Kim,K.H., Heo,I., Kim,S.K., Kim,O., Kim,H.K., Yoon,J.Y., Kim,H.S., Kim,d.J., Lee,S.J., Yoon,H.J., Kim,S.J., Lee,B.G., Song,H.K., Kim,V.N., Park,C.M., & Suh,S.W. (2007). Structural and functional insights into Dom34, a key component of no-go mRNA decay. *Mol.Cell*, 27(6), 938-950.
- Lee,Y., Hur,I., Park,S.Y., Kim,Y.K., Suh,M.R., & Kim,V.N. (2006). The role of PACT in the RNA silencing pathway. *The EMBO Journal*, 25(3), 522-532.
- Lehner,B., Fraser,A.G., & Sanderson,C.M. (2004). Technique review: how to use RNA interference. *Brief.Funct.Genomic.Proteomic.*, 3(1), 68-83.
- Levis,R., Weiss,B.G., Tsiang,M., Huang,H., & Schlesinger,S. (1986). Deletion mapping of Sindbis virus DI RNAs derived from cDNAs defines the sequences essential for replication and packaging. *Cell*, 44(1), 137-145.
- Li,G.P. & Rice,C.M. (1989). Mutagenesis of the in-frame opal termination codon preceding nsP4 of Sindbis virus: studies of translational readthrough and its effect on virus replication. *J.Virol.*, 63(3), 1326-1337.
- Li,H., Li,W.X., & Ding,S.W. (2002a). Induction and suppression of RNA silencing by an animal virus. *Science*, 296(5571), 1319-1321.
- Li,M.L., Wang,H.L., & Stollar,V. (1997). Complementation of and interference with Sindbis virus replication by full-length and deleted forms of the nonstructural protein, nsP1, expressed in stable transfectants of Hela cells. *Virology*, 227(2), 361-369.
- Li,W., Li,Y., Kedersha,N., Anderson,P., Emar,M., Swiderek,K.M., Moreno,G.T., & Brinton,M.A. (2002b). Cell proteins TIA-1 and TIAR interact with the 3' stem-loop of the West Nile virus complementary minus-strand RNA and facilitate virus replication. *J.Virol.*, 76(23), 11989-12000.
- Li,W.X., Li,H., Lu,R., Li,F., Dus,M., Atkinson,P., Brydon,E.W., Johnson,K.L., Garcia-Sastre,A., Ball,L.A., Palese,P., & Ding,S.W. (2004). Interferon antagonist proteins of influenza and vaccinia viruses are suppressors of RNA silencing. *Proc.Natl.Acad.Sci.U.S.A*, 101(5), 1350-1355.

- Liu,H., Rodgers,N.D., Jiao,X., & Kiledjian,M. (2002). The scavenger mRNA decapping enzyme DcpS is a member of the HIT family of pyrophosphatases. *The EMBO Journal*, 21(17), 4699-4708.
- Liu,J., Carmell,M.A., Rivas,F.V., Marsden,C.G., Thomson,J.M., Song,J.J., Hammond,S.M., Joshua-Tor,L., & Hannon,G.J. (2004). Argonaute2 is the catalytic engine of mammalian RNAi. *Science*, 305(5689), 1437-1441.
- Liu,Q., Greimann,J.C., & Lima,C.D. (2006). Reconstitution, activities, and structure of the eukaryotic RNA exosome. *Cell*, 127(6), 1223-1237.
- Liu,W.F., Zhang,A., Cheng,Y., Zhou,H.M., & Yan,Y.B. (2009). Allosteric regulation of human poly(A)-specific ribonuclease by cap and potassium ions. *Biochem.Biophys.Res.Commun.*, 379(2), 341-345.
- Liu,Y.P., Haasnoot,J., ter,B.O., Berkhout,B., & Konstantinova,P. (2008). Inhibition of HIV-1 by multiple siRNAs expressed from a single microRNA polycistron. *Nucleic Acids Res.*, 36(9), 2811-2824.
- Lopez,S., Bell,J.R., Strauss,E.G., & Strauss,J.H. (1985). The nonstructural proteins of Sindbis virus as studied with an antibody specific for the C terminus of the nonstructural readthrough polyprotein. *Virology*, 141(2), 235-247.
- Lu,S. & Cullen,B.R. (2004). Adenovirus VA1 noncoding RNA can inhibit small interfering RNA and MicroRNA biogenesis. *J Virol.*, 78(23), 12868-12876.
- Lu,Y.E., Cassese,T., & Kielian,M. (1999). The cholesterol requirement for sindbis virus entry and exit and characterization of a spike protein region involved in cholesterol dependence. *J.Virol.*, 73(5), 4272-4278.
- Lund,J.M., Alexopoulou,L., Sato,A., Karow,M., Adams,N.C., Gale,N.W., Iwasaki,A., & Flavell,R.A. (2004). Recognition of single-stranded RNA viruses by Toll-like receptor 7. *Proc.Natl.Acad.Sci.U.S.A*, 101(15), 5598-5603.
- Lykke-Andersen,J. (2002). Identification of a human decapping complex associated with hUpf proteins in nonsense-mediated decay. *Mol.Cell Biol.*, 22(23), 8114-8121.
- Lykke-Andersen,J., Shu,M.D., & Steitz,J.A. (2000). Human Upf proteins target an mRNA for nonsense-mediated decay when bound downstream of a termination codon. *Cell, Vol.*, 103, 1121-1131.
- MacRae,I.J., Ma,E., Zhou,M., Robinson,C.V., & Doudna,J.A. (2008). In vitro reconstitution of the human RISC-loading complex. *Proc.Natl.Acad.Sci.U.S.A*, 105(2), 512-517.
- Martinez,J., Ren,Y.G., Nilsson,P., Ehrenberg,M., & Virtanen,A. (2001). The mRNA cap structure stimulates rate of poly(A) removal and amplifies processivity of degradation. *J.Biol Chem.*, 276(30), 27923-27929.

- Martinez,J., Ren,Y.G., Thuresson,A.C., Hellman,U., Astrom,J., & Virtanen,A. (2000). A 54-kDa fragment of the Poly(A)-specific ribonuclease is an oligomeric, processive, and cap-interacting Poly(A)-specific 3' exonuclease. *J Biol.Chem.*, 275(31), 24222-24230.
- Matranga,C., Tomari,Y., Shin,C., Bartel,D.P., & Zamore,P.D. (2005). Passenger-strand cleavage facilitates assembly of siRNA into Ago2-containing RNAi enzyme complexes. *Cell*, 123(4), 607-620.
- Matsumoto,M., Kikkawa,S., Kohase,M., Miyake,K., & Seya,T. (2002). Establishment of a monoclonal antibody against human Toll-like receptor 3 that blocks double-stranded RNA-mediated signaling. *Biochem.Biophys.Res. Commun.*, 293(5), 1364-1369.
- Mendell,J.T., Sharifi,N.A., Meyers,J.L., Martinez-Murillo,F., & Dietz,H.C. (2004). Nonsense surveillance regulates expression of diverse classes of mammalian transcripts and mutes genomic noise. *Nat.Genet.*, 36(10), 1073-1078.
- Mi,S., Durbin,R., Huang,H.V., Rice,C.M., & Stollar,V. (1989). Association of the Sindbis virus RNA methyltransferase activity with the nonstructural protein nsP1. *Virology*, 170(2), 385-391.
- Mitrovich,Q.M. & Anderson,P. (2005). mRNA surveillance of expressed pseudogenes in *C. elegans*. *Curr.Biol.*, 15(10), 963-967.
- Mullen,T.E. & Marzluff,W.F. (2008). Degradation of histone mRNA requires oligouridylation followed by decapping and simultaneous degradation of the mRNA both 5' to 3' and 3' to 5'. *Genes Dev.*, 22(1), 50-65.
- Muller,S., Moller,P., Bick,M.J., Wurr,S., Becker,S., Gunther,S., & Kummerer,B.M. (2007). Inhibition of filovirus replication by the zinc finger antiviral protein. *J.Virol.*, 81(5), 2391-2400.
- Murray,K.E., Roberts,A.W., & Barton,D.J. (2001). Poly(rC) binding proteins mediate poliovirus mRNA stability. *RNA.*, 7(8), 1126-1141.
- Narayanan,K., Huang,C., Lokugamage,K., Kamitani,W., Ikegami,T., Tseng,C.T., & Makino,S. (2008). Severe acute respiratory syndrome coronavirus nsp1 suppresses host gene expression, including that of type I interferon, in infected cells. *J.Virol.*, 82(9), 4471-4479.
- Nguyen,L.H., Espert,L., Mechti,N., & Wilson,D.M., III (2001). The human interferon- and estrogen-regulated ISG20/HEM45 gene product degrades single-stranded RNA and DNA in vitro. *Biochemistry*, 40(24), 7174-7179.
- Nilsson,P., Henriksson,N., Niedzwiecka,A., Balatsos,N.A., Kokkoris,K., Eriksson,J., & Virtanen,A. (2007). A multifunctional RNA recognition motif in poly(A)-specific ribonuclease with cap and poly(A) binding properties. *J.Biol.Chem.*, 282(45), 32902-32911.

- Ohno,K., Sawai,K., Iijima,Y., Levin,B., & Meruelo,D. (1997). Cell-specific targeting of Sindbis virus vectors displaying IgG-binding domains of protein A. *Nat.Biotechnol.*, 15(8), 763-767.
- Opyrchal,M. (2005). The Sindbis Virus 3' Untranslated Region Inhibits mRNA Decay in Mosquito Cell Extracts. University of Medicine and Dentistry of New Jersey).
- Opyrchal,M., Anderson,J.R., Sokoloski,K.J., Wilusz,C.J., & Wilusz,J. (2005). A cell-free mRNA stability assay reveals conservation of the enzymes and mechanisms of mRNA decay between mosquito and mammalian cell lines. *Insect Biochem.Mol.Biol.*, 35(12), 1321-1334.
- Orban,T.I. & Izaurralde,E. (2005). Decay of mRNAs targeted by RISC requires XRN1, the Ski complex, and the exosome. *RNA.*, 11(4), 459-469.
- Ou,J.H., Strauss,E.G., & Strauss,J.H. (1981). Comparative studies of the 3'-terminal sequences of several alpha virus RNAs. *Virology*, 109(2), 281-289.
- Pandey,N.B. & Marzluff,W.F. (1987). The stem-loop structure at the 3' end of histone mRNA is necessary and sufficient for regulation of histone mRNA stability. *Mol.Cell Biol.*, 7(12), 4557-4559.
- Parrish,S. & Moss,B. (2007). Characterization of a second vaccinia virus mRNA-decapping enzyme conserved in poxviruses. *J.Virol.*, 81(23), 12973-12978.
- Parrish,S., Resch,W., & Moss,B. (2007). Vaccinia virus D10 protein has mRNA decapping activity, providing a mechanism for control of host and viral gene expression. *Proc.Natl.Acad.Sci.U.S.A*, 104(7), 2139-2144.
- Paulding,W.R. & Czyzyk-Krzeska,M.F. (1999). Regulation of tyrosine hydroxylase mRNA stability by protein-binding, pyrimidine-rich sequence in the 3'-untranslated region. *J.Biol.Chem.*, 274(4), 2532-2538.
- Paynton,B.V. & Bachvarova,R. (1994). Polyadenylation and deadenylation of maternal mRNAs during oocyte growth and maturation in the mouse. *Mol.Reprod.Dev.*, 37(2), 172-180.
- Pfeffer,M., Kinney,R.M., & Kaaden,O.R. (1998). The alphavirus 3'-nontranslated region: size heterogeneity and arrangement of repeated sequence elements. *Virology*, 240(1), 100-108.
- Pfeffer,S., Sewer,A., Lagos-Quintana,M., Sheridan,R., Sander,C., Grasser,F.A., van Dyk,L.F., Ho,C.K., Shuman,S., Chien,M., Russo,J.J., Ju,J., Randall,G., Lindenbach,B.D., Rice,C.M., Simon,V., Ho,D.D., Zavolan,M., & Tuschl,T. (2005). Identification of microRNAs of the herpesvirus family. *Nat.Methods*, 2(4), 269-276.
- Piccirillo,C., Khanna,R., & Kiledjian,M. (2003). Functional characterization of the mammalian mRNA decapping enzyme hDcp2. *RNA.*, 9(9), 1138-1147.

- Read,G.S. & Patterson,M. (2007). Packaging of the virion host shutoff (Vhs) protein of herpes simplex virus: two forms of the Vhs polypeptide are associated with intranuclear B and C capsids, but only one is associated with enveloped virions. *J.Virol.*, 81(3), 1148-1161.
- Renz,D. & Brown,D.T. (1976). Characteristics of Sindbis virus temperature-sensitive mutants in cultured BHK-21 and *Aedes albopictus* (Mosquito) cells. *J.Virol.*, 19(3), 775-781.
- Rice,A.P. & Roberts,B.E. (1983). Vaccinia virus induces cellular mRNA degradation. *J.Virol.*, 47(3), 529-539.
- Robb,G.B. & Rana,T.M. (2007). RNA helicase A interacts with RISC in human cells and functions in RISC loading. *Mol.Cell*, 26(4), 523-537.
- Roberts,W.K., Hovanessian,A., Brown,R.E., Clemens,M.J., & Kerr,I.M. (1976). Interferon-mediated protein kinase and low-molecular-weight inhibitor of protein synthesis. *Nature*, 264(5585), 477-480.
- Rosemond,H. & Sreevalsan,T. (1973). Viral RNAs associated with ribosomes in Sindbis virus-infected HeLa cells. *J.Virol.*, 11(3), 399-415.
- Ross,J. (1995). mRNA stability in mammalian cells. *Microbiol Rev*, 59(3), 423-450.
- Rothenfusser,S., Goutagny,N., DiPerna,G., Gong,M., Monks,B.G., Schoenemeyer,A., Yamamoto,M., Akira,S., & Fitzgerald,K.A. (2005). The RNA helicase Lgp2 inhibits TLR-independent sensing of viral replication by retinoic acid-inducible gene-I. *J.Immunol.*, 175(8), 5260-5268.
- Rowe,M., Glaunsinger,B., van,L.D., Zuo,J., Sweetman,D., Ganem,D., Middeldorp,J., Wiertz,E.J., & Rensing,M.E. (2007). Host shutoff during productive Epstein-Barr virus infection is mediated by BGLF5 and may contribute to immune evasion. *Proc.Natl.Acad.Sci.U.S.A.*, 104(9), 3366-3371.
- Rubach,J.K., Wasik,B.R., Rupp,J.C., Kuhn,R.J., Hardy,R.W., & Smith,J.L. (2009). Characterization of purified Sindbis virus nsP4 RNA-dependent RNA polymerase activity in vitro. *Virology*, 384(1), 201-208.
- Rutherford,M.N., Hannigan,G.E., & Williams,B.R. (1988). Interferon-induced binding of nuclear factors to promoter elements of the 2-5A synthetase gene. *The EMBO Journal*, 7(3), 751-759.
- Safrany,S.T., Caffrey,J.J., Yang,X., Bembenek,M.E., Moyer,M.B., Burkhart,W.A., & Shears,S.B. (1998). A novel context for the 'MutT' module, a guardian of cell integrity, in a diphosphoinositol polyphosphate phosphohydrolase. *The EMBO Journal*, 17(22), 6599-6607.

- Saleh,S.M., Poidinger,M., Mackenzie,J.S., Broom,A.K., Lindsay,M.D., & Hall,R.A. (2003). Complete genomic sequence of the Australian south-west genotype of Sindbis virus: comparisons with other Sindbis strains and identification of a unique deletion in the 3'-untranslated region. *Virus Genes*, 26(3), 317-327.
- Salles,F.J., Richards,W.G., & Strickland,S. (1999). Assaying the polyadenylation state of mRNAs. *Methods*, 17(1), 38-45.
- Sawicki,D.L. & Sawicki,S.G. (1985). Functional analysis of the A complementation group mutants of Sindbis HR virus. *Virology*, 144(1), 20-34.
- Sawicki,D.L., Sawicki,S.G., Keranen,S., & Kaariainen,L. (1981). Specific Sindbis Virus-Coded Function for Minus-Strand RNA Synthesis. *J.Virol.*, 39(2), 348-358.
- Schaeffer,D., Tsanova,B., Barbas,A., Reis,F.P., Dastidar,E.G., Sanchez-Rotunno,M., Arraiano,C.M., & van,H.A. (2009). The exosome contains domains with specific endoribonuclease, exoribonuclease and cytoplasmic mRNA decay activities. *Nat.Struct.Mol.Biol.*, 16(1), 56-62.
- Scheller,N., Resa-Infante,P., de la,L.S., Galao,R.P., Albrecht,M., Kaestner,L., Lipp,P., Lengauer,T., Meyerhans,A., & Diez,J. (2007). Identification of PatL1, a human homolog to yeast P body component Pat1. *Biochim.Biophys.Acta*, 1773(12), 1786-1792.
- Schwede,A., Ellis,L., Luther,J., Carrington,M., Stoecklin,G., & Clayton,C. (2008). A role for Caf1 in mRNA deadenylation and decay in trypanosomes and human cells. *Nucleic Acids Res.*, 36(10), 3374-3388.
- Sheth,U. & Parker,R. (2003). Decapping and decay of messenger RNA occur in cytoplasmic processing bodies. *Science*, 300(5620), 805-808.
- Shirako,Y. & Strauss,J.H. (1990). Cleavage between nsP1 and nsP2 initiates the processing pathway of Sindbis virus nonstructural polyprotein P123. *Virology*, 177(1), 54-64.
- Shyu,A.B., Belasco,J.G., & Greenberg,M.E. (1991). Two distinct destabilizing elements in the c-fos message trigger deadenylation as a first step in rapid mRNA decay. *Genes Dev*, 5(2), 221-231.
- Silverman,R.H., Wreschner,D.H., Gilbert,C.S., & Kerr,I.M. (1981). Synthesis, characterization and properties of ppp(A2'p)nApCp and related high-specific-activity 32P-labelled derivatives of ppp(A2'p)nA. *Eur.J.Biochem.*, 115(1), 79-85.
- Singh,G., Popli,S., Hari,Y., Malhotra,P., Mukherjee,S., & Bhatnagar,R.K. (2009). Suppression of RNA silencing by Flock house virus B2 protein is mediated through its interaction with the PAZ domain of Dicer. *FASEB J.*

- Sittman,D.B., Graves,R.A., & Marzluff,W.F. (1983). Histone mRNA concentrations are regulated at the level of transcription and mRNA degradation. *Proc.Natl.Acad.Sci.U.S.A.*, 80(7), 1849-1853.
- Smibert,C.A., Johnson,D.C., & Smiley,J.R. (1992). Identification and characterization of the virion-induced host shutoff product of herpes simplex virus gene UL41. *J.Gen.Virol.*, 73 (Pt 2), 467-470.
- Smit,J.M., Bittman,R., & Wilschut,J. (1999). Low-pH-dependent fusion of Sindbis virus with receptor-free cholesterol- and sphingolipid-containing liposomes. *J.Virol.*, 73(10), 8476-8484.
- Snyder,H.W. & Sreevalsan,T. (1974). Proteins specified by Sindbis virus in HeLa cells. *J.Virol.*, 13(2), 541-544.
- Sokoloski,K., J.R.Anderson, & J.Wilusz (2007). Development of an in vitro mRNA decay system in insect cells. In J.Wilusz (Ed.), *Methods in Molecular Biology Humana Press*.
- Spangberg,K., Goobar-Larsson,L., Wahren-Herlenius,M., & Schwartz,S. (1999). The La protein from human liver cells interacts specifically with the U-rich region in the hepatitis C virus 3' untranslated region. *J.Hum.Virol.*, 2(5), 296-307.
- Spangberg,K., Wiklund,L., & Schwartz,S. (2000). HuR, a protein implicated in oncogene and growth factor mRNA decay, binds to the 3' ends of hepatitis C virus RNA of both polarities. *Virology*, 274(2), 378-390.
- Spangberg,K., Wiklund,L., & Schwartz,S. (2001). Binding of the La autoantigen to the hepatitis C virus 3' untranslated region protects the RNA from rapid degradation in vitro. *J.Gen.Virol.*, 82(Pt 1), 113-120.
- Stefanovic,B., Hellerbrand,C., Holcik,M., Briendl,M., Aliebbhaber,S., & Brenner,D.A. (1997). Posttranscriptional regulation of collagen alpha1(I) mRNA in hepatic stellate cells. *Mol.Cell Biol.*, 17(9), 5201-5209.
- Stoecklin,G., Mayo,T., & Anderson,P. (2006). ARE-mRNA degradation requires the 5'-3' decay pathway. *EMBO Rep.*, 7(1), 72-77.
- Strauss,J.H. & Strauss,E.G. (1994). The alphaviruses: gene expression, replication, and evolution. *Microbiol.Rev.*, 58(3), 491-562.
- Taylor,R., Kebaara,B.W., Nazarens,T., Jones,A., Yamanaka,R., Uhrenholdt,R., Wendler,J.P., & Atkin,A.L. (2005). Gene set coregulated by the *Saccharomyces cerevisiae* nonsense-mediated mRNA decay pathway. *Eukaryot.Cell*, 4(12), 2066-2077.
- Taylor,R.M., Hurlbut,H.S., Work,T.H., Kingston,J.R., & Frothingham,T.E. (1955). Sindbis virus: a newly recognized arthropodtransmitted virus. *Am.J.Trop.Med.Hyg.*, 4(5), 844-862.

- Thal,M.A., Wasik,B.R., Posto,J., & Hardy,R.W. (2007). Template requirements for recognition and copying by Sindbis virus RNA-dependent RNA polymerase. *Virology*, 358(1), 221-232.
- Tharun,S., He,W., Mayes,A.E., Lennertz,P., Beggs,J.D., & Parker,R. (2000). Yeast Sm-like proteins function in mRNA decapping and decay. *Nature*, 404, 515-518.
- Tharun,S., Muhlrاد,D., Chowdhury,A., & Parker,R. (2005). Mutations in the *Saccharomyces cerevisiae* LSM1 gene that affect mRNA decapping and 3' end protection. *Genetics*, 170(1), 33-46.
- Tharun,S. & Parker,R. (2001). Targeting an mRNA for decapping: displacement of translation factors and association of the Lsm1p-7p complex on deadenylated yeast mRNAs. *Mol.Cell*, 8(5), 1075-1083.
- Thisted,T., Lyakhov,D.L., & Liebhaber,S.A. (2001). Optimized RNA targets of two closely related triple KH domain proteins, heterogeneous nuclear ribonucleoprotein K and alphaCP-2KL, suggest Distinct modes of RNA recognition. *J.Biol.Chem.*, 276(20), 17484-17496.
- Tohya,Y., Narayanan,K., Kamitani,W., Huang,C., Lokugamage,K., & Makino,S. (2009). Suppression of Host Gene Expression by Nsp1 Proteins of Group 2 Bat Coronaviruses. *J.Virol.*
- Townley-Tilson,W.H., Pendergrass,S.A., Marzluff,W.F., & Whitfield,M.L. (2006). Genome-wide analysis of mRNAs bound to the histone stem-loop binding protein. *RNA*, 12(10), 1853-1867.
- Tucker,M., Valencia-Sanchez,M.A., Staples,R.R., Chen,J., Denis,C.L., & Parker,R. (2001). The transcription factor associated Ccr4 and Caf1 proteins are components of the major cytoplasmic mRNA deadenylase in *Saccharomyces cerevisiae*. *Cell*, 104, 377-386.
- Ubol,S., Tucker,P.C., Griffin,D.E., & Hardwick,J.M. (1994). Neurovirulent strains of Alphavirus induce apoptosis in bcl-2-expressing cells: role of a single amino acid change in the E2 glycoprotein. *Proc.Natl.Acad.Sci.U.S.A*, 91(11), 5202-5206.
- Unno,Y., Shino,Y., Kondo,F., Igarashi,N., Wang,G., Shimura,R., Yamaguchi,T., Asano,T., Saisho,H., Sekiya,S., & Shirasawa,H. (2005). Oncolytic viral therapy for cervical and ovarian cancer cells by Sindbis virus AR339 strain. *Clin.Cancer Res.*, 11(12), 4553-4560.
- Unterholzner,L. & Izaurralde,E. (2004). SMG7 acts as a molecular link between mRNA surveillance and mRNA decay. *Mol.Cell*, 16(4), 587-596.
- van Dijk,E., Cougot,N., Meyer,S., Babajko,S., Wahle,E., & Seraphin,B. (2002). Human Dcp2: a catalytically active mRNA decapping enzyme located in specific cytoplasmic structures. *The EMBO Journal*, 21(24), 6915-6924.

- van Hoof,A., Frischmeyer,P.A., Dietz,H.C., & Parker,R. (2002). Exosome-mediated recognition and degradation of mRNAs lacking a termination codon. *Science*, 295(5563), 2262-2264.
- Vasiljeva,L., Merits,A., Auvinen,P., & Kaariainen,L. (2000). Identification of a novel function of the alphavirus capping apparatus. RNA 5'-triphosphatase activity of Nsp2. *J.Biol.Chem.*, 275(23), 17281-17287.
- Wahlfors,J.J., Zullo,S.A., Loimas,S., Nelson,D.M., & Morgan,R.A. (2000). Evaluation of recombinant alphaviruses as vectors in gene therapy. *Gene Ther.*, 7(6), 472-480.
- Wang,K.S., Schmaljohn,A.L., Kuhn,R.J., & Strauss,J.H. (1991a). Antiidiotypic antibodies as probes for the Sindbis virus receptor. *Virology*, 181(2), 694-702.
- Wang,X., Kiledjian,M., Weiss,I.M., & Liebhaber,S.A. (1995). Detection and characterization of a 3' untranslated region ribonucleoprotein complex associated with human alpha-globin mRNA stability. *Mol.Cell Biol.*, 15(3), 1769-1777.
- Wang,Y.F., Sawicki,S.G., & Sawicki,D.L. (1991b). Sindbis virus nsP1 functions in negative-strand RNA synthesis. *J.Virol.*, 65(2), 985-988.
- Wang,Y.F., Sawicki,S.G., & Sawicki,D.L. (1994). Alphavirus nsP3 functions to form replication complexes transcribing negative-strand RNA. *J.Virol.*, 68(10), 6466-6475.
- Wang,Z., Jiao,X., Carr-Schmid,A., & Kiledjian,M. (2002). The hDcp2 protein is a mammalian mRNA decapping enzyme. *Proc.Natl.Acad.Sci.U.S.A*, 99(20), 12663-12668.
- Wang,Z., Ren,L., Zhao,X., Hung,T., Meng,A., Wang,J., & Chen,Y.G. (2004). Inhibition of severe acute respiratory syndrome virus replication by small interfering RNAs in mammalian cells. *J Virol.*, 78(14), 7523-7527.
- Weil,J.E. & Beemon,K.L. (2006). A 3' UTR sequence stabilizes termination codons in the unspliced RNA of Rous sarcoma virus. *RNA.*, 12(1), 102-110.
- Weil,J.E., Hadjithomas,M., & Beemon,K.L. (2009). Structural characterization of the Rous sarcoma virus RNA stability element. *J.Virol.*, 83(5), 2119-2129.
- Weiss,B., Nitschko,H., Ghattas,I., Wright,R., & Schlesinger,S. (1989). Evidence for specificity in the encapsidation of Sindbis virus RNAs. *J.Virol.*, 63(12), 5310-5318.
- Wengler,G., Wengler,G., & Gross,H.J. (1978). Studies on virus-specific nucleic acids synthesized in vertebrate and mosquito cells infected with flaviviruses. *Virology*, 89(2), 423-437.
- Wilson,T. & Treisman,R. (1988). Removal of poly(A) and consequent degradation of c-fos mRNA facilitated by 3' AU-rich sequences. *Nature*, 336(6197), 396-399.

- Wilusz, J. & Shenk, T. (1988). A 64 kd nuclear protein binds to RNA segments that include the AAUAAA polyadenylation motif. *Cell*, 52(2), 221-228.
- Wittmann, J., Hol, E.M., & Jack, H.M. (2006). hUPF2 silencing identifies physiologic substrates of mammalian nonsense-mediated mRNA decay. *Mol. Cell Biol.*, 26(4), 1272-1287.
- Wreschner, D.H., McCauley, J.W., Skehel, J.J., & Kerr, I.M. (1981). Interferon action--sequence specificity of the ppp(A²p)nA-dependent ribonuclease. *Nature*, 289(5796), 414-417.
- Wu, M., Nilsson, P., Henriksson, N., Niedzwiecka, A., Lim, M.K., Cheng, Z., Kokkoris, K., Virtanen, A., & Song, H. (2009). Structural basis of m(7)GpppG binding to poly(A)-specific ribonuclease. *Structure.*, 17(2), 276-286.
- Yamashita, A., Chang, T.C., Yamashita, Y., Zhu, W., Zhong, Z., Chen, C.Y., & Shyu, A.B. (2005). Concerted action of poly(A) nucleases and decapping enzyme in mammalian mRNA turnover. *Nat. Struct. Mol. Biol.*, 12(12), 1054-1063.
- Yoneyama, M., Kikuchi, M., Natsukawa, T., Shinobu, N., Imaizumi, T., Miyagishi, M., Taira, K., Akira, S., & Fujita, T. (2004). The RNA helicase RIG-I has an essential function in double-stranded RNA-induced innate antiviral responses. *Nat. Immunol.*, 5(7), 730-737.
- Yu, J. & Russell, J.E. (2001). Structural and functional analysis of an mRNP complex that mediates the high stability of human beta-globin mRNA. *Mol. Cell Biol.*, 21(17), 5879-5888.
- Zamore, P.D., Tuschl, T., Sharp, P.A., & Bartel, D.P. (2000). RNAi: double-stranded RNA directs the ATP-dependent cleavage of mRNA at 21 to 23 nucleotide intervals. *Cell*, 101(1), 25-33.
- Zangar, R.C., Hernandez, M., Kocarek, T.A., & Novak, R.F. (1995). Determination of the poly(A) tail lengths of a single mRNA species in total hepatic RNA. *Biotechniques*, 18(3), 465-469.
- Zaric, B., Chami, M., Remigy, H., Engel, A., Ballmer-Hofer, K., Winkler, F.K., & Kambach, C. (2005). Reconstitution of two recombinant LSM protein complexes reveals aspects of their architecture, assembly, and function. *J. Biol. Chem.*, 280(16), 16066-16075.
- Zelus, B.D., Stewart, R.S., & Ross, J. (1996). The virion host shutoff protein of herpes simplex virus type 1: messenger ribonucleolytic activity in vitro. *J. Virol.*, 70(4), 2411-2419.
- Zhang, Y., Burke, C.W., Ryman, K.D., & Klimstra, W.B. (2007). Identification and characterization of interferon-induced proteins that inhibit alphavirus replication. *J. Virol.*, 81(20), 11246-11255.

Zheng,D., Ezzeddine,N., Chen,C.Y., Zhu,W., He,X., & Shyu,A.B. (2008). Deadenylation is prerequisite for P-body formation and mRNA decay in mammalian cells. *J.Cell Biol.*, 182(1), 89-101.

Zhou,A., Hassel,B.A., & Silverman,R.H. (1993). Expression cloning of 2-5A-dependent RNAase: a uniquely regulated mediator of interferon action. *Cell*, 72(5), 753-765.

Zhou,A., Paranjape,J.M., Hassel,B.A., Nie,H., Shah,S., Galinski,B., & Silverman,R.H. (1998). Impact of RNase L overexpression on viral and cellular growth and death. *J.Interferon Cytokine Res.*, 18(11), 953-961.

Zuker,M. (2003). Mfold web server for nucleic acid folding and hybridization prediction. *Nucleic Acids Res.*, 31(13), 3406-3415.

Zuo,J., Thomas,W., van,L.D., Middeldorp,J.M., Wiertz,E.J., Rensing,M.E., & Rowe,M. (2008). The DNase of gammaherpesviruses impairs recognition by virus-specific CD8+ T cells through an additional host shutoff function. *J.Virol.*, 82(5), 2385-2393.

APPENDIX A

ABBREVIATIONS

293T	Human embryonic kidney cell line transformed by SV40 T-antigen
Ago2	Argonaute 2
AR339	Strain of Sindbis isolated in 1952 in Sindbis, Egypt
ARE	AU-Rich Element
ATP	Adenosine Triphosphate, unit of energy in cell
Bcl-2	Anti-apoptotic protein
BGLF5	Alkaline exonuclease encoded by EBV
BHK-21	Baby Hamster Kidney cells
C6/36	Mosquito larval cell line
Caf1p	Ccr4p-Associated Factor 1
Ccr4p	Carbon Catabolite Repressor 4
Ccr4-Not	Large complex of proteins (NOT=Negative on TATA)
cDNA	Complimentary DNA
CIAP	Calf Intestinal Alkaline Phosphatase
CSE	Conserved Sequence Element
DAN	Deadenylating Nuclease
Dcp1	Decapping protein 1
Dcp2	Decapping Protein 2
DcpS	Scavenger decapping enzyme
Dis3p	Accessory exosome component, also called Rrp44
DNA	Deoxyribonucleic Acid
Dom34p	eRF1 paralogue in <i>Saccharomyces cerevisiae</i>
dsRNA	Double-stranded RNA
E1 and E2	Envelope proteins of Sindbis virus
E3L	Vaccinia virus encoded protein
EBV	Epstein-Barr virus

EJC	Exon Junction Complex
eRF1	Eukaryotic Release Factor 1 (translation termination)
eRF3	Eukaryotic Release Factor 3 (translation termination)
Exo9	Exosome component 9, also known as Rrp45 and Pm/Scf-75
G3BP1 and 2	rasGAP SH3 binding protein 1 and 2
Hbs1p	eRF3 paralogue in <i>Saccharomyces cerevisiae</i>
Hedls	Human enhancer of decapping large subunit
HeLa	Human cervical cancer cell line
HIV-1	Human Immunodeficiency Virus 1
HuR	Human antigen R
IFN	Interferon
ISG	Interferon stimulated genes
ISG20	Interferon stimulated gene 20
KSHV	Kaposi's sarcoma-associated virus
LLM-PAT	Linker-Ligation Mediated Poly(A) Tail Assay
LM-PAT	Ligation-Mediated Poly(A) Tail Assay
Lsm1-7	Sm-like protein complex 1-7
MDA5	Retinoic Acid Inducible Gene I
Mfold	RNA structure prediction computer program based on thermodynamic stability
mRNA	Messenger RNA
mRNP	Messenger Ribonucleoprotein
NMD	Nonsense-Mediated Decay
NS1	Non-Structural Protein, Influenza A virus
nsP	Non-structural protein, Sindbis virus
Nsp1	Non-structural protein 1, SARS
NTP	Nucleotide Triphosphate
OAS	Oligo-adenylate synthetase
PACT	Protein activator of the interferon-induced protein kinase, PKR
Pan2-Pan3	Poly(A) binding protein (Pab1p) dependent poly(A) nuclease 2 and 3

PAP	Pokeweed Antiviral Protein
PARN	Poly(A) Ribonuclease, originally termed DAN
Pat1	Protein associated with topoisomerase II
PAZ	Domain in PIWI, Argo and Zwillie proteins
P-bodies	Processing Bodies
PCR	Polymerase Chain Reaction
PEG	Polyethylene Glycol
PH	Pleckstrin homology domain
PIWI	P-element induced wimpy testis in <i>Drosophila melanogaster</i> , domain within the Ago2 protein which has endonucleolytic activity
PNK	Polynucleotide kinase
PNRC2	Proline-rich nuclear receptor coregulatory protein 2
Poly(C)bp	Poly-Cytosine binding protein
Poly(rC)	Poly-Cytosine binding protein
PRE	Pyrimidine-rich element
PTB	Poly-pyrimidine Tract Binding protein
PTC	Premature Termination Codon
qRT-PCR	Quantitative Real-Time Polymerase Chain Reaction
Rck/p54	Decapping accessory protein in humans
RHA	RNA helicase A
RISC	RNA induced silencing complex
RNA	Ribonucleic Acid
RNAi	RNA interference
RPA	RNase Protection Assay
Rrp44	Ribosomal RNA processing protein 44, accessory exosome component, also called Dis3p
RSE	Repeat Sequence Element
S100	100 Svedberg Units
SARS	Severe Acute Respiratory Syndrome
shRNA	Short hairpin RNA

siRNA	Small interfering RNA
Ski7	“Superkiller” 7, molecular tRNA mimic
SLBP	Stem-Loop binding protein
Smg1, 5, 6 & 7	Originally named for its action as a suppressor with morphogenetic effect on genitalia
SOX	Shut off and exonuclease protein encoded by KSHV
Sp6	DNA-dependent RNA polymerase
ssRNA	Single-stranded RNA
SURF	Smg1-Upf1-eRF1-eRF3 complex
TIA-1	T-cell intracellular antigen
TIAR	TIA-1 related protein
TLR3	Toll-like receptor 3, recognizes dsRNA
TLR7/8	Toll-like receptor 7 and 8, recognize ssRNA
TRBP	HIV-1 transactivating response RNA-binding protein
ts6	Temperature-sensitive strain 6 of Sindbis virus derived from AR339 heat resistant strain
U	Units
Upf1	Originally titled Up Frame shift protein 1, core protein in NMD
Upf2	Originally titled Up Frame shift protein 2, core protein in NMD
Upf3	Originally titled Up Frame shift protein 3, core protein in NMD
URE	U-Rich Element
UTR	Untranslated Region
VA1	Virus associated RNA 1, low molecular weight adenovirus RNA
Vhs	Virion host shutoff protein, Herpes simplex virus
WNV	West Nile Virus
Xrn1	Exoribonuclease 1, originally termed Ski11
ZAP	Zinc-finger Antiviral Protein
Δ	Denotes a deletion when used with the 3' UTR, and knockdown when used in front of a protein

APPENDIX B

STUDENT'S T-DISTRIBUTION FOR A 95% CONFIDENT INTERVAL

(Adapted from http://en.wikipedia.org/wiki/Student's_t-distribution)

Where: v = degrees of freedom

<u>v</u>	<u>95%</u>
1	6.314
2	2.920
3	2.353
4	2.132
5	2.015
6	1.943

APPENDIX C

LIST OF AUTHOR'S PUBLICATIONS

Garneau, N.L., C.J. Wilusz and J. Wilusz. In Vivo Analysis of the Decay of Transcripts Generated by Cytoplasmic RNA Viruses. *Methods in Enzymology*. 2008;449:97-123.

Garneau, N.L., K.J. Sokoloski, M. Opyrchal, C.P. Neff, C.J. Wilusz and J. Wilusz. The 3' Untranslated Region of Sindbis Virus Represses the Deadenylation of Viral Transcripts in Mosquito and Mammalian Cells. *Journal of Virology*. 2008 Jan;82(2):880-92.

Garneau, N.L., J. Wilusz and C.J. Wilusz. The highways and byways of mRNA decay. *Nature Reviews Molecular Cell Biology*. 2007 Feb;8(2):113-26.

Vasudevan S., **N. Garneau**, D. Tu Khounh and S.W. Peltz. p38 mitogen-activated protein kinase/Hog1p regulates translation of the AU-rich-element-bearing MFA2 transcript. *Molecular and Cellular Biology*. 2005 Nov;25(22):9753-63.